



UNIVERSITÀ DEGLI STUDI DI CATANIA  
DIPARTIMENTO DI SCIENZE  
BIOLOGICHE, GEOLOGICHE ED AMBIENTALI

---

---

*Salvatore Distefano*

*Stratigraphic, structural and geomorphological  
features of the Sicilian continental shelf:  
study cases from Southern Tyrrhenian  
and Sicily Channel*

---

---

**Ph.D Thesis**

---

---

Relatore: *Chiar.ma Prof.ssa Agata Di Stefano*

Correlatore: *Dr. Fabiano Gamberi*

--- *XXX CICLO* ---  
*2014-2017*

---

Ph.D Thesis: *Stratigraphic, structural and geomorphological features of the Sicilian continental shelf: study cases from Southern Tyrrhenian and Sicily Channel.*

## **INDEX**

### **GENERAL INTRODUCTION**

#### **PART I: METHODOLOGY**

1.0 INTRODUCTION

1.1 SONAR PRINCIPLES IN THE WATER

1.2 ECHOSOUNDING

1.3 MULTIBEAM

1.4 CHIRP SUB-BOTTOM

1.5 SPARKER SYSTEM

1.6 BATHYMETRIC AND SEISMIC INTERPRETATION SOFTWARES

1.6.1 GLOBAL MAPPER

1.6.2 SWANPRO™

1.6.3 GEOSUITE ALLWORKS

1.7 SEISMIC STRATIGRAPHY PRINCIPLES

1.8 THE SEISMIC RESOLUTION

#### **PART II: CONTINENTAL SHELF ENVIRONMENT: STRUCTURAL-STRATIGRAPHIC EVOLUTION OF LAMPEDUSA ISLAND AND SOUTH-EAST SICILY OFFSHORE**

2.0 INTRODUCTION

2.1 PHYSIOGRAPHIC FEATURES OF THE CONTINENTAL SHELF

2.2 DEPOSITIONAL ENVIRONMENTS: AUTOGENIC AND ALLOGENIC CONTROLS

2.3 SEQUENCE STRATIGRAPHY

2.3.1 SEQUENCE STRATIGRAPHIC UNITS

2.3.2 SEQUENCE STRATIGRAPHIC SURFACES

2.4 LATE MIOCENE TO QUATERNARY STRUCTURAL EVOLUTION OF THE LAMPEDUSA ISLAND OFFSHORE

#### 2.4.1 GEOLOGICAL SETTING

#### 2.4.2 DATA DESCRIPTION AND INTERPRETATION

##### *2.4.2.1 Northern sector*

##### *2.4.2.2 Southern Sector*

##### *2.4.2.3 Eastern sector*

#### 2.4.3 DISCUSSION

#### 2.4.4 CONCLUSIONS

### 2.5 STRUCTURAL AND STRATIGRAPHIC RECONSTRUCTION OF THE SOUTH-EAST SICILY CONTINENTAL SHELF

#### 2.5.1 GEOLOGICAL SETTING

#### 2.5.2 DATA DESCRIPTION AND INTERPRETATION

#### 2.5.3 DISCUSSION

#### 2.5.4 CONCLUSIONS

## **PART III: SHALLOW-WATER DEPOSITIONAL SYSTEM: GEOMORPHOLOGICAL EVOLUTION OF THE NORTH-EAST SICILY**

### 3.0 INTRODUCTION

### 3.1 TRANSGRESSIVE WAVE-DOMINATED COASTS

### 3.2 PHYSICAL PROCESSES AND MAIN SEDIMENTARY STRUCTURES

#### 3.2.1 RIPPLES AND HUMMOCKY CROSS-STRATIFICATION

#### 3.2.2 PLANAR STRATIFICATION

#### 3.2.3 DUNES

#### 3.2.4 BARRIERS AND BEACHES

### 3.3 DELTA

#### 3.3.1 PHYSIOGRAPHIC AND RECONSTRUCTION OF A DELTAIC SYSTEM



### 3.4 GEOMORPHOLOGICAL RECONSTRUCTION OF THE NORTH-EAST SICILY CONTINENTAL SHELF

#### 3.4.1 GEOLOGICAL SETTING

#### 3.4.2 DATA DESCRIPTION AND INTERPRETATION

##### *3.4.2.1 Shelf sector n. 1*

##### *3.4.2.2 Shelf sector n. 2*

##### *3.4.2.3 Shelf sector n. 3*

#### 3.4.3 DISCUSSION

##### 3.4.3.1 LAST TRANSGRESSIVE STAGE RECONSTRUCTION

#### 3.4.4 CONCLUSIONS

## REFERENCES

Ph.D Thesis: *Stratigraphic, structural and geomorphological features of the Sicilian continental shelf: study cases from Southern Tyrrhenian and Sicily Channel.*

## GENERAL INTRODUCTION

The main aims of this Ph.D Thesis are the characterization of the structural-stratigraphic evolution of the continental shelf deposits in offshore areas and the definition of its morphological features, through the interpretation of seismic profiles and bathymetric data.

The methodological study represented an important study phase, because the knowledge of the physical principles and of the technologies used in Marine Geology is the basis of a good interpretation of the acquired data. In particular, the geophysical technologies employed to acquisition of bathymetric data and seismic profiles interpreted in this Thesis are: the Multibeam system, Sparker system and Sub-Bottom CHIRP.

The Multibeam system allows to investigate the bathymetry of the seabed and, therefore, constituted an important instrument for defining the morphological characteristics of the study areas. The CHIRP Sub-bottom is a technology used in marine geology to acquire high resolution sub-bottom lines that represent acoustic sections below the seabed, along the route of the ship during the acquisition phases. The depth of the investigation and the resolution of the seismic data depend on the best compromise between source energy and signal frequency. The Sparker System is another high-resolution seismic-acoustic source and differs from Sub-bottom CHIRP mainly for the type of acoustic wave trigger and for the frequency (50-4000 Hz) of the acoustic signal. The study areas, lying in the inner part of the continental shelf, are the Lampedusa Island, the south-east and the north-east Sicily offshore. In order to develop coherent tectonic-stratigraphic models, the regional geodynamic context of the study areas was always considered during the seismic stratigraphic interpretation phase. In the following, the main results of the seismic interpretation in these three areas are reported.

The Pelagian Archipelago (Lampedusa, Lampione and Linosa Islands) is located in a complex and wide geodynamic system characterized by the occurrence of two independent tectonic processes acting simultaneously: convergence along the Apennine-Maghrebian accretionary wedge and late Miocene-early Pliocene rifting in the Sicily Channel. Through high resolution single-channel seismic reflection profiles (Sparker

System) recently acquired around the Lampedusa Island offshore, the reconstruction of an updated structural setting of this area and its regional correlation has been performed.

The late Miocene-early Pliocene rifting affects directly the structural evolution of the Lampedusa plateau, with the development of a graben and half-graben setting in most of the offshore area, widely filled with the syn-rift deposits. A different distribution of these depositional units in the various sectors (northern, southern and eastern) of the Lampedusa plateau is shown. In the northern sector, the activity of the normal faults associated with the rifting is active up to the early Pliocene, whereas it is quiescent since late Miocene in southern sector. This current fabric of the Lampedusa plateau derives by its involvement in regional extensional regime, lying in a dextral-transpressive zone and marked by pull-apart basins. In particular, two systems of the normal faults in the Lampedusa offshore have been recognized. The Master Extensional Faults oriented WNW-ESE represent the main structural alignment of the Lampedusa offshore and reflect the extensional trending of the Sicily Channel. The Second order of Extensional Faults, oriented NNW-SSE, bounds smaller pull-apart basins and are probably associated with the main dextral-transpressive regional regime.

From the comparison with some preexisting models known in literature, an updated stratigraphic-structural model is proposed also to the southeastern continental shelf between the Gela-Catania foredeep and the Hyblean foreland offshore, along the Marina di Ragusa offshore.

The seismo-stratigraphic interpretation shows a NE-SW extensional faults system that involves only the late Miocene formations, probably connected to history of the Scicli Line and to polyphase kinematic evolution of the N50 oriented faults. Furthermore, the late Miocene extensional tectonic activity involves widely affects the offshore portions of the Hyblean foreland and its ramp, but it does not show evidences that this activity has involved the Plio-Pleistocene succession. The deposition of the Gessoso-Solfifera Formation has been widely recognized in the Hyblean foreland ramp, demonstrating that the evaporitic deposition does not is a peculiarity only of the deposits within the semi-isolated and marginal sub-basins or of the thrust top mini-basins of the Apennine-Maghrebides belt, but extends also in areas where the extensional tectonic have been dominant, at least during the pre-Messinian age.

Through Multibeam bathymetric data, an update characterization of the geomorphological setting of the north-east Sicily continental shelf, between Milazzo Promontory and the area offshore from the Saponara River, is provided in the Chapter 6. Furthermore, through high-resolution CHIRP seismic profiles interpretation, a reconstruction of the evolution of the last eustatic sea level cycle is performed, on the basis of the morpho-stratigraphic description of the transgressive and highstand wedges. The lowstand succession, corresponding with the foreset of the prograding clinofolds of the continental margin deposits, determines the accommodation space for the depositional processes that occur during the rise of the sea level. In fact, the evolution of the transgressive and highstand wedges is strongly influenced by the geometry of the underlying lowstand succession. The transgressive wedge is developed in the 80-100 m bathymetric range and consists of the relict geomorphic elements that represent past landscape. These elements tracked the variations in coastline position during the last sea-level rise, formed during an interval of relatively reduced rate of sealevel rise. With the support of 3D bathymetric maps, a reconstruction of the geomorphological evolution of the past coastal systems during the last transgressive stage is provided. The highstand wedge consists of the Corriolo, Muto, Niceto, Cocuzzaro and Rometta delta deposits that widely develop on the offshore portions of the inner continental shelf.

Ph.D Thesis: *Stratigraphic, structural and geomorphological features of the Sicilian continental shelf: study cases from Southern Tyrrhenian and Sicily Channel.*

## **PART I: METHODOLOGY**

### **1.0 INTRODUCTION**

Part I of this Thesis represents a detailed methodological study of the geophysical technologies used during the data acquisition in the study areas (Lampedusa island, south-east and north-east Sicily). In particular, a short review of the main physical principles about the propagation of the sound in water introduces the description of these technologies, the bathymetric and seismic interpretation softwares and the seismic stratigraphy principles.

In particular, the stratigraphic and morpho-structural setting of the Lampedusa Island offshore and the part of the northeastern and southeastern offshore of Sicily, is reconstructed in this Thesis through the accurate analysis of seismic profiles and bathymetric data acquired with three SONAR technologies: *EM710 Reason SeaBat 7111 Multibeam*, *Teledyne BENTHOS III CHIRP* and *Marine Multi-Tip Sparker System, Geo-Source 200 Light Weight model*.

In **Table 1.1** are reported some information about the oceanographic cruises during which the seismo-bathymetric data have been acquired.

Year	Project	Institute	Ship	Data acquired
2009	MAGIC	CNR_ISMAR_BO	Urania	Sub-Bottom CHIRP
2009-2010	MAGIC	CNR_ISMAR_BO	Maria Grazia	Multibeam
2011	MAGIC	CNR_ISMAR_BO	Urania	Multibeam
2014	MARBEEP	CNR_ISMAR_BO	Urania	Sub-Bottom CHIRP
2015	SIMIT	UNI_CT	Neptune 1	Sparker System

**Table 1.1** – *The oceanographic cruises and the projects with which the geophysical data interpreted in this thesis were acquired.*

In the following, the main technical features of the oceanographic ships are described.

The Urania oceanographic ship (**Fig. 1.1A**) is managed by the CNR (Consiglio Nazionale delle Ricerche). It has 45 days of self-sufficiency and can accommodate up to 36 persons between scientific staff and crew. The speed range for continuous detection varies between 1.5 and 11 knots. The propulsion system consists of two variable pitch propellers driven by two 1000 KW engines and a 220 kW propeller. The ship is equipped with a Simrad Dynamic Positioning System for precision maneuvers. The ship hosts laboratories for analysis, geological sampling, chemical and radiological laboratories, and allows the elaboration of navigation data, geophysics and data captured using the Remote Operated Vehicle (ROV) and multiparameter probe. Geophysical instruments include a Chirp Datasonic profiler, a Sparker, a 3.5KHz Sub-Bottom Profile, a Uniboom, a 100 - 500KHz side scan sonar and a magnetometer. As for the sampling systems (operating up to the deepest depths of the Mediterranean), gravity and piston samplers, box corers and buckets (Shipek and Van Veen) are available.



**Fig. 1.1** – A. The Urania oceanographic ship; B. The Maria Grazia oceanographic ship; C. The Neptune 1 oceanographic boat.

The Maria Grazia oceanographic ship (**Fig. 1.1B**) is enabled for unlimited Mediterranean navigation and has a maximum operating autonomy of approximately 30 days. It can host up to 8 crew members and 10 scientific/technical staff. It has a length of 42 meters and reaches about 16 knots of maximum speed thanks to two 433 kW motors. The ship can perform: geophysical surveys (Multibeam echo sounder, Singlebeam echo sounder, Sub Bottom Profiler), surface data collection, CTD, continuous water sampling, ADCP, dredges, box corer, bucket; support for geomorphological inspections with Sparker, Uniboom, Side Scan Sonar, Magnetometer, ROV and AUV.



The Neptune 1 (Geonautics s.r.l.) (**Fig. 1.1C**) oceanographic boat is equipped with 100 HP Volkswagen Marine motorization that allows fast moving. Through the trolling valve system, it maintains extremely low speeds for long periods, a key factor for the goodness of a survey. On board there are two pc stations and a TV monitor for ROV analysis. The navigation system allows to connect GPS, magnetometer, USBL, motion sensors. The boat can be equipped with Sub Bottom CHIRP, Sparker and Multibeam system.

### **1.1 SONAR PRINCIPLES IN THE WATER**

Acoustic waves move quite efficiently through water. As an example, the whales use sound to communicate over distances of 10s kilometers. The ability of sound to travel over such great distances is at the basis of the remote sensing technique in the submarine environment. Sound travels in water in a moving series of pressure fronts known as a compressional wave. These pressure fronts move at a specific speed in water, named the local speed of sound. The local speed of sound can change depending on the conditions of the water such as its salinity, pressure, and temperature, but it is independent of the characteristics of the sound itself. In a typical ocean environment, the speed of sound is about 1500 m/s.

The physical distance between pressure fronts in a traveling sound wave is its *wavelength*. The number of pressure fronts that pass a stationary point in the water per unit time is the *frequency* of the wave. Wavelength, if measured in meters (m), and frequency, if measured in cycles per second (Hz), are related to each other through the speed of sound, which is measured in meters per second (m/s):

$$\textit{speed of sound} = \textit{frequency} \times \textit{wavelength}$$

When a sound wave meets a change in the local speed of sound, its wavelength changes, but its frequency remains constant. For this reason, sound waves are generally described in terms of their frequency.

A sound wave carries a certain amount of acoustic energy. This energy can be measured by a device called a hydrophone, which measures the oscillations in pressure. The size of these oscillations is the *amplitude* of the wave (**Fig. 1.2**).

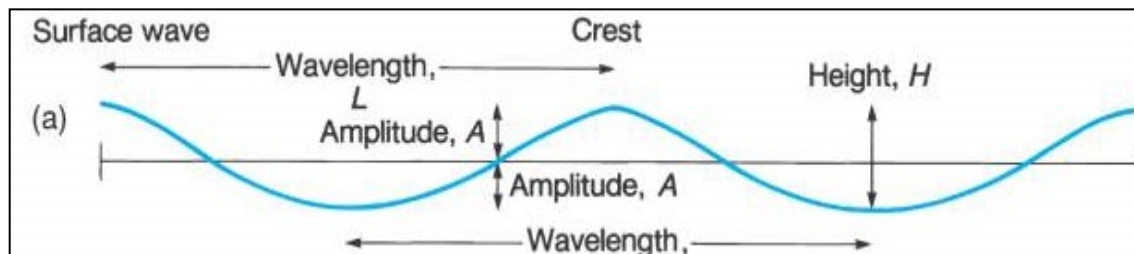


**Fig. 1.2** – Graphic representation of an acoustic wave.

As a sound wave propagates, it loses some of its acoustic energy. This happens because the transfer of pressure differences between molecules of water is not 100% efficient, but some energy is lost as generated heat. The energy lost by propagating waves is called *attenuation*. As a sound wave is attenuated, its amplitude is reduced. Sound waves are useful for remote sensing in a water environment because some of them can travel for hundreds of kilometers without significant attenuation. The level of attenuation of a sound wave is dependent on its frequency: high frequency sound is attenuated rapidly, while low frequency is attenuated with great distances.

When a moving sound pulse encounters another medium, only a fraction of its energy propagates into the new material. How much of the energy is transmitted is dependent on several factors, including the *impedance* of the new material (a product of the material's density and the speed of sound within it), the *angle of incidence* of the impinging pulse (the angle at which the sound pulse strikes the new medium), and the *roughness* of the new medium's surface. The energy that is not transmitted into the new material must go back into the original medium: the water. Some amount of it is reflected off the surface of the material: essentially it rebounds in a direction that depends on the angle of incidence. The remainder is scattered in all directions (**Fig. 1.3**).

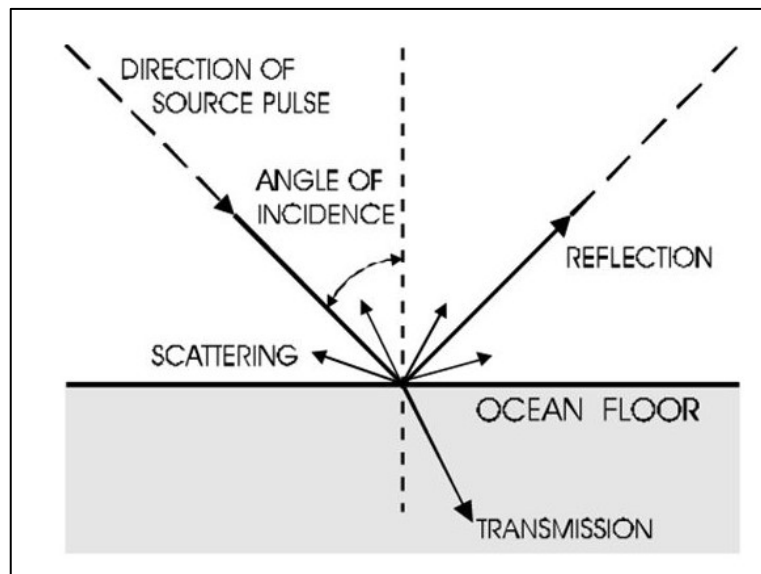


**Fig. 1.3** - *Components of an Echo Event on the Ocean Floor (by Multibeam Sonar, Theory and Operation, 2000)*

How much energy goes into reflection and how much goes into scattering depends on the characteristics of the material and the angle of incidence. The energy returned to the water is called an *echo*. The echo maintains the frequency attributes of the source wave.

## 1.2 ECHOSOUNDING

The echo sounding is a technique for measuring water depths by transmitting acoustic pulses from the ocean surface and recording for their reflection (or echo) from the sea floor. This technique has been used since the early twentieth century and has allowed the ships to navigate in safety through the world's oceans. In addition, the information derived from echo sounding has aided in laying trans-oceanic telephone cables, exploring and drilling for off-shore oil and improving our understanding of the Earth's geological processes.

The echo sounder is a tool that generates acoustic waves through transducers, devices that converts energy from one form to another and analyzes the return signal. Until the early 1960s, most depth sounding used single-beam echo sounders. These devices make a single depth measurement with each acoustic pulse and include both wide and narrow beam systems. Over the years, the scientific progress has reached the

best compromise between the acoustic amplitude (greater area coverage) and the acoustic energy (higher resolution), experimenting successfully a new system named *multiple narrow beam*. This system allows mapping of the sea bottom through a simultaneously emission of a beam of acoustic waves, reducing the navigation times and the costs.

The multiple narrow beam and, in general, the transmission of the acoustic waves through the water column represent the physical concepts at the basis of the instruments for the data acquisition interpreted in this PhD thesis: multibeam, sub-bottom chirp and sparker system.

### **1.3 MULTIBEAM**

The Multibeam system allows to investigate the bathymetry of the seabed. It can operate in shallow and deep waters, properly changing the frequency and the energy of the acoustic wave. The instrument, assembled below the keel of the ship, emits the acoustic pulses that are reflected by the seawater-seafloor interface and back to the surface, where they are recorded by the transducers. The *backscatter* is the physical feature for which a part of the acoustic energy emitted is reflected and diffused by the seabed roughness. It represents a different parameter, through which it is possible to acquire additional information on the morphological and textural characteristics of the seabed investigated.

For each acoustic pulse, the time it takes for a reflection from a particular boundary to arrive at the geophone is called the *travel time*. For a simple vertically traveling wave, the travel time from the surface to the reflector and back is called the *Two-Way Time* (TWT) and is given by the formula:

$$\text{Time} = 2 (\text{depth} / \text{wave velocity})$$

Therefore, the Multibeam is a multiple impulse system: more waves at different angles are generated at the same time. During the emission, a beam of the acoustic pulses (*swath*) investigates the seabed orthogonally to the axis of the ship. With a

constant angular aperture of the acoustic beam, the seabed area investigated (*footprint*) gradually increases toward deeper bathymetry (**Fig. 1.4**)

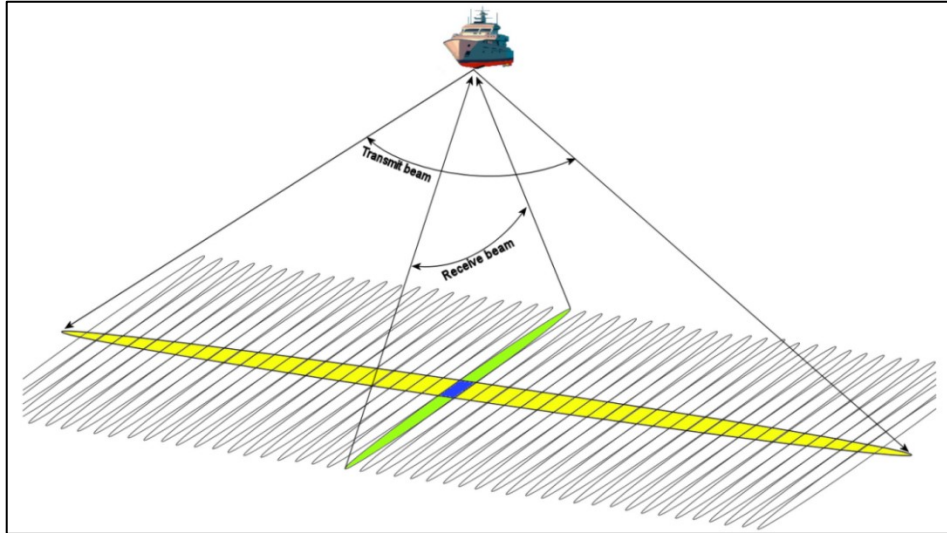


**Fig. 1.4** – Schematic functioning of the Multibeam system.

During the survey acquisition, the navigation routes tend to be parallel, with partial overlapping of the swaths in order to allow the full coverage of the study area. The lateral beams travel longer way and with an incidence angle greater than the central ones. Then, they are more susceptible to the dispersion of the original acoustic energy. In fact, if necessary, the beam aperture can be changed until the optimal emission angle is achieved.

The main Multibeam system components are shown in **Fig. 1.5**.

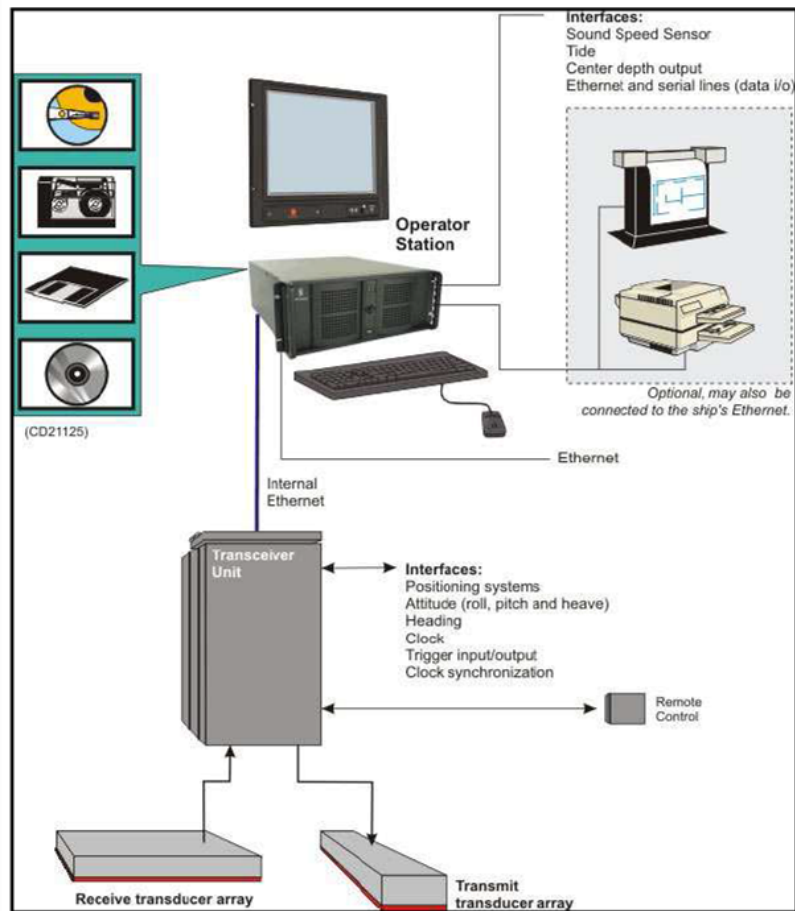


**Fig. 1.5** – Hardware components of the Multibeam system (*Multibeam Sonar, Theory and Operation, 2000*).

The batimetric data interpreted in this PhD thesis was mainly acquired through the EM3002d and EM710 Reason SeaBat 7111 Multibeam (**Fig. 1.6**).



**Fig. 1.6** - EM710 Reason SeaBat 7111 Multibeam and an integrated monitor.

The EM3002d and EM710 Reason SeaBat 7111 are two 455 kHz Ultra High Resolution Focused Multibeam Echosounder (MBES) systems, which measure the relative water depth across a swath perpendicular to the vessel's track. The SeaBat 7111 uses high frequency focused near-field beam forming to provide a good level of detail. The five standard components of the SeaBat 7111 system are described in the following.

- The Sonar Processor can be mounted in the operating space. It is the source of operating power for the Sonar Head and all system I/O connections are made at the processor's rear panel;

- the Processor to Sonar Head Signal and Control cable is a multi-conductor cable of water-blocked construction with a molded waterproof pressure immune connector at the wet end and an MS-type connector at the dry end. The standard cable is 25 meters in length;

- the Sonar Head is compact, with no moving parts. It may be temporarily mounted on a retractable structure or permanently on an extension through the hull in a moon pool, sea-chest configuration, or on a Remotely Operated Vehicle (ROV);

- the Color Video Monitor is a standard PC-type S-VGA monitor.

The maximum selectable range scale is 600 meters. However, maximum swath width typically occurs at a water depth of 400 meters. At depths greater than 400 meters, accurate bottom surveys are still possible, but with a corresponding decrease in swath width. The Seabat 7111 system illuminates a swath on the sea floor that is 120° across track by 1° along track. The swath consists of 240 individual 0.5° by 1.0° beams at the center and 1.0° by 1.0° at the outer ends. The bottom detection range resolution is 2.5 cm. During the acquisition phases, in order to know the sound velocity along the water column and thus to minimize the errors of the depth investigated, a Reson SVP-C probe was used at regular intervals.

The data was acquired with the SIS and PDS2000 softwares and subsequently processed with CARIS HIPS & SIPS softwares by the technologists of the ISMAR (Istituto di Scienze Marine) of the CNR (Consiglio Nazionale delle Ricerche) of Bologna (Italy). The final output is a Digital Terrain Model (DTM) of the submerged sectors of the North-East Sicily, with a spatial resolution of about 1 m within the shelf area and 5 m within continental escarpment. In particular, The Digital Terrain Model (DTM) used for the

interpretation of the geomorphology of the study area was compiled from data acquired with different multibeam systems on board several oceanographic vessels. High resolution bathymetric data were acquired during two cruises in the upper slope and shelf area, carried out on board R/V Mariagrazia in 2009 and 2010 using a hull-mounted Kongsberg EM3002D (300 kHz) and a pole-mounted Reson 7111 (100 kHz) multibeam system respectively. In 2011 some sectors of the outer shelf were re-mapped with a hull-mounted Kongsberg EM710 (70–100 kHz) multibeam system on board R/V Urania.

The Multibeam data interpreted in this Thesis cover an area of about 75 Km<sup>2</sup> of the northwestern Sicily offshore, from a depth of 40 m to 150 m and represent a tool of fundamental importance to define the morphological characteristics of the study area.

#### **1.4 CHIRP SUB-BOTTOM**

The Chirp Sub-bottom is a technology used in Marine Geology to acquire high resolution subbottom lines, that represent acoustic sections below the seabed, along the route of the ship during the acquisition phases. The depth of the investigation and the resolution of the seismic data depend on the best compromise between source energy and signal frequency.

Together with the multibeam data acquisition, high resolution CHIRP seismic profiles were acquired on board R/V Mariagrazia and Urania with a hull-mounted Teledyne BENTHOS III CHIRP system having a frequency modulation between 2 and 20 kHz (Gamberi et al., 2014).

Teledyne BENTHOS III CHIRP is an instrument belonging to high-resolution seismic sources. Benthos is a pioneer in Chirp technology and was the first to bring a commercial Chirp sub-bottom profiling system to the market. Teledyne Benthos continues that advancement with the Chirp III sub-bottom profiling system. Its versatile system configuration has been designed to operate with a wide variety of tow-vehicles and sound sources.

The main components (**Fig. 1.7**) of the Teledyne BENTHOS III CHIRP are:

- Tow-vehicle (TTV-290 Series): it is designed for hydrodynamic stability in most towing applications. The stainless steel midplate construction provides users



with a rigid and stable platform to mount additional sensors. TTV-290 tow vehicle includes a 2x2 Low frequency (2-7 kHz), transducer array (AT-471), high frequency (10-20 kHz) transmit projector, receiving hydrophone and all interconnect cables;

- Chirp III transceiver (DSP-6651): it includes a 4KW power amplifier, heave compensation delay key, analog preamplifier gain 0, + 15dB,+30dB and dual analog input channel, DSP hardware which provides the user with matched filter or digital processing for analog sources and multi-task operations;

- Personal Computer with a monitor: it represents the acquisition system and allows the visualization in real time of the data acquired and the processing of the digital signal. The acquisition system performs a digital recording in .SEGY format.



**Fig. 1.7** - Main components of the Teledyne BENTHOS III CHIRP.

One or more hydrophones detect the reflected seismic waves that are transformed in an analogic electrical signal, subsequently filtered and transformed in digital signals. Finally, the seismic data are processed and analyzed on paper or monitor for the seismic stratigraphy interpretation.

In order to provide an accurate stratigraphic-structural characterization of the northwestern Sicily offshore, the interpretation of several CHIRP seismic profiles has been

performed. In particular, 90 seismic profiles acquired during the MARBEEP survey and 78 seismic profiles acquired during the MAGIC survey were interpreted, covering a surface of about 80 Km<sup>2</sup> and comparing the results with the batimetric data of the Digital Terrain Model.

### 1.5 SPARKER SYSTEM

The Sparker System is another high-resolution seismo-acoustic source and differs from Sub-bottom CHIRP mainly for the type of acoustic wave trigger and for the frequency (50-4000 Hz) of the acoustic signal. Following the release of a high-voltage and lower-power electrical discharge between two or more electrodes submerged in water, the Sparker System generates a shock wave, followed by bubble pulses produced by expansion-contraction of further gas bubbles.

Also in this case, the output data are the seismic profiles but that involve a greater depth of the investigation (up to 500 m, as a function of the lithology) and a lower vertical resolution (up to 20 cm) than the Sub-bottom CHIRP (**Fig. 1.8**).

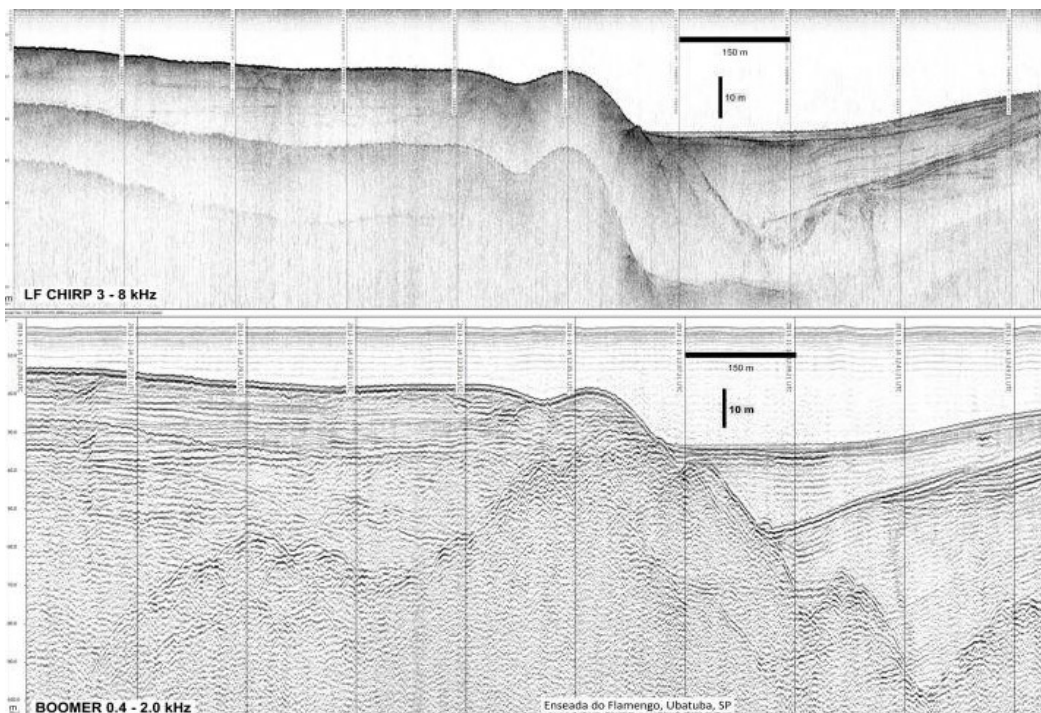


**Fig. 1.8** – Comparison of the different resolutions between CHIRP and Sparker System (named also Boomer).

The seismic data of the Lampedusa Island offshore described and interpreted in this Thesis have been acquired with the *Marine Multi-Tip Sparker System, Geo-Source 200 Light Weight model*. Designed to be towed by small boats, it uses a maximum power of 1000 Joules to cover depths between 2 and 500 m, reaching an average penetration of 200-300 ms and a vertical resolution up to 20-30 cm. The Geo-Source 200 is made up of three main components (**Fig. 1.9**):

- the Geo-Spark 1000 Pulsed Power Supply consists of dozens of electrodes that develop a negative electric charge with a high-voltage flexible cable of standard length of 25 m;
- the Single Channel Array is a Mini-Streamer (50-100 meters) with 8, 16, 24 or 48 hydrophones, created to capture a high frequency spectrum;
- the Solid State Pulse Power Supplies generates the acoustic signal; it is designed to avoid electric oscillations and to work at a power of 100 up to 1000 Joules.



**Fig. 1.9** – Main components of *Marine Multi-Tip Sparker System, Geo-Source 200 Light Weight model*. A. *Geo-Spark 1000 Pulsed Power Supply*; B. *Mini-Streamer (16 hydrophones)*; C. *Solid State Pulsed Power Supplies*.

In this work a grid of 21 seismic profiles with the Sparker System was acquired, consisting of both dip and strike lines in the northern, eastern and southern offshore of the Lampedusa Island. The technical features and some characteristics of the acquisition phase are reported in **Table 1.2**.

Technology	Geo-Spark 1000 Pulsed Power Supply
Energy	600 J
Sampling frequency	10000 Hz
Capture window	500 ms
Vertical resolution	Decimeters
N° seismic lines	21
Total length	145 km
Spacing	2-4 km

**Table 1.2** - *Some technical data of the Geo-Spark 1000 Pulsed Power Supply system, employed during the acquisition phase.*

All the seismic profiles were acquired in .SEGY format and interpreted using the Geo-Suite software. The acoustic penetration (about 250-300 ms TWT) allowed a good imaging of the upper part of the sedimentary succession and tectonic fabric of the Lampedusa offshore. The thickness of the deposits and the throw of extensional faults were calculated using an average velocity model of 2000 m/sec.

## **1.6 BATHYMETRIC AND SEISMIC INTERPRETATION SOFTWARES**

### **1.6.1 GLOBAL MAPPER**

Global Mapper is a viewer capable of displaying the most popular GIS raster, elevation and vector datasets, allowing users to easily view, edit and export the bathymetric data in multiple formats (**Fig. 1.10**).

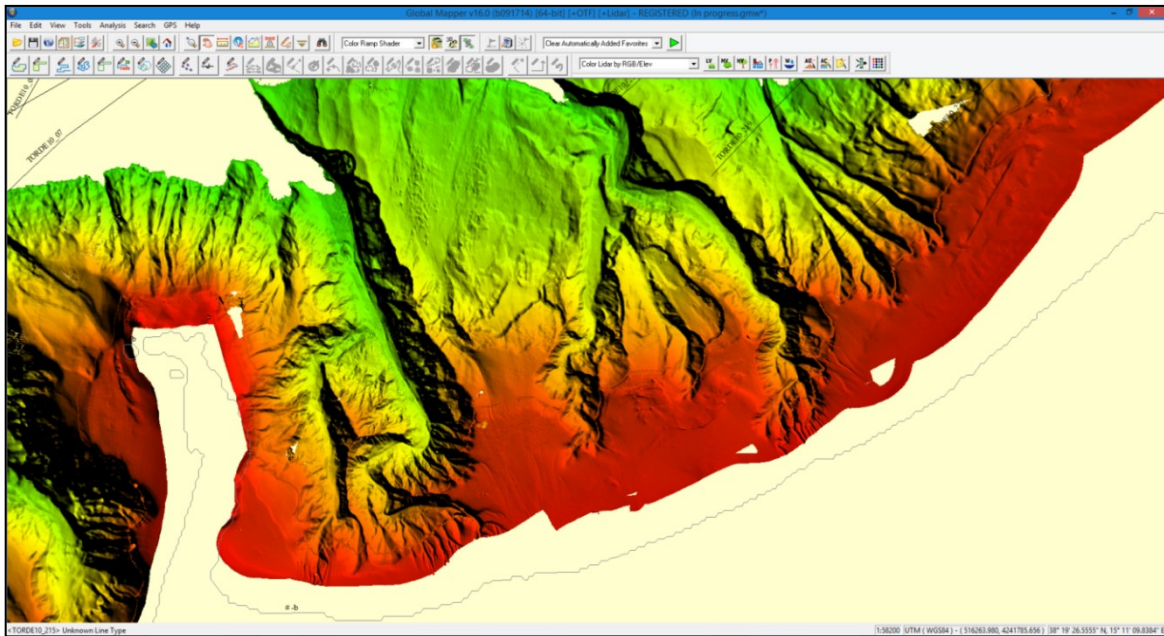


**Fig. 1.10** – Screenshot of Global Mapper software, showing a frame of the northeastern Sicily offshore.

The main tools used in the bathymetric interpretation are:

- loading and visualization of the Digital Terrain Model;
- creation of the elevation profile graphs;
- creation of the contours from the Digital Terrain Model;
- creation of the points, lines and areas;
- export of the contours to .DWG or SHP formats.
- creation and export of 3D mesh;
- simulation of the variation of the sea level in 3D view.

Developed by Blue Marble Geographics for Windows OS, the main quality of the Global Mapper software is the simple interface that allows an immediate access to advanced analysis tools and a fast processing of the large number of spatial data interpreted along the northeastern Sicily coastline.

### **1.6.2 SWANPRO™**

SwanPro™ (Communication Technology) is innovative software for real time data acquisition of sea floor imaging systems and seismic systems. It digitizes in real time, records and processes true 16 bits/sample signals and combines the imagery with the navigation inputs to geo-reference the data in real-time. This software interfaces with sub



bottom profilers CHIRP (**Fig. 1.11**) and other seismic systems (also the Sparker System). It runs under any 32 and 64 bit Microsoft Windows operating system and is very flexible and user friendly.

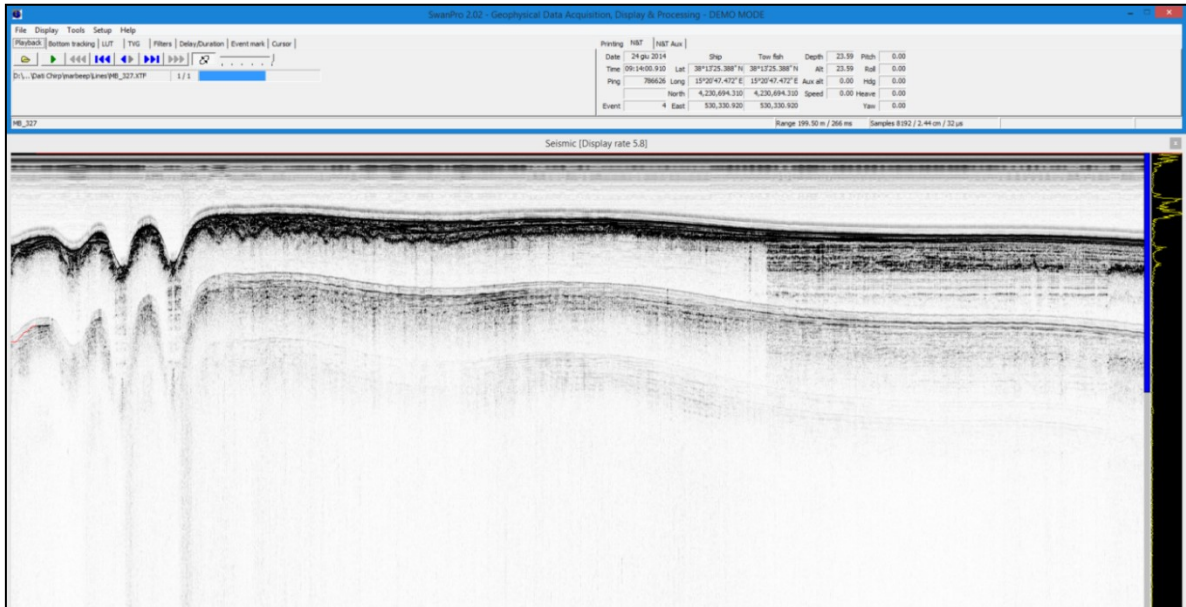


**Fig. 1.11** - Screenshot of SwanPro™ software, showing a Sparker seismic profile of the Lampedusa island offshore.

SwanPro™ supports several digital formats, including .SEGY format. The main tools used to seismic interpretation are:

- loading and visualization of the seismic profiles;
- variation of the “gain” (LUT function), that is the change in the amplitude of electrical signal from the original input to the amplified output;
- automatic conversion time-space for the determination of the distances between the acoustic reflectors.

All the seismic profiles reported in this Thesis have been described and interpreted also through SwanPro™.

### 1.6.3 GEOSUITE ALLWORKS

GeoSuite AllWorks (Geo Marine Survey Systems) is a comprehensive environment for the processing and the interpretation of the seismic profiles and related data resources. Through this software, standalone seismic data viewer or project to process different seismic data types can be performed. In particular, a project allows to investigate

the survey area with a wide set of dedicated tools for seismic profiles processing and interpretation in a GIS environment (**Fig. 1.12**).

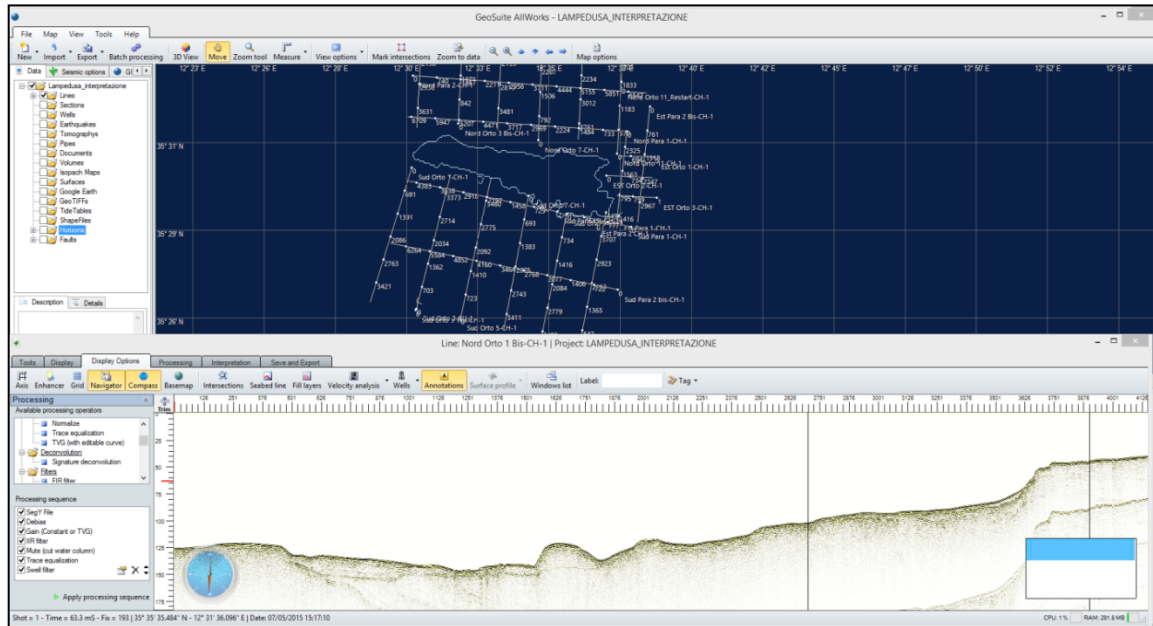


**Fig. 1.12** - Screenshot of GeoSuite AllWorks software, showing the geographic location of the seismic Sparker profiles acquired along the Lampedusa island offshore and the view for their interpretation.

The main tools used to the seismic interpretation are:

- loading and visualization of the seismic profiles (also in 3D view);
- processing sequence (debias-gain-IIR filter-Mute to cut water column-Trace equalization-Swell filter);
- resizing of the seismic traces, through the “traces/cm” and “ms/cm” functions;
- interpolation mode (none, bilinear or bicubic);
- variation of the “gain”, that is the change in the amplitude of electrical signal from the original input to the amplified output;

picking horizons and picking faults. All the seismic profiles reported in this Thesis have been described and interpreted also through GeoSuite AllWorks.

## 1.7 SEISMIC STRATIGRAPHY PRINCIPLES

The seismic reflectors (named here also acoustic horizons) generally correspond to physical surfaces that separate media with different value of *acoustic impedance* (product of the material's density and the speed of sound within it). For example, the stratification surfaces within a sedimentary succession (or the reflections generated by fluids with a different density) produce phenomena of reflection-refraction of the acoustic waves. However, the gradual facies lateral variations normally do not produce distinct reflections and, in addition, not all reflectors correspond to well-recognizable physical surfaces.

The seismic profiles processed and interpreted in this Thesis have a horizontal scale expressed in Shots, corresponding to times in the acquisition phases and recorded by progressive numeration. Instead, the vertical scale is expressed in time. Specifically, the vertical scale represents the time between the instant in which the acoustic pulse was generated and the instant in which the return energy is recorded by the hydrophone. This value is twice the time that the acoustic wave employs from the surface of the sea to the reflector: for this reason the time scale is commonly expressed in TWTT (Two-Way Travel Time) (**Fig. 1.13**).

During the interpretation phase, a 6x vertical exaggeration was applied in each Chirp and Sparker seismic profiles. In this way, the vertical and horizontal scale ratios have changed, favoring the visualization of the acoustic reflectors.

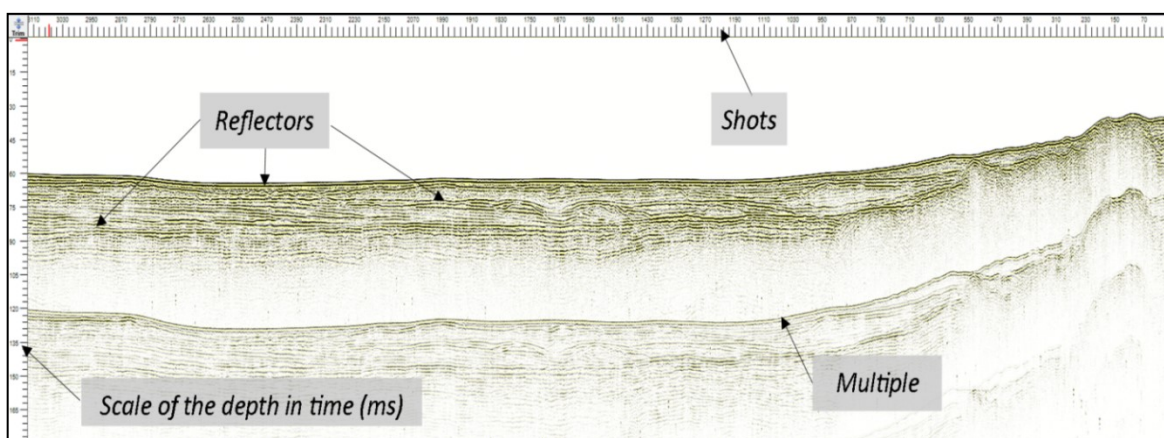


**Fig. 1.13** – Example of a Sparker System seismic profile and main components within the interpretation window in GeoSuite Allworks software.



The seismic profiles often show numerous interferences, defined *noises*, which are mainly due to the surrounding environment or to the navigation processes.

The *multiples* are a type of seismic noise due to successive reflections of a same horizon. In a seismic profile the multiple of a reflector appear as its acoustic repetition at a multiple depth and with a greater inclination (**Fig. 1.13**).

The *diffraction hyperbola* are another type of seismic noise and are generated when the seismic wave strikes a point of discontinuity of a horizon, such as a tectonic discontinuity. In according with the Huygens-Fresnel principle, this point becomes a source of secondary spherical waves that propagate inside the medium producing a series of false signals (**Fig. 1.14**).

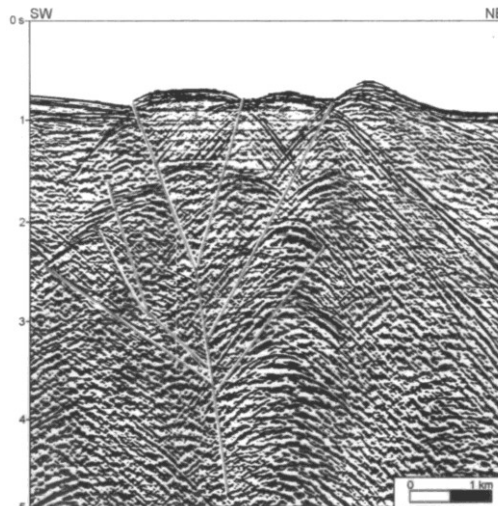


**Fig. 1.14** - Close to the faults, numerous diffraction hyperbola can be generated, overlapping with the real signals.

The *ringing effect* creates an interference caused by the absorption and resonance of the acoustic pulse emitted by the source. Frequently recognized in seismic profiles, the ringing consists in a series of reflective surfaces that are repeated with a regular spacing (**Fig. 1.15**).

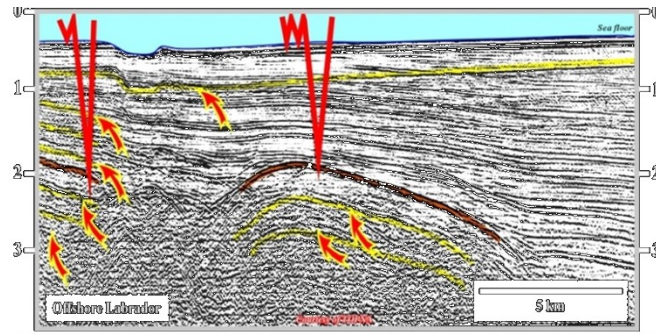


**Fig. 1.15** - "Ringing" effect of the bottom of the sea.

In the seismic interpretation of this work, the real reflectors are assembled in *seismic facies* that have homogeneous and different acoustic features than those of the adjacent units. The seismic facies can provide useful information on the environments and on the sedimentary processes. Furthermore, their variations in amplitude and the lateral continuity of the reflectors provide useful indications about the lithological features of the investigated stratigraphic units.

## 1.8 THE SEISMIC RESOLUTION

In seismic stratigraphy the vertical resolution is the minimum vertical distance between two interfaces, necessary to achieve a single reflection (Emery and Meyers, 1996).

The seismic acquisition depends by some physical parameters:

**Pe**: energy of the pulse;

**Bw**: amplitude of the spectrum frequency;

**PI**: pulse duration.

The resolution **R** (in meter) is:

$$R: PI \times Vs / 2$$

where **Vs** is the acoustic speed in the medium.

This mathematical relation shows as the wave amplitude and the acoustic energy influences directly the vertical resolution and the penetration depth of the signal: high frequency corresponds usually with increasing in the resolution. For example, the geophysical acquisition systems generate signal with less than 1 kHz of frequency and acquire low-resolution data but with a high penetration rate, such as the systems air/water-guns. Instead, the technologies belonging to the high resolution system class use frequency spectra comprised between 1 and 30 kHz, such as Sub Bottom Chirp.

The lateral resolution is the minimum distance between two points of the same surface and depends on the *shot rate* and the speed of the ship during the acquisition phases.



**PART II: CONTINENTAL SHELF ENVIRONMENT:**  
**STRUCTURAL-STRATIGRAPHIC EVOLUTION OF LAMPEDUSA ISLAND**  
**AND SOUTH-EAST SICILY OFFSHORE**

**2.0 INTRODUCTION**

The study areas (Lampedusa Island, Marina di Ragusa and North-East Sicily offshore) lie, from a physiographic point of view, along the continental shelves, that is the submarine areas closest to land and where the fluvial sediment transport to the offshore in combination with the oceanographic processes is the main control for the development of geomorphic elements (Gamberi et al., 2014). In fact, in all study areas, the continental shelf represents the common physiographic and environmental context along which the new seismic and bathymetric data have been acquired. The physiographic features of this depositional environment are briefly described in this Part, highlighting that the autogenic and allogenic factors directly control the stratigraphic evolution of the depositional units detected. Furthermore, the influence on the depositional systems of the global scale factors (eustatic variations, climatic variations, morpho-structural setting) and local-scale factors (physical erosion and transport processes) are also discussed. In the following sections, the concept of sequence stratigraphy is carefully studied, because an accurate knowledge of the various stratigraphic sequence units (sequences in s.s., parasequences and system tracts) was crucial during the seismic-interpretation phase.

In particular, through the interpretation of high-resolution seismic profiles (Sparker System) are described and discussed two areas in this part of the Thesis:

1 - Lampedusa Island offshore, with the reconstruction of current structural evolution of the area and its regional significance;

2 - Marina di Ragusa offshore, with the proposal of new stratigraphic-structural model that connect the Gela-Catania foredeep and the Hyblean foreland ramp and the description of the Plio-Pleistocene succession and its areal distribution.

## 2.1 PHYSIOGRAPHIC FEATURES OF THE CONTINENTAL SHELF

The *coastal zone*, as described by Inman & Brush (1973), is essentially represented by three sub-environments: *coastal plain, shoreface and continental shelf s.s.* (Fig.2.1).

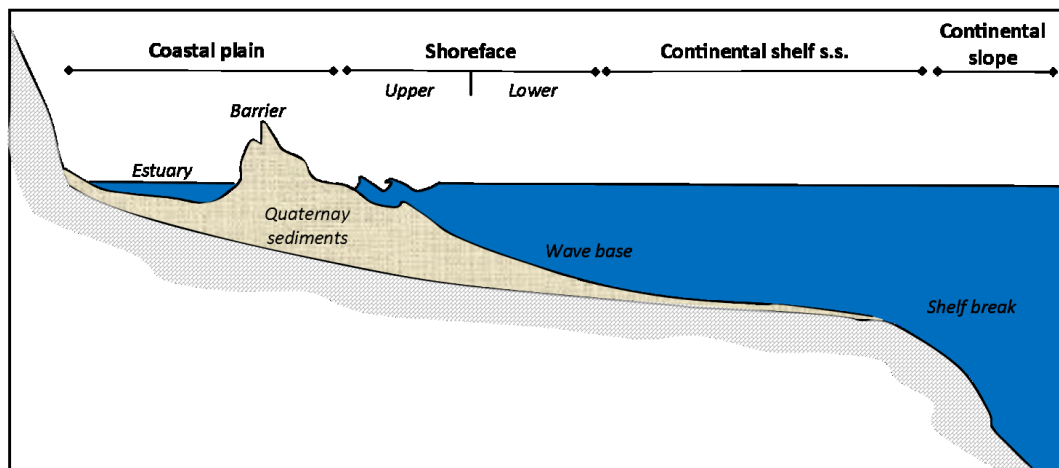


**Fig. 2.1** – Physiographic schematic setting of the continental shelf (modified by Masselink & Hughes, 2003)

The *coastal plain* is an area of flat, low-lying land adjacent to a seacoast and separated from the interior by other topographic features.

The *shoreface* is that portion of the shelf that lies above the low-tide, and which is dominated by swash and backwash of breaking waves. It is the narrow zone seaward from the low watermark in which sand and gravel are moved by the waves and the currents. And in particular, *lower shoreface* refers to the portion of the seafloor that lies below the maximum depth at which a water wave's passage causes significant water motion (*wave base*). Instead, the *upper shoreface* refers to the portion of the seafloor that is shallow enough to be agitated by the wave action.

The *continental shelf s.s.* is a submerged shelf of land that begins at a continental shoreline (lower boundary of the shoreface), slopes downward gradually at an angle of about  $0.1^\circ$  for a variable distance, and ends at the top of a much steeper downward slope (*continental slope*) at an angle of about  $3^\circ$  to  $6^\circ$  until it reaches the ocean floor. The abrupt slope breaking that limits the two areas is mainly controlled by structural factors and isostasy processes of large scale (Southard & Stanley, 1976).

The morphology and stratigraphy of continental shelf areas are controlled by factors, such as global eustatic variations and local morpho-structural and climatic features. Secondly, physical erosion and transportation processes also contribute to modeling superficial sedimentary cover and thus affect the continental shelf physiography.

Although the surface of continental shelf is involved with variable hydraulic conditions, also in short periods of time, it can be considered as an area of dynamic equilibrium.

Here, in absence of relevant sea-level changes, during the sedimentation processes, the sedimentary prism aggrades and the ratio of sediment deposited and transported decreases until the achievement of the base wave. An ideal non-deposition surface (*topset*) tends to form. It is slightly inclined towards the sea, while the depositional area moves towards the deeper areas (continental slope). According to this dynamic process, the time-surfaces assume *clinoform morphology*, typical of shelf deposits (**Fig. 2.2**).

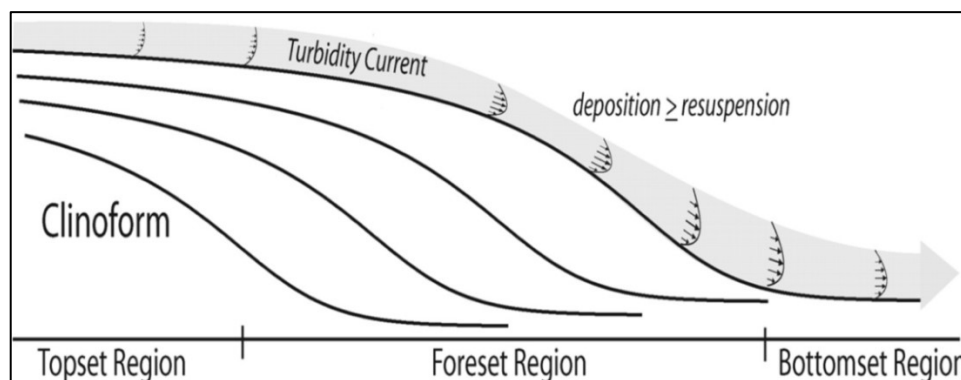


**Fig. 2.2** - Typical *clinoform morphology* in the shelf deposits.

The slope breaking, close to the lower limit of influence of the wave motion, is defined *offlap break*. It separates the *topset region* from the *foreset* that is the steepest portion of the clinoform, where dominate the gravitational mechanisms of transport and deposition (*foreset region*) (Rich, 1951; Mitchum, 1977; Friedman et al., 2001). Towards the sea, the deposition processes consist mainly of the fall-out of fine grain sediments: in this area, the deposits tend to have a sub-horizontal geometry (*bottomset region*).

In function of the physical external conditions, new equilibrium surfaces tend to form. Therefore, the continental shelf consists of several depositional sequences, reflecting the changes triggered by these factors. According to these methods, the continental margins tend to assume a common morphological configuration. The role of the marine geologist is, then, to interpret this configuration, taking into account the different regional structural setting of each continental shelf.

## **2.2 DEPOSITIONAL ENVIRONMENTS: AUTOGENIC AND ALLOGENIC CONTROLS**

Siliciclastic sediments accumulate in wide range of setting, from mountainous areas, through low-lying alluvial-plain and coastal environments, to shallow- and deep-marine setting. The nature of depositional environments and the deposits created within them is a function of many variables, which can be divided in two broad groups.

The first of these are those processes that are intrinsic to the environment and are termed *autogenic*. They are the distinctive physical features of an environment. For example: the fluvial environments are dominated by unidirectional currents and the coasts experience the wave action and tidal current in various combinations. Within each of these settings, the intrinsic processes create a distinctive geomorphology: the currents tend to create channels and the waves produce beaches and shorefaces. Therefore, there is a feedback between the geomorphology, the processes and the available sediment such that particular geomorphic settings are characterized by specific types of deposits.. In particular, the coastal zone and its associated shallow-marine environments are uniquely complex because the interaction of both terrestrial and marine processes. This zone is also especially sensitive to changes in accommodation, as reflected in change in relative sea level (Boyd et al., 1992; Harris et al., 2002). Coastal environments are most commonly subdivided on the basis of the dominant physical process, where the “dominance” is assigned to the process that transports and deposits the greatest volume of sediment because this process is responsible for producing the characteristics of the deposits.

The second group of variables is those that are external to local environment. They include the *accommodation space*, *tectonic setting* and *climate*. These *allogenic* factors



create the broader context in which the environment sits and thereby have an influence on the grain size supplied to the environment, the precise nature of the processes that operate (e.g., the relative influence of wave and tides) and the large-scale evolution of the environment.

- Accommodation: is the space available for the potential sediment accumulation and is the most fundamental control because *the accommodation at any location determines whether sediment accumulates or not* (Catuneanu, 2006). If the accommodation is zero (the equilibrium profile coincides with the sediment surface), the site is an area of sediment bypass with no deposition or erosion. If the accommodation is negative (the equilibrium profile lies below the sediment surface), net erosion occurs. Accumulation can only take place where there is positive accommodation, with deposition occurring until the sediment surface. Eustatic sea-level change, tectonic activity and change in energy level are all phenomena that determine changes in the accommodation space.

- Tectonic setting: it exerts an important control on the nature of the depositional system. In particular: i) it influences the features of the source area and the steepness of the transport system; ii) it determines the spatial distribution of the subsidence and accommodation, influencing also the grain size of the sediments.

- Climate: it determines the siliciclastic sedimentation, because influences the rate of the erosion and deposition through its control on the temperature (Allen, 1997). The variation in sediment supply produced by climatic changes can cause rivers to incise and can produce an alternation in fluvial style between braided and meandering (Blum and Tornqvist, 2000). The climate, as governed by astronomically determined changes in solar insolation (Milankovitch cyclicity), also drives eustatic sea-level change.

### **2.3 SEQUENCE STRATIGRAPHY**

Sequence stratigraphy began almost 70 years ago when Sloss et al, (1949) coined the term sequence for a stratigraphic unit bounded by large-magnitude, regional

unconformities which spanned most of North America. Wheeler (1957, 1958) proposed, instead, a model building to provide a theoretical foundation for the development of unconformities and consequent sequences. It was not until the early 1960s that Sloss (1963) fully developed the concept and named six sequences which occurred throughout North America. Sloss (1963) recognized the major unconformities that bounded the sequences through empirical science and he interpreted as tectonic uplift episodes. In summary, by the mid-1960s, sequence stratigraphy was characterized by two separate approaches, one of data-driven empiricism as exemplified by the work of Sloss (1963) and the other of model-driven deduction as used by Wheeler (1957, 1958).

In 1970s, the first seismic data refresh the sequence stratigraphy concept. In fact, the seismic stratigraphy is defined as perhaps best way to study the sequence stratigraphy. Vail et al., (1977) demonstrated, through the use of seismic sections, that the sedimentary record consists of a series of units that are partially bound by unconformities (Vail et al, 1977). These units were termed “depositional sequences”. Shortly after, Mitchum et al., (1977) modified the *sequence* definition, specifying “bounded by unconformities or their correlative conformities”, where an *unconformity* is defined as a stratigraphic surface across which there is a significant gap in the stratigraphic record. Salvador (1994) specifies that the unconformity is a change in depositional trend from deposition to non-deposition and back again to deposition, and adds that it can also be created by submarine erosion or by non-deposition alone.

Finally, Catuneanu (2011) defines the actual concept of the sequence stratigraphy, defining it as a methodology that provides a framework for the elements of any depositional setting, facilitating paleogeographic reconstructions and the prediction of facies and lithologies away from control points. The sequence stratigraphic framework also provides the context within which to interpret the evolution of depositional systems through space and time.

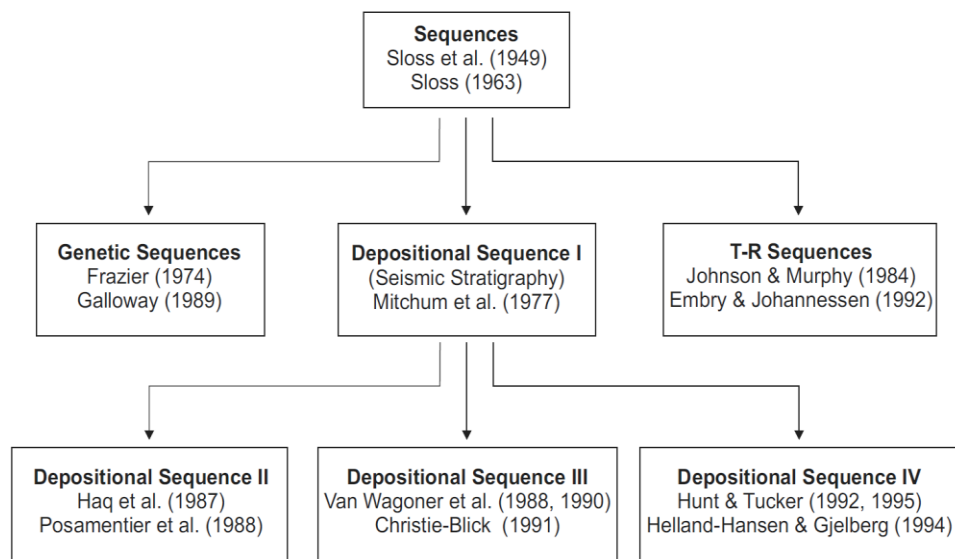


**Fig. 2.3** - Evolution of sequence stratigraphic approaches (from Catuneanu et al. 2010).

Although the stratigraphic-sequential method is of common use in stratigraphic analyzes and despite some concepts are largely recognized in literature, a unique model is not currently accepted and used. This reflects the existence of a variety of alternative approaches (Fig. 2.3). Researchers usually choose the conceptual model that is best adapted to the depositional system they are studying, which naturally has led to a multitude of different definitions of the sequence stratigraphic units and surfaces.

### 2.3.1 SEQUENCE STRATIGRAPHIC UNITS

In general, a sequence stratigraphic framework may consist of three different types of stratigraphic units:

- sequences s.s.: *“a succession of strata deposited during a full cycle of change in accommodation or sediment supply”* (Catuneanu et al., 2009);
- parasequences: *“an upward-shallowing succession of facies bounded by marine flooding surfaces”* (Van Wagoner et al., 1988; 1990);
- systems tracts: *“a linkage of contemporaneous depositional systems, forming the subdivision of a sequence”* (Brown and Fisher, 1977).

The definition of these units is independent of temporal-spatial scales and each type of unit is defined by specific stratal stacking patterns and bounding surfaces.

In particular, the systems tracts are interpreted on the basis of stratal stacking patterns, position within the sequence, and types of bounding surface (Van Wagoner et al. 1987, 1988, 1990; Posamentier et al. 1988; Van Wagoner 1995; Posamentier and Allen 1999). A systems tract consists of a relatively conformable succession of genetically related strata bounded by conformable or unconformable sequence stratigraphic surfaces.

The system tracts are commonly interpreted to form during five specific phases of the relative sea-level cycle (Posamentier et al. 1988; Hunt and Tucker 1992; Posamentier and Allen 1999; Catuneanu 2006; Catuneanu et al. 2009) (**Fig. 2.4**):

**1. Falling-Stage Systems Tract (FSST):** includes all the regressional deposits that accumulated after the onset of a relative sea-level fall and before the start of the next relative sea-level rise. The FSST is the product of a forced regression and lies directly on the sequence boundary, capped by the overlying lowstand systems tract sediments.

**2. Lowstand Systems Tract (LST):** includes deposits that accumulate after the onset of relative a sea-level rise. This systems tract lies directly on the upper surface of the falling stage systems tract and is capped by the transgressive surface formed when the sediments onlap onto the shelf margin;

**3. Transgressive systems tract (TST):** comprises the deposits that accumulated from the onset of coastal transgression until the time of maximum transgression of the coast, just prior to the renewed regression of the HST. The TST lies directly on the transgressive surface (TS) formed when the sediments onlap the underlying LST and is overlain by the maximum flooding surface (MFS) formed when marine sediments reach their most landward position.

**4. Highstand systems tract (HST):** Comprises the progradational deposits that form when the sediment accumulation rates exceed the rate of increase in accommodation space. This HST constitutes the upper systems tract of a stratigraphic sequence, and lies directly on the maximum flooding surface (mfs) formed when marine sediments reached

their most landward position. This systems tract is capped by the subaerial unconformity (1999).

**5. Regressive System Tract (RST):** lies above a TST and is overlain by the initial transgressive surface of the overlying TST. The sediments of this systems tract include the HST, FSST and LST systems tracts defined above. The complete sequence is known as a Transgressive-Regressive (T-R) Sequence (Johnson and Murphy 1984; Embry and Johannessen 1992).

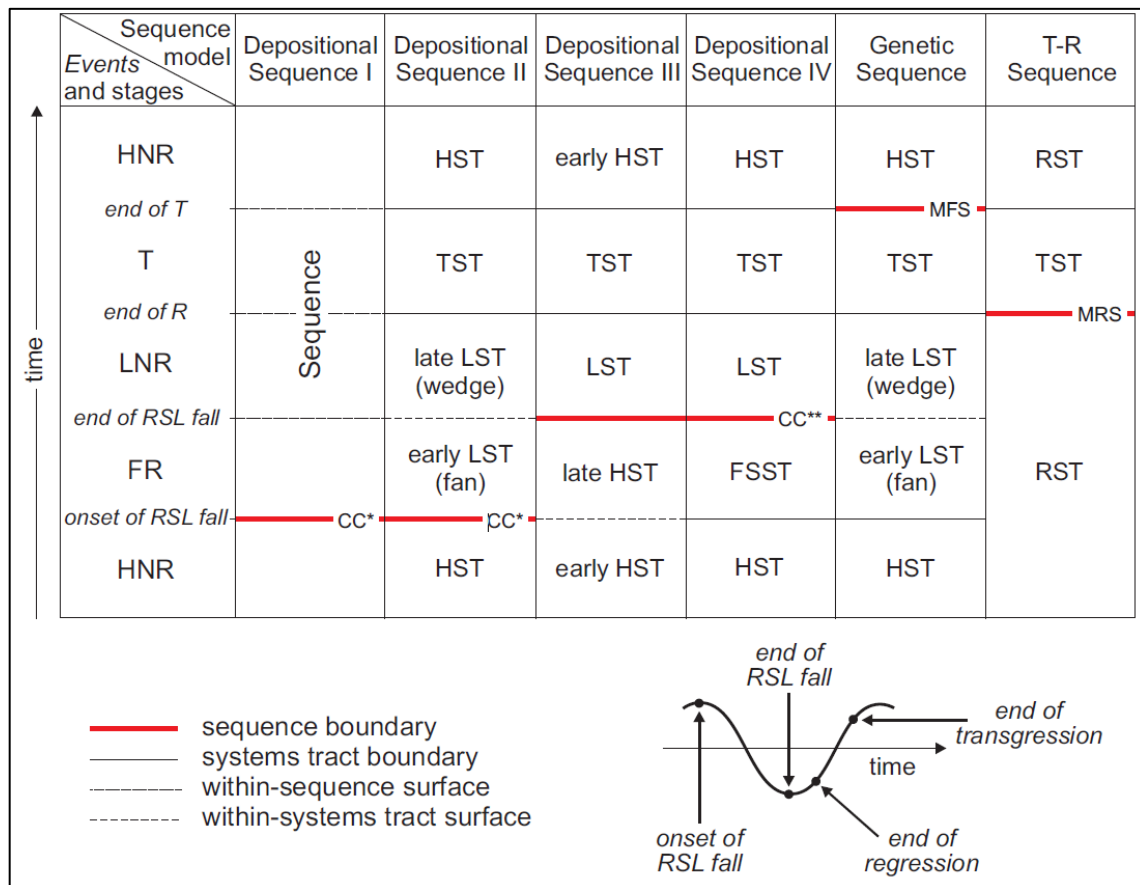


**Fig. 2.4 - Nomenclature of systems tracts, and timing of sequence boundaries for the various sequence stratigraphic approaches (modified from Catuneanu et al. 2010).** Abbreviations: RSL – relative sea level; T – transgression; R – regression; FR – forced regression; LNR – lowstand normal regression; HNR – highstand normal regression; LST – lowstand systems tract; TST – transgressive systems tract; HST – highstand systems tract; FSST – falling-stage systems tract; RST – regressive systems tract; T-R – transgressive-regressive; CC\* – correlative conformity in the sense of Posamentier and Allen (1999); CC\*\* – correlative conformity in the sense of Hunt and Tucker (1992); MFS – maximum flooding surface; MRS – maximum regressive surface. References for the proponents of the various sequence models are provided in Fig. 3 (Catuneanu et al., 2011).

### 2.3.2 SEQUENCE STRATIGRAPHIC SURFACES

Sequence stratigraphic surfaces mark the changes in stratal stacking pattern. They are surfaces that can serve as systems tract boundaries. Unconformable sequence stratigraphic surfaces typically have a physical expression and the main are: *subaerial unconformity*, *correlative conformity*, *the maximum flooding surface*, *maximum regressive surface*, *transgressive ravinement surfaces* and *regressive surface of marine erosion*.

The *subaerial unconformity* forms under subaerial conditions as a result of fluvial erosion or bypass, pedogenesis, wind degradation, or dissolution and karstification (Sloss et al., 1949). Subaerial unconformities may form during forced regression, during transgression accompanied by coastal erosion, during periods of negative fluvial accommodation or during relative sea-level fall exposing carbonate platforms and reefs to karstification (Posamentier et al., 1988; Leckie, 1994; Blum, 1994).

The *correlative conformity* is a marine stratigraphic surface that marks the change in stratal stacking patterns from highstand normal regression to forced regression. It is the paleo-seafloor at the onset of forced regression. An alternative term is *basal surface of forced regression* (Hunt and Tucker 1992) (**Fig. 2.5**).

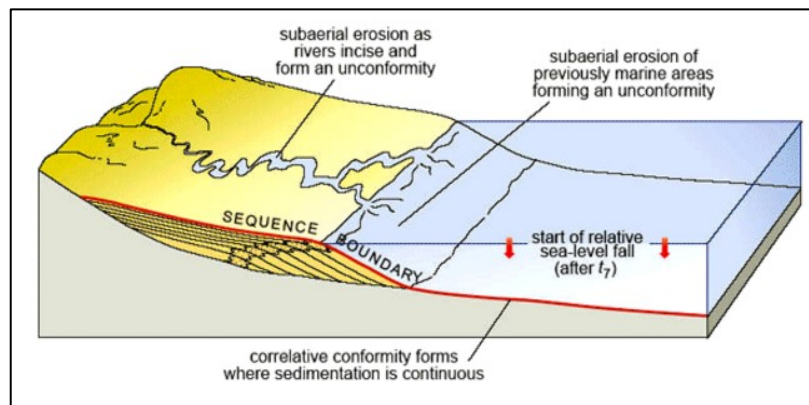


**Fig. 2.5** - *Correlative conformity in the depositional context of the continental shelf (Catuneanu, 2006).*

The *maximum flooding surface* (Frazier 1974; Posamentier et al. 1988; Van Wagoner et al. 1988; Galloway 1989) is a stratigraphic surface that marks a change in stratal stacking patterns from transgression to highstand normal regression. It is the

paleo-seafloor at the end of transgression, and its correlative surface within the nonmarine setting (**Fig. 2.6**).

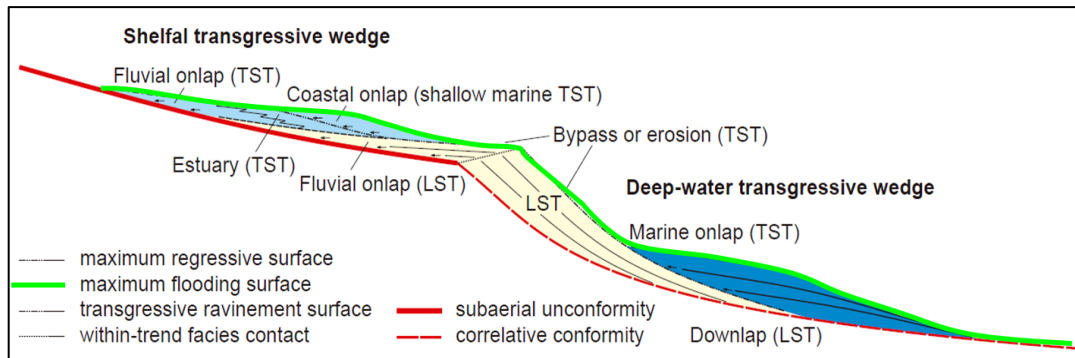


**Fig. 2.6** – The Maximum Flooding Surface (MFS) marks the time of maximum flooding of the shelf and it separates the transgressive and highstand systems tract (Catuneanu, 2006).

The *maximum regressive surface* (Helland-Hansen and Martinsen, 1996) is a stratigraphic surface that marks a change in stratal stacking patterns from lowstand normal regression to transgression. It is the paleo-seafloor at the end of lowstand normal regression.

The *transgressive ravinement surfaces* (Nummedal and Swift, 1987) are erosional surfaces that form by means of wave scouring (wave-ravinement surfaces; Swift 1975) or tidal scouring (tidal-ravinement surfaces; Allen and Posamentier 1993) during transgression in coastal to shallow-water environments. An alternative term for either type of transgressive ravinement surface is the *transgressive surface of erosion* (Posamentier and Vail, 1988).

The *regressive surface of marine erosion* (Plint, 1988) is an erosional surface that forms typically by means of wave scouring during forced regression in wave dominated shallow-water settings due to the lowering of the wave base relative to the seafloor. The regressive surface of marine erosion is diachronous, younging basinward with the rate of shoreline regression. Alternative terms include: *regressive ravinement surface* (Galloway, 2001) and *regressive wave ravinement* (Galloway 2004) (**Fig. 2.7**).

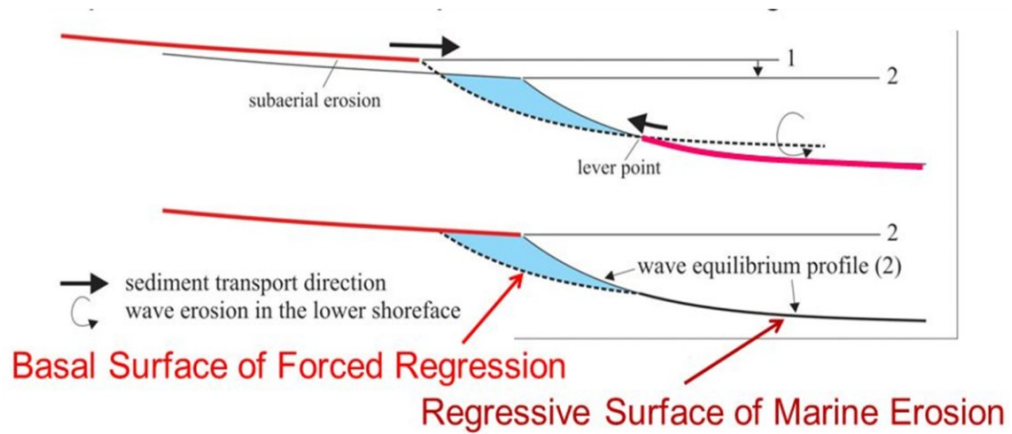


**Fig. 2.7** – Regressive surface of marine erosion is a subaqueous surface of marine erosion formed during a relative sea-level fall.



## **2.4 LATE MIOCENE TO QUATERNARY STRUCTURAL EVOLUTION OF THE LAMPEDUSA ISLAND OFFSHORE**

### **2.4.1 GEOLOGICAL SETTING**

With a surface of 20 km<sup>2</sup>, Lampedusa is the largest island of the Pelagian Archipelago that also comprises the islands of Linosa and Lampione. It is located in the Sicily Channel, within the central Mediterranean Sea, about 210 km south of Sicily (**Fig. 2.8**). The island stretches for 11 km in E-W direction, with tabular morphology, and it reaches the maximum topographic elevation of 134 m a.s.l. in correspondence of Albero Sole Mt, in the northwestern sector. The island is characterized, in its southern and eastern parts, by low-lying coasts, with numerous bays and inlets coinciding with the mouth of valleys cutting the carbonate plateau. Conversely, the northern coast consists of sub-vertical cliffs, up to about 120 m high (Segre, 1960; Grasso and Pedley, 1985, 1988; Buccheri et al., 1999; Giraudi et al., 2004; Baldassini et al., 2015).

Lampedusa lies on the northern edge of the Tunisian continental shelf and represents a small emerged portion of the Pelagian Block (Grasso et al., 1986; Grasso et al., 1990; Buroillet et al., 1978; Winnock, 1981; Giraudi, 2004). This last represents the foreland domain of the Apennine-Maghrebide fold and thrust belt (Colantoni, 1975; Boccaletti et al., 1984; Ben-Avraham & Grasso, 1990; Gardiner et al., 1995; Gamberi and Argnani, 1995; Tavarnelli et al., 2003; Finetti and Del Ben, 2005; Finetti et al. 2005), associated with the Mesozoic collision between African and European plates (Grasso et al., 1999) (**Fig. 2.8**).

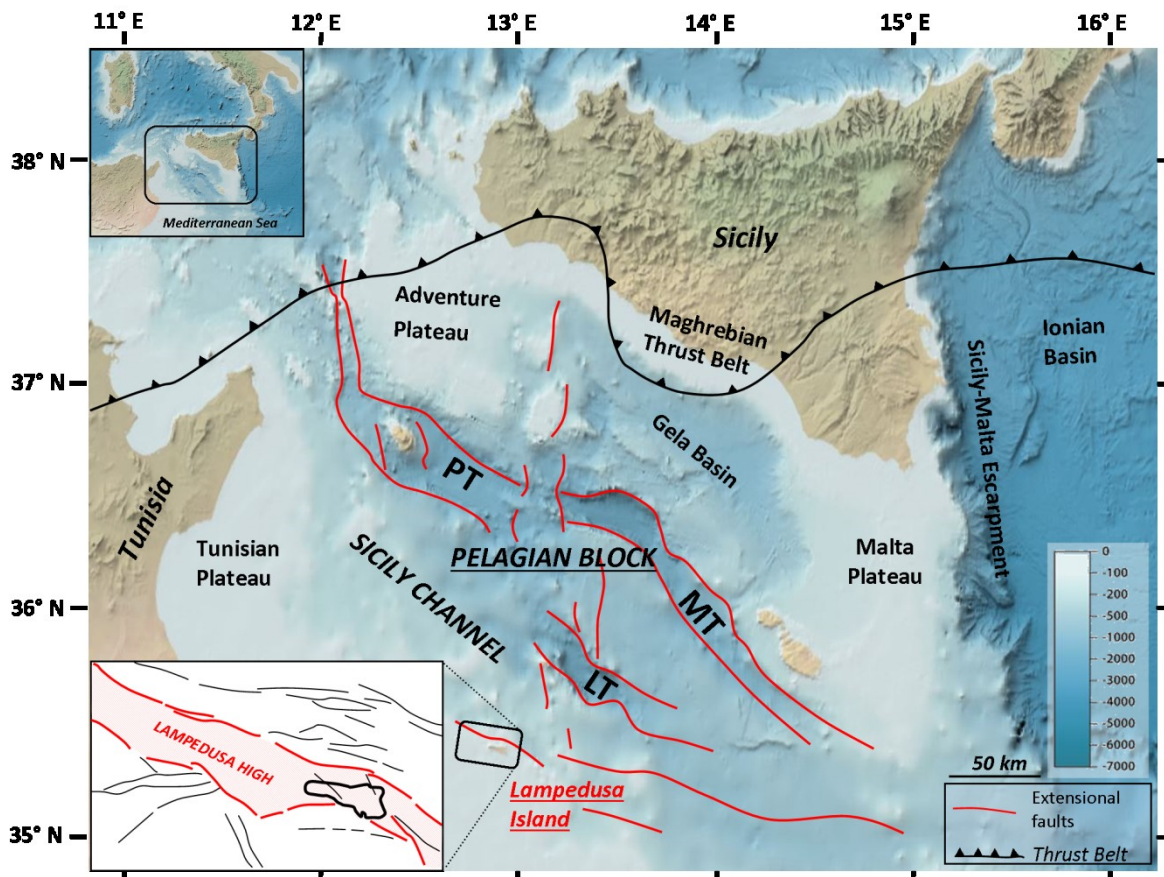


**Fig. 2.8** - Bathymetric (from NOAA: National Oceanic and Atmospheric Administration) and schematic structural map of the central Sicily Channel, with the front (black line) of the Maghrebian Thrust Belt (Colantoni, 1975; Boccaletti et al., 1984, Lipparini et al., 2009). Note the distribution of the WNW, NW and NS-trending normal faults (in red), bounding the main grabens of the area (Pantelleria, Malta and Linosa) (Boccaletti et al., 1987; Cello, 1987; Dart et al., 1993; Catalano et al., 2009; Civile et al., 2015) and the Tunisian and Lampedusa plateaus (Torelli et al., 1995). PT: Pantelleria trough; MT: Malta trough; LT: Linosa trough.

The Sicily Channel is a complex geodynamic sector, where extensional tectonics interacts with the Africa-Europe convergence (Hollenstein et al., 2003; D'Agostino and Selvaggi, 2004; Serpelloni et al., 2007; Catalano et al., 2008). In the specific, the area has suffered two main rifting phases (Antonelli et al., 1988; Argnani, 1990), the youngest of which, occurring since late Miocene, has controlled the evolution of the sedimentary basin where the deposits characterizing the Lampedusa Island formed. During this rifting event, the extensional activity mainly develops through a set of WNW-ESE and NW-SE trending normal faults, dissecting a shallow-water continental shelf (Malta, Tunisia and Adventure plateaus), giving rise to a zone of stretched lithosphere between Sicily and

Tunisia (Reuther and Eisbacher, 1985; Grasso et al., 1990) reported as Sicily Channel Rift Zone (SCRZ) (e.g. Finetti et al., 1984; Boccaletti et al., 1987).

The SCRZ normal faults, associated to a dextral strike-slip regime (Boccaletti et al., 1984, 1987; Cello et al., 1985; Reuther and Eisbacher, 1985; Reuter et al., 1993) and dissected by transverse N-S oriented normal faults, bound three main troughs (Pantelleria, Linosa and Malta) (Cello, 1987; Dart et al., 1993; Boccaletti et al., 1987; Corti et al., 2006; Catalano et al., 2009; Civile et al., 2010), interpreted as pull-apart basins (Boccaletti et al., 1984, 1987; Cello et al., 1985; Reuther and Eisbacher, 1985; Cavallaro et al., 2016).

As far as the Neogene to Quaternary structural evolution of the Lampedusa offshore concerns, Torelli et al. (1995) show that it was largely affected by extensional tectonics, which produced differential uplifted and subsided areas. The latter authors recognize in the Lampedusa High (**Fig. 2.8**), bounded by WNW-ESE and NW-SE trending extensional faults, the most prominent structural high of the Sicily Channel. In particular, the Lampedusa High is bounded, on its eastern part, by the NNW-SSE Cala Creta fault (Grasso and Pedley, 1985), which is interpreted as a late Miocene syn-sedimentary transtensional structure, locally connected with an oblique left lateral motion (Jongsma et al. 1985).

From a stratigraphic point of view, the Lampedusa Island shows similar features with respect to the Hyblean Plateau (Patacca et al., 1979; Grasso & Lentini, 1982; Dall'Antonia et al., 2001) and the Maltese islands (Baldassini & Di Stefano, 2015, 2017). In the specific it is made up of the Lampedusa Formation (Grasso and Pedley, 1985), a late Miocene (Tortonian to lower Messinian) neritic carbonate succession (Winnock, 1981) slightly tilted southwards, which is covered by lower Pleistocene calcarenite and upper Pleistocene sand deposits (Grasso & Pedley, 1985, 1988). The Lampedusa Formation includes three distinct members, which have been lithologically described and chronostratigraphically framed by Grasso and Pedley (1985) (**Fig. 2.9a**): the oldest is the Cala Pisana Member (made up of coarse grained wackstones, packstones and grainstones, Tortonian in age), which crops out in the eastern and southern portions of the island and represents the pre-rift deposits (Grasso and Pedley, 1985, 1988); the intermediate is the Capo Grecale Member (made up of carbonate mudstone and

wackstones, late Tortonian in age), which outcrops in eastern, southwestern and in the central portions of Lampedusa, unconformably overlying the Cala Pisana Member, and represents the syn-rift deposits (**Fig. 2.9b**); the youngest is the Vallone della Forbice Member (made up of grey dolomite packstones to pure dolomite, early Messinian in age), which is the thickest member of the Lampedusa Formation and crops out in the central part of the island, representing the syn-rift succession. The latter formation is incised, during late Miocene, by a widespread erosional surface connected with the onset of the Messinian salinity crisis (Hsü et al., 1973, 1977; Rouchy and Caruso, 2006; Roveri et al., 2008, 2012).

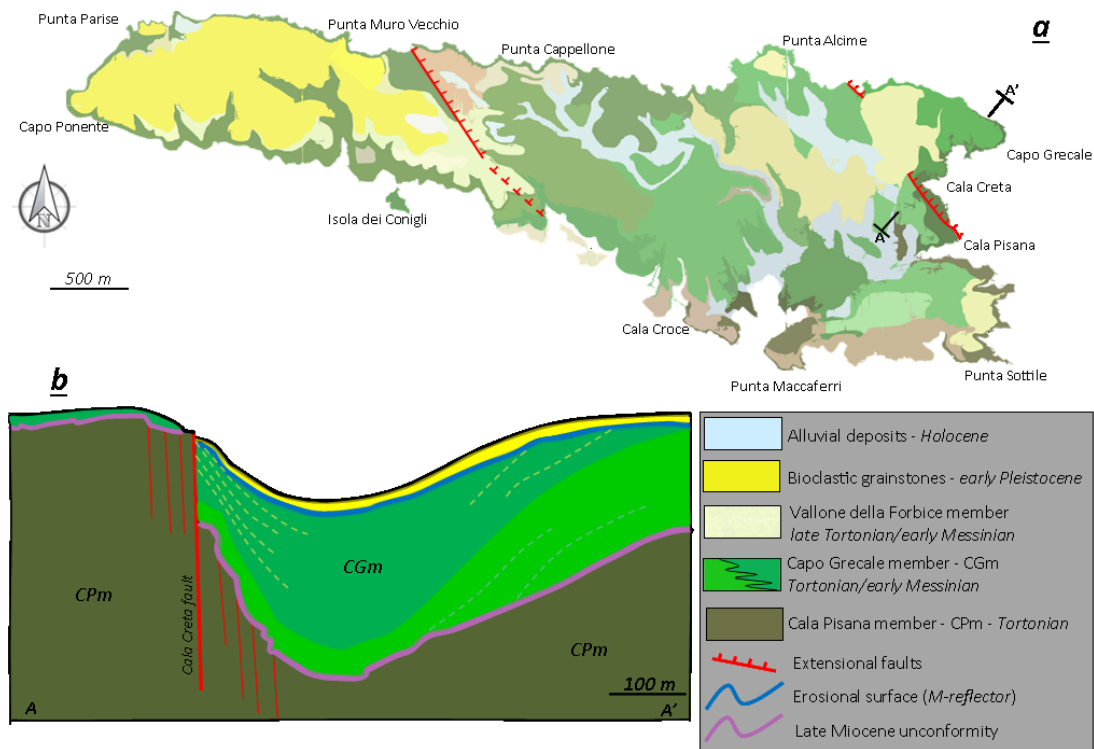


**Fig. 2.9a** - Schematic geological map of the Lampedusa Island (modified after Grasso & Pedley, 1985); note the two main faults outcropping on-shore in Cala Creta and in Punta Muro Vecchio area. **Fig. 2.9b** - NE-SW stratigraphic section in the eastern sector of the Lampedusa Island (modified after Grasso and Pedley, 1985), showing the stratigraphic relationship between the late Miocene (pre- and syn-rift deposits) and Pleistocene post-rift deposits, with in evidence the main unconformities.

In this thesis, through the interpretation of high-resolution seismic profiles, recently (July 2015) acquired in the offshore of the Lampedusa Island, we aim at detailing the current structural evolution of the area and its regional significance.

#### **2.4.2 DATA DESCRIPTION AND INTERPRETATION**

In order to contribute to improving the knowledge concerning the geodynamic scenery of the Sicily Channel we present data from some of the new seismic profiles, which outline the Lampedusa offshore stratigraphic-structural setting. For greater clarity in description, the investigated area has been subdivided into three main sectors: northern, southern and eastern.

In all of the surveyed area, a common feature is represented by a laterally persistent horizon with an erosional character, associated to the Messinian erosional surface ("M-reflector") and highlighted by an intense contrast of acoustic impedance and often truncating the underlying units. The M-reflector separates the late Miocene syn-rift members of the Lampedusa Formation from the Plio-Quaternary deposits. Only in the northeastern sector of the Lampedusa offshore, the M-reflector is cut by tectonic structures. The continuity and sub-parallel setting of the seismic unit above the M-reflector is the evidence of a regular post-Messinian sedimentation that in general healed previously formed topography of the seabed. The latter recognition emphasizes that the Plio-Quaternary units were affected by an early Pliocene extensional tectonic phase only in the northern sector. The map in **Fig. 2.10** shows the reconstruction of the tectonic setting of the Lampedusa Island offshore and the syn-rift depositional basins connected with the late Miocene-early Pliocene rifting phase.

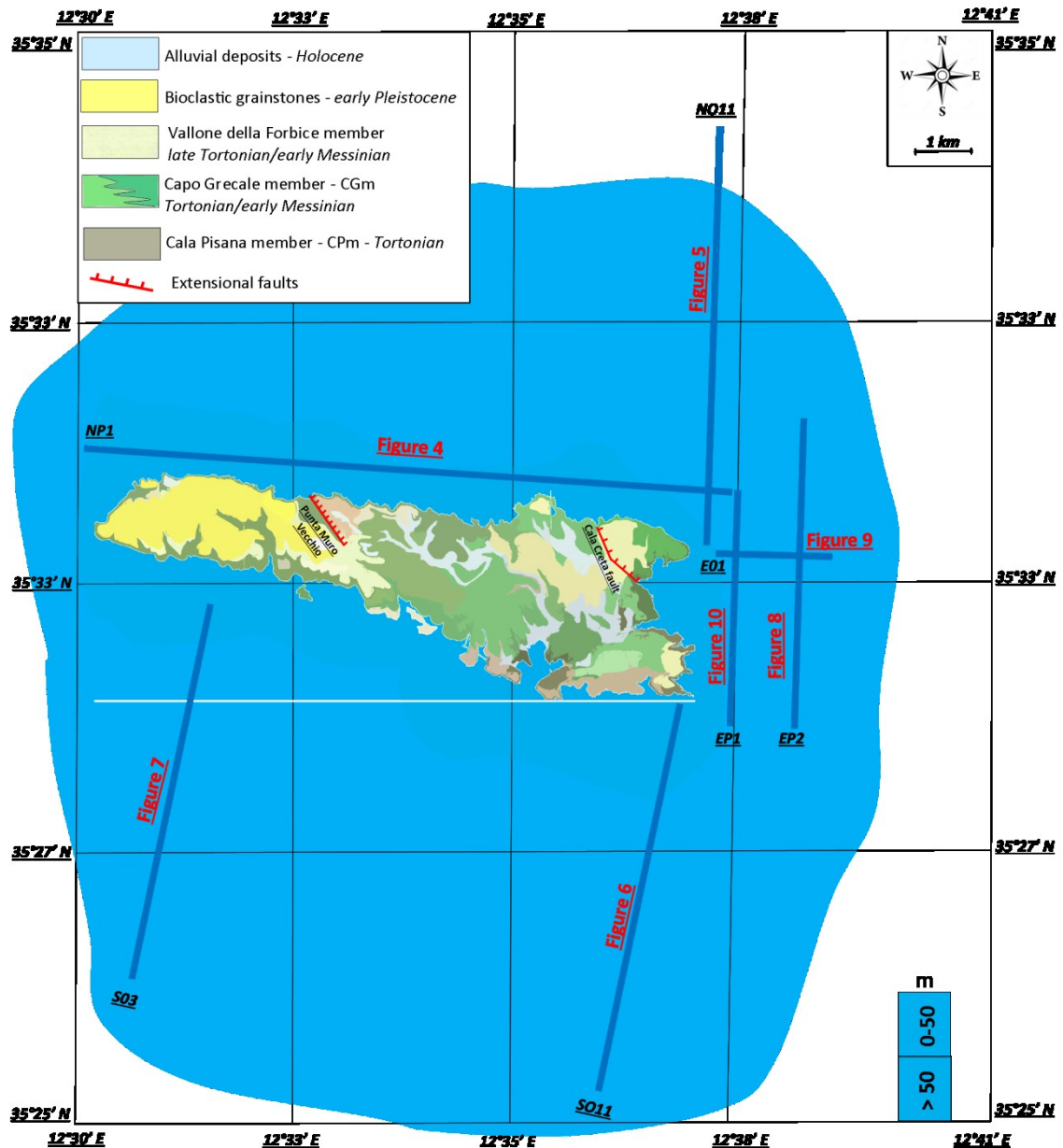


**Fig. 2.10** - Schematic geological map of the Lampedusa Island with location of the seismic grid of the single-channel Sparker seismic reflection lines interpreted in this study.

#### 2.4.2.1 Northern sector

The North Para 1 (NP1) seismic profile is oriented in a W-E direction, running very close to the coastline (**Fig. 2.11A**). The western part of the profile (**Fig. 2.11b**) is dominated by a structural high (H1) bounded to the west by a near-vertical fault dipping westwards, and to the east by a similar structure dipping eastwards. The eastern fault lengthens along the continental shelf for at least 4 km in NW-SE direction, and probably represents the offshore continuation of a normal fault cropping out in the Punta Muro



Vecchio area (**Fig. 3.3**), recognized on land by Grasso & Pedley (1985). As a whole, H1 has an E-W maximum extension of about 2 km.

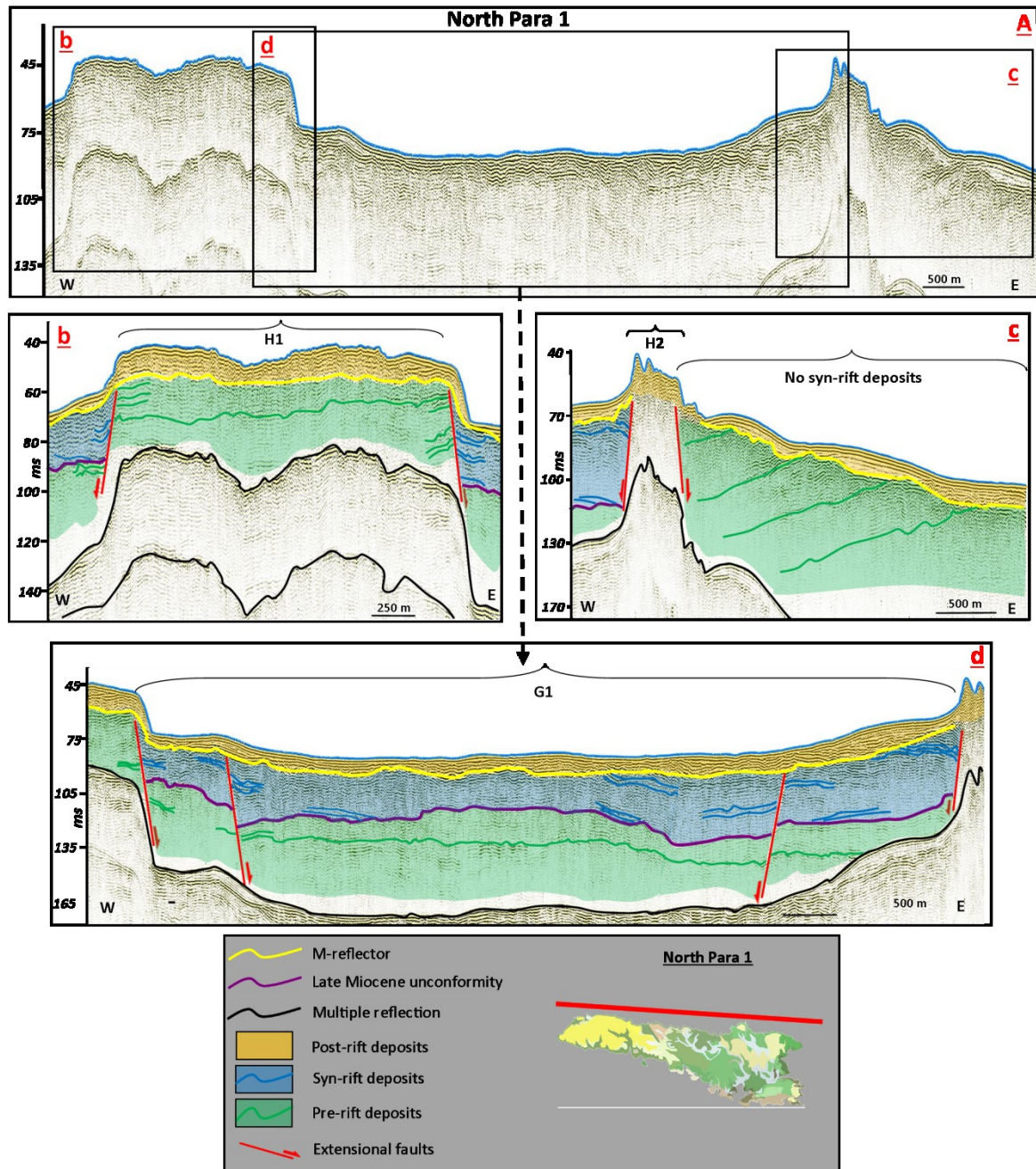


**Fig. 2.11A** - North Para 1 seismic profile. **Fig. 2.11b** - Western portion of the North Para 1 seismic profile, showing the Horst 1 (H1) and the stratigraphic relationships between pre-, syn- and post-rift deposits. **Fig. 2.11c** - Eastern portion of the North Para 1 seismic profile, showing the Horst 2 (H2) and the stratigraphic relationships between the depositional units. **Fig. 2.11d** - Central portion of the North Para 1 seismic profile, showing the Graben 1 (G1) and the stratigraphic relationships between pre-, syn- and post-rift deposits.

In the eastern part (**Fig. 2.11b**) a less developed structural high occurs (H2), showing a W-E extension of about 300 m. This horst is delimited by two sub-vertical normal faults, respectively dipping east- and westwards. The eastern fault, which very likely represents the offshore continuation of the Cala Creta fault (**Fig. 2.10**) (Grasso and Pedley, 1985), extends in NNW-SSE direction for about 2 km in the Lampedusa offshore.

The central portion, delimited by H1 and H2 (**Fig. 2.11d**), represents a structural depression (G1) filled with pre- and syn-rift deposits, cut by two additional normal faults, showing the same trend of the main structures bounding the graben itself. The syn-rift deposits, as expected, show increased thickness close to the normal faults, where they assume wedge shapes, and thin in the axial part of the basin (**Fig. 2.11d**). The seismic facies below the M-reflector is subdivided into two units separated by a prominent unconformity (Late Miocene Unconformity=LMU), highlighted out by a main acoustic horizon (**Fig. 2.11d**) that separates pre- from syn-rift deposits.

The M-reflector does not seem to be affected by the fault activity, and is continuously present both on the horsts and within the graben; above it, the post-rift deposits unconformably lie, showing undisturbed subparallel reflections (**Fig. 2.11d**).

In the eastern part of the profile (**Fig. 2.11c**), the H2 delimits an half-graben, filled with a seismic unit displaying tilted acoustic horizons, dipping 25° to the west and truncated by the M-horizon. We interpret these acoustic facies as pre-rift deposits. The Plio-Quaternary deposits (above the M-reflector) unconformably cover the pre-rift deposits, while syn-rift deposits are absent. The tilting of the pre-rift units is probably associated to the activity of the vertical normal fault bounding the sedimentary basin (**Fig. 2.11c**), which acted before the late Miocene rifting phase.

The North Orto 11 (NO11, **Fig. 2.12A**) seismic profile extends for about 7 km in a S-N direction. In its southern portion, 40° southward dipping horizons occur, truncated by the M-reflector (**Fig. 5b**). These deposits represent the pre-rift succession, and become horizontal northwards, where they are interrupted by a near-vertical tectonic discontinuity (**Fig. 2.12b**). This latter forms a sub-vertical discontinuity dipping to the north cutting the M-reflector with a vertical displacement of about 50 m and represents the southern tectonic boundary of a half-graben (HG1, **Fig. 2.12c**). The latter is approximately oriented NW-SE and filled with post-Messinian sediments up to 50 m thick. It is controlled



by the contemporaneous activity of the fault (late syn-rift deposits), which should be active also during Pliocene, or even in more recent times (**Fig. 2.12c**). The post-rift deposits, directly overlying the M-reflector in the southern area (**Fig. 2.12b**), rest in the basinal area on the late syn-rift deposits.

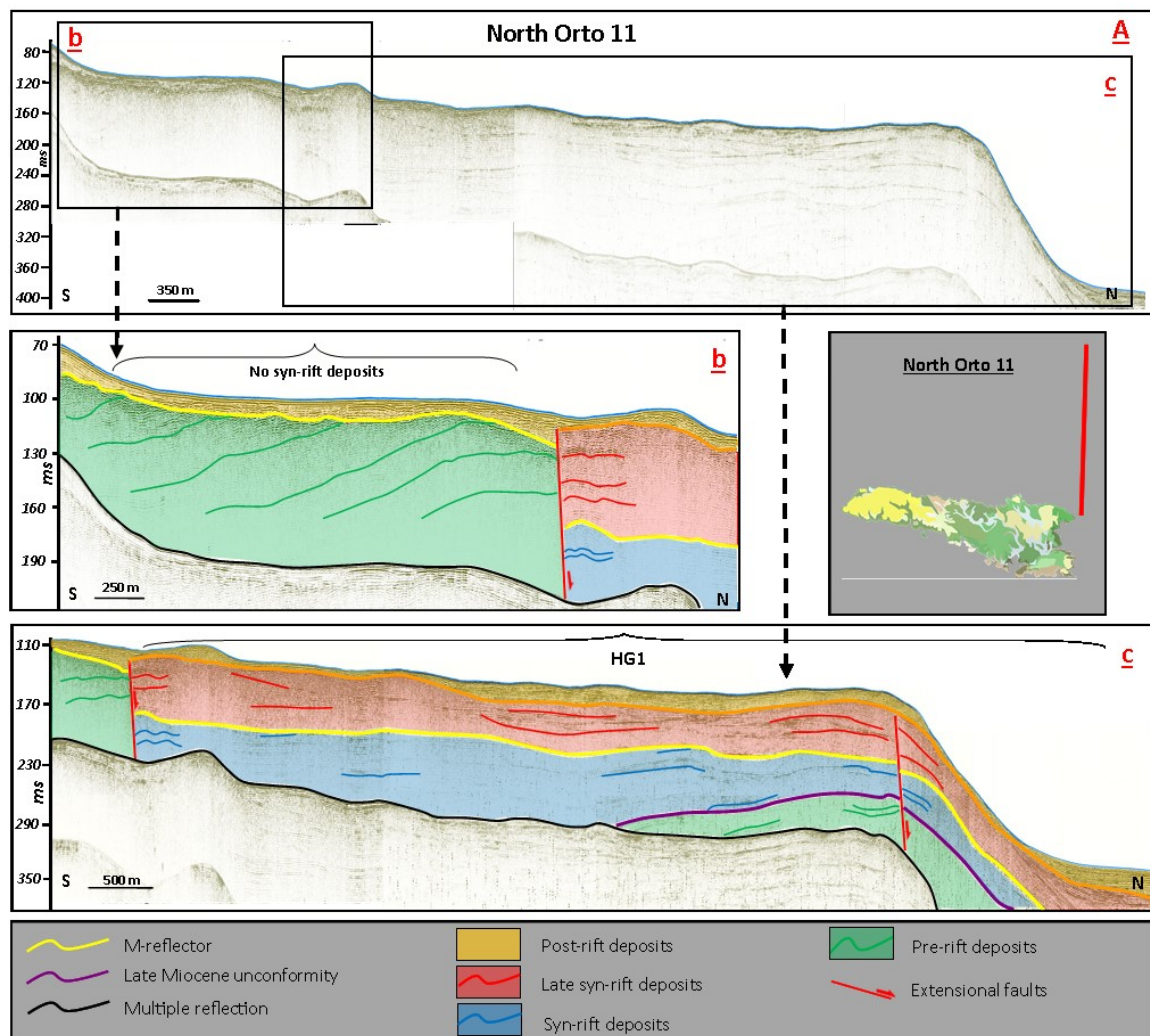


**Fig. 2.12A** - North Orto 11 seismic profile. **Fig. 2.12b** - Southern portion of the North Orto 11 seismic profile: the fault bounds a structural depression, where syn- and late syn-rift deposits occurred. **Fig. 2.12c** - Central and northern portions of the North Orto 11 seismic profile, showing the Half-Graben 1 (HG1) filled with of late syn-rift deposits. The post-rift deposits in the basinal area rest on the late syn-rift deposits.

In the northern part of the line (**Fig. 2.12c**), another normal fault bounds a high seafloor escarpment, coinciding with the continental shelf outer limit. Even this fault cuts the M-reflector involving the Plio-Quaternary deposits.

### 2.4.2.2 Southern Sector

In the South Orto 11 seismic profile (SO11, **Fig. 2.13A**), shot in the south-eastern area with a N-S trend, the seismic facies below the M-reflector is subdivided into two units separated by the LMU. This surface is less evident in the southernmost portion of the profile, due to the low penetration of the seismic signal. Pre- and syn-rift sequences are affected by a set of extensional structures which form, in the whole, a horst-and-graben system (H3 and G2), extended in a NW-SE direction, truncated at the top by the M-reflector. The syn-rift wedge shaped deposits show variable thickness, up to 35 m in correspondence of the tectonic depressions, while they are absent above the structural highs (Fig. 2.13b).

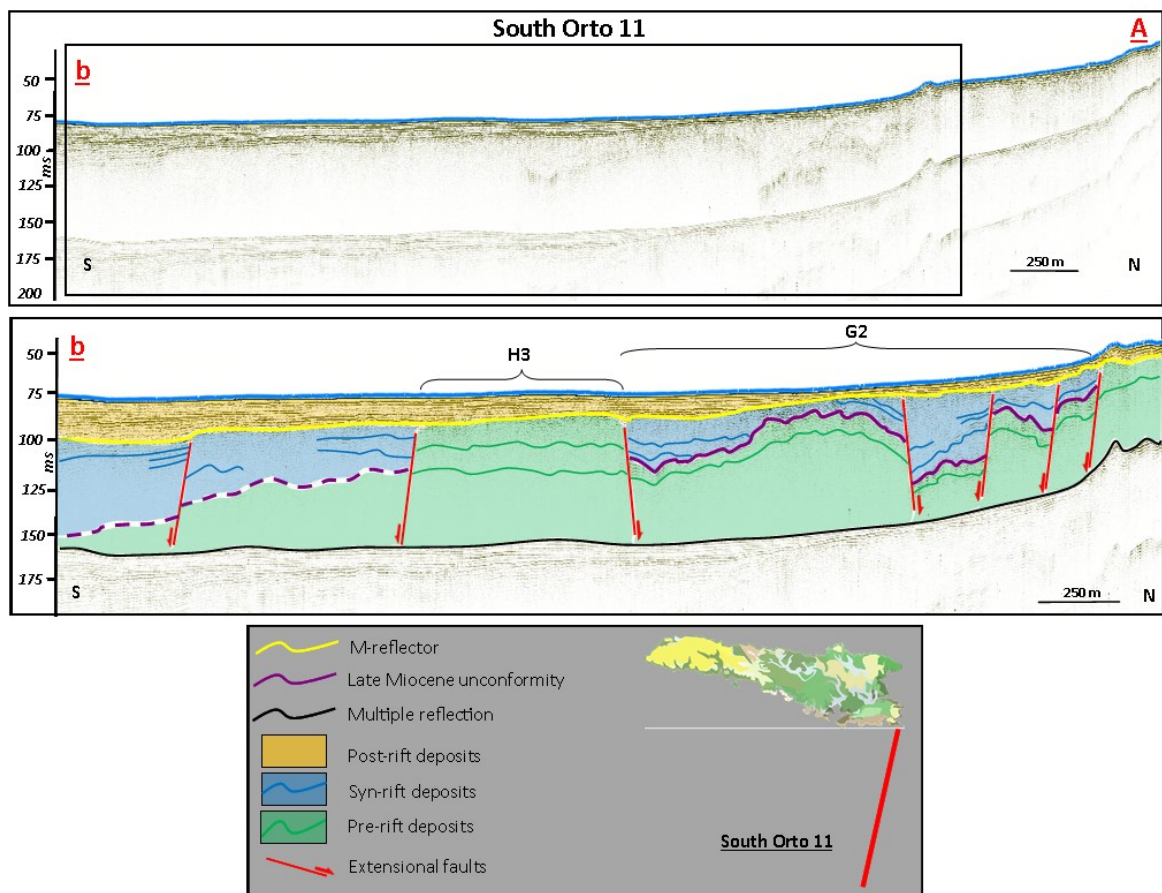


**Fig. 2.13A** - South Orto 11 seismic profile. **Fig. 2.13b** - It shows pre- and syn-rift sequences affected by a set of extensional structures, which form a horst-and-graben system (H3 and G2) truncated at the top by the M-reflector.

Above the M-reflector, the post-rift deposits are characterized by undisturbed parallel acoustic horizons, showing thickness up to about 25 m. The deposition of the

post-rift succession does not reflect pre-Messinian tectonic deformation, displaying their maximum thickness in correspondence of the ancient structural highs.

In the southwestern portion of the Lampedusa offshore, the South Orto 3 seismic profile (SO3, **Fig. 2.14A**) is characterized by N-S dip orientation. Also in this line, it is possible to observe the pre- and syn-rift deposits affected by near-vertical normal faults, which clearly depict a graben structure (G3, **Fig. 2.14b**). The syn-rift deposits are recognizable only in the structural depression, where they reach thickness up to 50 m and are clearly separated from the pre-rift deposits by a well evident LMU.

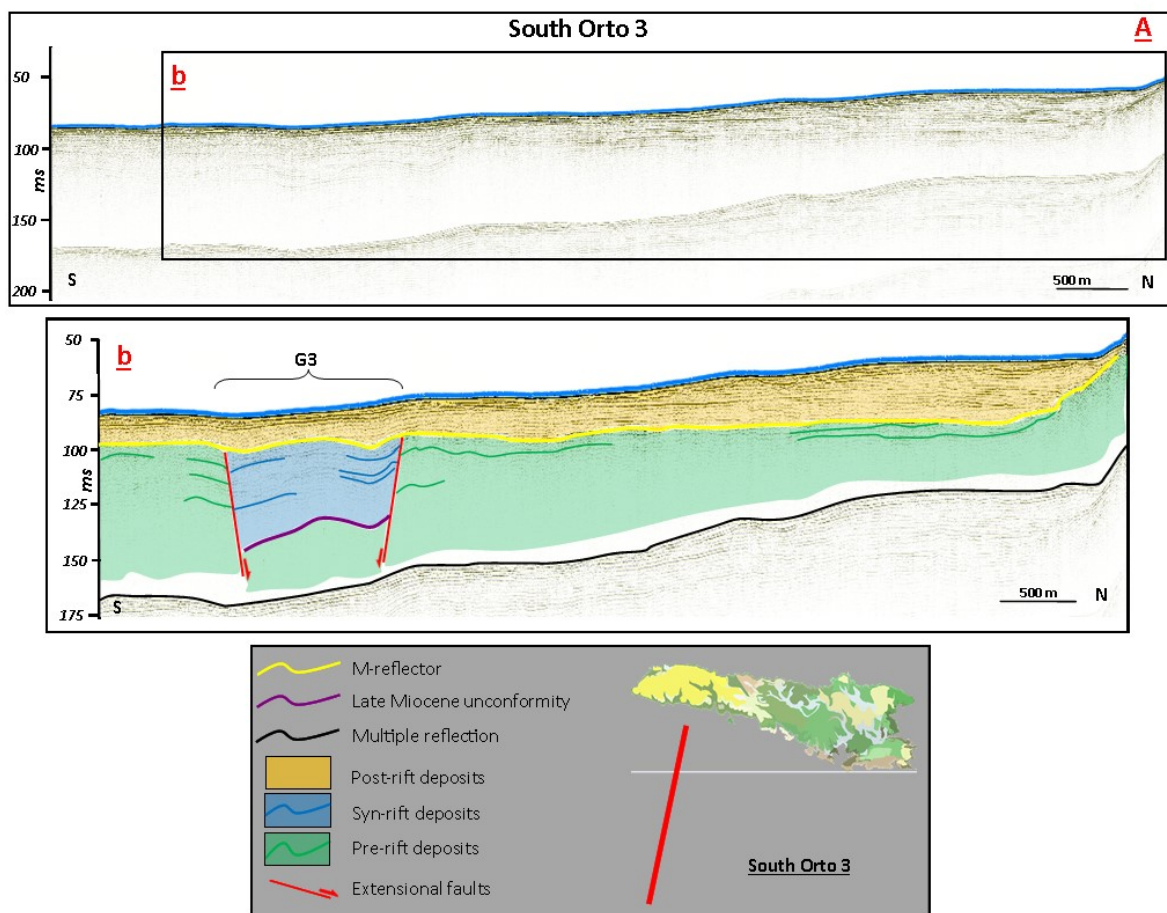


**Fig. 2.14A** - South Orto 3 seismic profile. **Fig. 2.14b** – In this seismic profile is possible to observe the pre- and syn-rift deposits affected by near-vertical normal faults, which depict a graben structure (G3).

This tectono-sedimentary setting is truncated by the M-reflector, which can be followed continuously until the coastline (to the north). Above the M-reflector, the undisturbed post-rift deposits show variable thickness, increasing northwards up to 20 m (**Fig. 2.14b**).



### 2.4.2.3 Eastern sector

The East Para 2 (EP2, **Fig. 2.15A**) seismic profile extends for about 6 Km in a N-S direction. In this line, two normal faults define a structural high southwards, and structural depressions northwards. The two faults delimit a half-graben (HG1) filled with pre- and syn-rift deposits, separated by the LMU, not visible in correspondence of the structural high, where syn-rift deposits are absent (**Fig. 2.15b**).

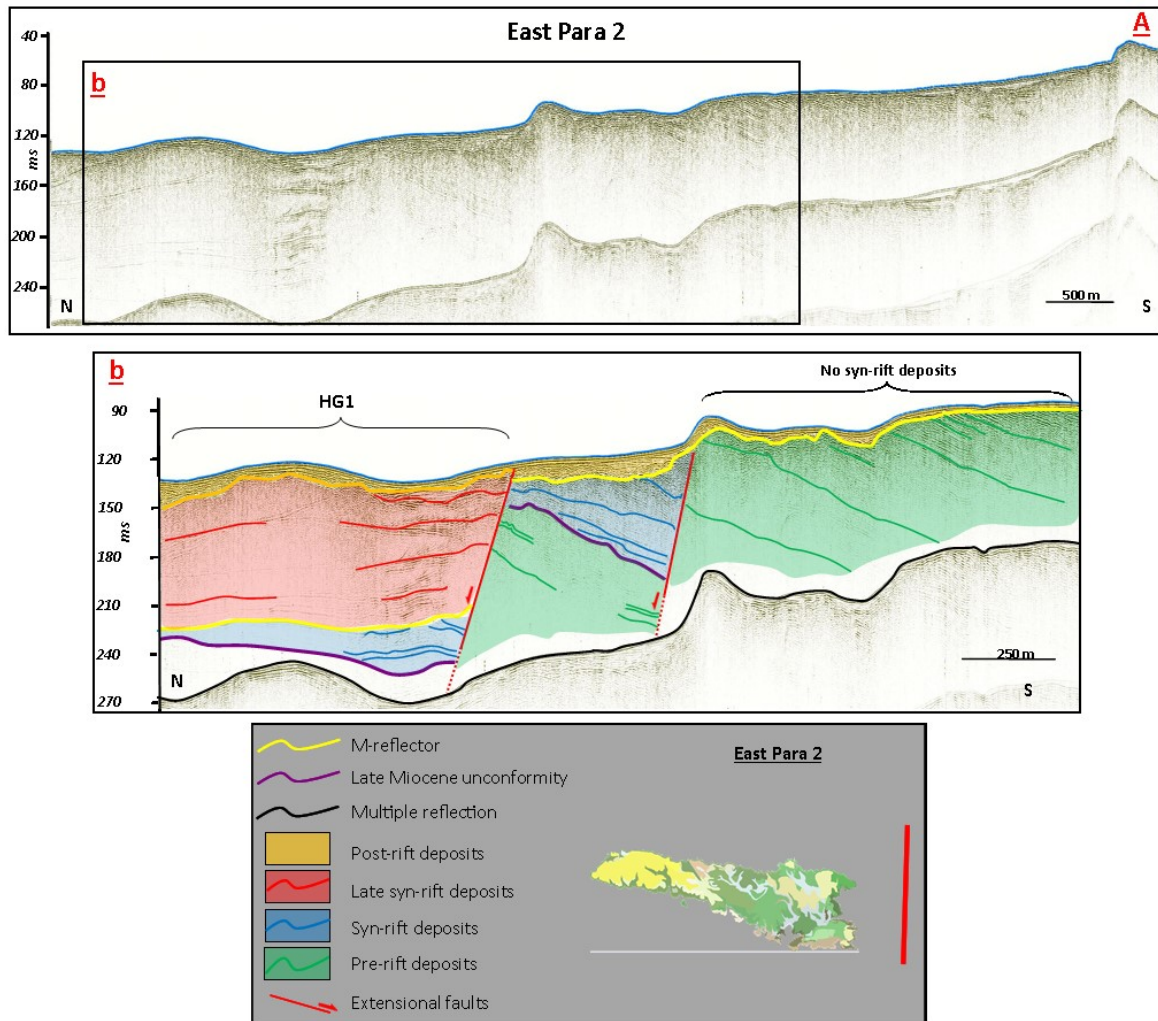


**Fig. 2.15A** - East Para 2 seismic profile. **Fig. 2.15b** – It shows two normal faults delimiting two structural depressions and the northernmost is filled with late syn-rift deposits.

Both pre- and syn-rift sequences show deformed reflections dipping of about 30° to south, probably due to the activity of the faults themselves. The northern fault interrupts the continuity of the M-reflector, with a vertical displacement up to about 70 m, thus indicating that the fault was active also after the Messinian age (see also Profile NO11 in **Fig. 2.15c**). The fault delimits a further structural depression, filled with what we already

called late syn-rift deposits, displaying a wedge shape and a thickness in consistence with the calculated amount of fault displacement recorded along the fault.

The post-rift deposits, from 10 to 5 m thick, unconformably rest on the M-reflector in the southern and central portion, while seem to follow in continuity the late syn-rift deposits (**Fig. 2.15b**) in the northern portion of the EP2 seismic profile.

The most significant element of East Orto 1 (EO1) seismic profile, oriented in a W-E direction (**Fig. 2.16A**), is a normal fault delimiting a structural high to the west and a structural depression to the east. The structural high is exclusively formed by pre-rift deposits, followed by the post-rift deposits, which unconformably rest upon the M-reflector. The structural depression is filled with wedge shaped syn-rift deposits, showing highest thickness close to the fault, separated by the pre-rift deposits by the LMU. Both the pre- and syn-rift deposits are deformed and incised by the M-reflector which cuts the LMU. The overlying post-rift deposits are characterized by a constant thickness of about 5 m (**Fig. 2.16b**).

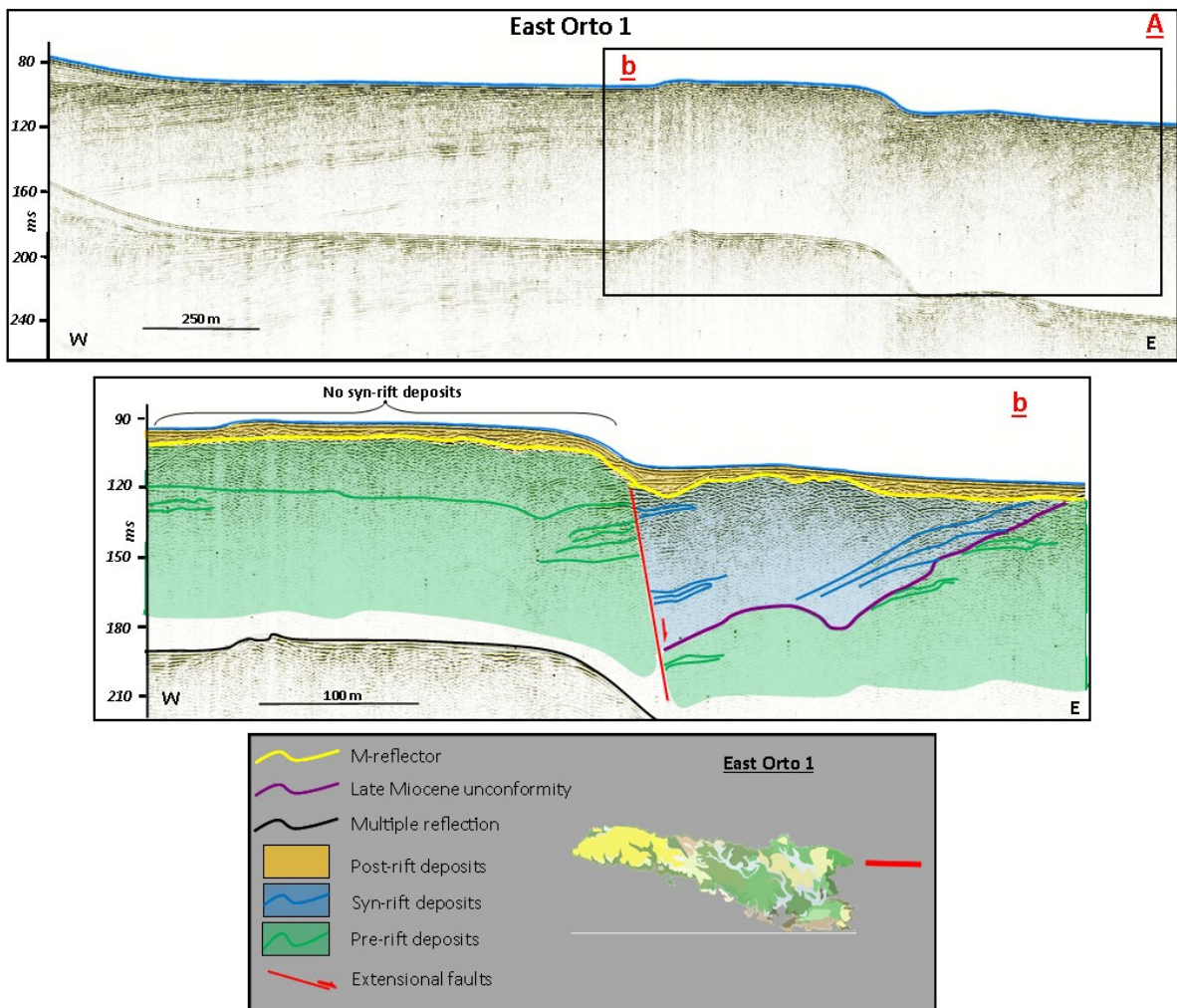


**Fig. 2.16A** - East Orto 1 seismic profile. **Fig. 2.16b** - It shows a normal fault delimiting a structural high to the west and structural depression to the east, filled with wedge shaped syn-rift deposits.

The East Para 1 (EP1) seismic profile, characterized by a S-N orientation (**Fig. 2.17A**), shows structural feature very similar to the previous one. In this line, two normal faults are observable, depicting a structural depression to the north, filled with syn-rift deposits (**Fig. 2.17b**). The southernmost fault probably represents the eastern continuation (at least 3 km) of the Cala Creta fault, outcropping on-land. The structural highs, to the south, are characterized by the pre-rift deposits, which show horizons dipping 10° to the south. The M-reflector is continuously present, delimiting the post-rift deposits.

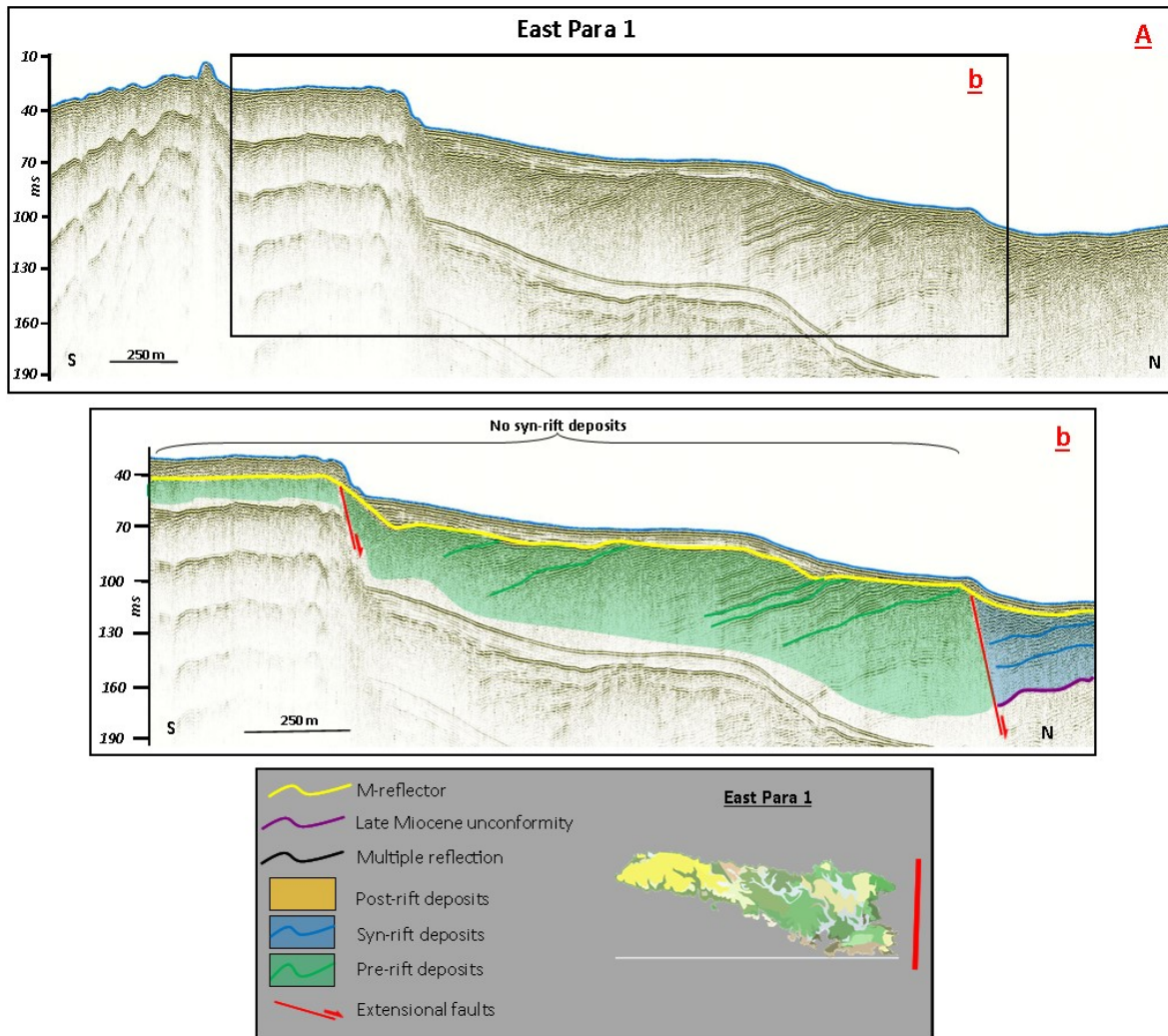


**Fig. 2.17A** - East Para 1 seismic profile. **Fig. 2.17b** - Two normal faults bound a structural depression to the north, filled with syn-rift deposits. The southernmost fault probably represents the eastern continuation of the Cala Creta fault (Grasso and Pedley, 1985).

### 2.4.3 DISCUSSION

The data here presented provide detailed information concerning the structural setting of the Lampedusa offshore, which perfectly fit the wider context of the Sicily Channel Rift Zone, described by previous Authors, deriving by the interconnection between an extensional tectonic regime, coupled with the convergence processes between the African and the European Plates.

In the area south of Lampedusa, the main structures are represented by extensional faults showing a WNW-ESE direction, which define a “horst-and-graben” structural context, characterized by pre- and syn-rift deposits, incised by the Messinian erosional surface. In this area, the post-Messinian deposits seem be unaffected by

tectonic activity. The northern sector is characterized by extensional faults displaying the same orientation, which, on the contrary, displace the Messinian erosional surface, thus indicating that they became active in more recent times.

An additional system of normal faults, with a NNW-SSE orientation and localized in proximity of the northern coastline of the Lampedusa Island (**Fig. 2.18**), represents a second order extensional faults, bounding as well a graben and horst system. Some of these normal faults represent the offshore prosecution of on-land structures (Punta Muro Vecchio and Cala Creta faults).



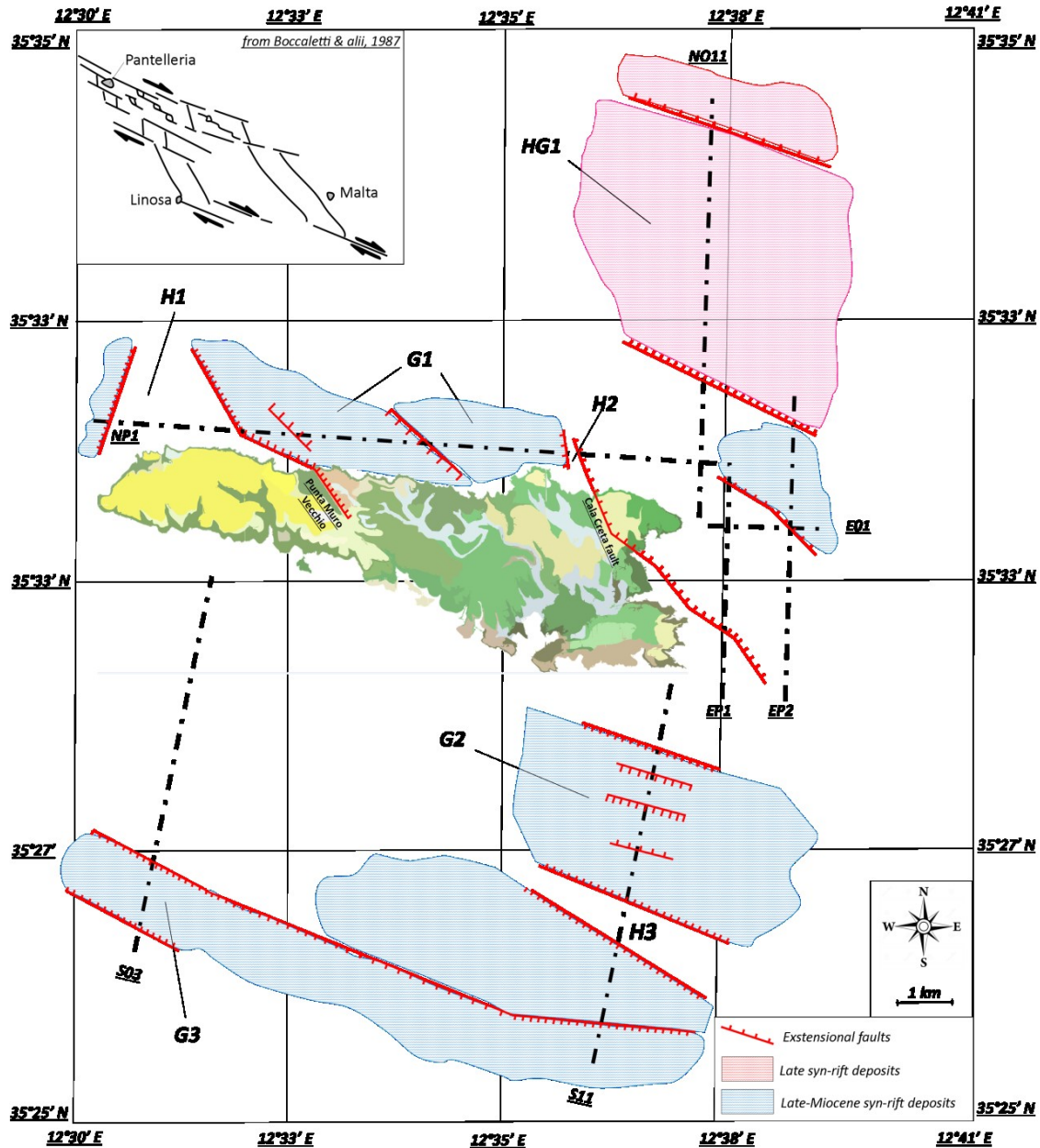


**Fig. 2.18** – Tectonic setting of the Lampedusa Island offshore and the syn-rift and late syn-rift depositional basins connected with the rifting phase. HG: Half-Graben; G: Graben; H: Horst.

In the whole, the proposed tectonic reconstruction, well fits with the model proposed by Boccaletti et al. (1987) and more recently by Catalano et al. (2008), showing WNW-ESE extensional faults, which, associated to the NW-SE convergence characterizing the Sicily Channel area, give rise to a dextral transtensional regime (Boccaletti et al., 1984, 1987; Cello et al., 1985; Reuther & Eisbacher, 1985, Catalano et al., 2008).

In this geodynamic framework, the main faults, combined with NNW-SSE second-order normal structures, originate pull-apart processes, with the development of basinal areas, where the deposition of syn- and late-syn-rift deposits occurred.

As far as the northern sector concerns, our findings match the reconstruction proposed by Torelli et al. (1995) that interpret the extensional faults in the Lampedusa offshore as associated with a late Miocene rifting phase, extended at least up to early Pliocene. On the other hand, the southern sector seems to have suffered an intense tectonic activity until the late Miocene only.

#### **2.4.4 CONCLUSIONS**

Based on the seismo-stratigraphic interpretation of seismic profiles recently acquired around the Lampedusa Island offshore, a more detailed structural framework of the area and its regional significance has been achieved. In addition, the timing of the recent-most rifting phase affecting the region is here provided.

The main results can be synthesized as follows:

1. The pre-Messinian tectonic activity can be depicted as “horst-and-graben” systems, where syn-rift sediments, characterized by a peculiar wedge shape and probably corresponding to the on-land CGM formation, accumulated.
2. The pre-Messinian tectonic phase deformed both the syn- and the pre-rift deposits, probably corresponding to the on-land CPM formation. Pre- and syn-rift deposits are separated by a clear unconformity (LMU), highlighted by a marked acoustic horizon.
3. In the southern sector of the Lampedusa Island, and along the northern coast, the rifting phase was active until the late Miocene, as the structures connected to this event are clearly sutured by the Messinian erosional surface.
4. In the northern sector the rifting phase extends up to the Pliocene; in fact, some normal faults connected with the late Miocene rift, cut the Messinian erosional surface, and bound tectonic depressions, filled with late syn-rift deposits.

5. The post-rift deposits, characterized by horizontal sub-parallel reflectors, unconformably rest on the syn-rift deposits and, in apparent continuity on the late syn-rift deposits. They probably correspond to the bioclastic grainstones deposits exposed onshore.
6. The tectonic setting reconstructed for the investigated offshore areas of the Lampedusa are consistent with the more general context of the Sicily Channel Rift Zone, where main WNW-ESE faults depict a dextral transtensive regime, resulted from the compressive processes linked to the Africa-Europe convergence and the extensional tectonic phase. This geodynamic framework originates pull-apart processes, with the formation of small basinal areas, delimited by second-order N-S oriented normal faults, where the deposition of syn-rift deposits took place.

## **2.5 STRUCTURAL AND STRATIGRAPHIC RECONSTRUCTION OF THE SOUTH-EAST SICILY CONTINENTAL SHELF**

### **2.5.1 GEOLOGICAL SETTING**

In the central Mediterranean Sea, the foreland of the Appennine-Magrebian chain consists of the slightly deformed continental areas of the Pelagian Block (Buroillet et al., 1978, Ben Avraham et al., 1990), belonging to the North African tectonic plate (Roure et al., 1990). The western boundary of the Pelagian Block is represented by a N-S left transcurrent fault, that separates the Atlas folds from the Sahel (Tunisia) underformed areas (Lentini, 2006). The eastern boundary is represented by the Hyblean-Malta escarpment (Grasso and Lentini, 1982), interpreted as a dextral transtensive tectonic system, active also during the Pliocene and Quaternary ages. The relatively undeformed sequences of the Pelagian Block crop out onshore in the Sahel region and in Libia (Lentini, 2006), extend along most of the Sicily Channel - emerging in Lampedusa, Lampione and the Maltese islands - and crop out extensively in the Sciacca area (western Sicily) and in the Hyblean Plateau (eastern Sicily).

The Hyblean Plateau is delimited to the northwest by a NE-SW normal faults system with dip to the NW (Bianca et al., 1999; Lentini and Carbone, 2014). The Gela-Catania foredeep (Torelli et al., 1998; Catalano et al., 2004) developed to the west of the Hyblean Plateau, during the Plio-Pleistocene age (Lentini and Carbone, 2014) being associated with the convergent geodynamic context and the progressive advancement of the allochthonous units of the Appennine-Maghrebides front (Cogan et al, 1989; Grasso and Pedley, 1990), namely Gela Nappe, towards the relatively undeformed foreland units (**Fig. 2.19**).

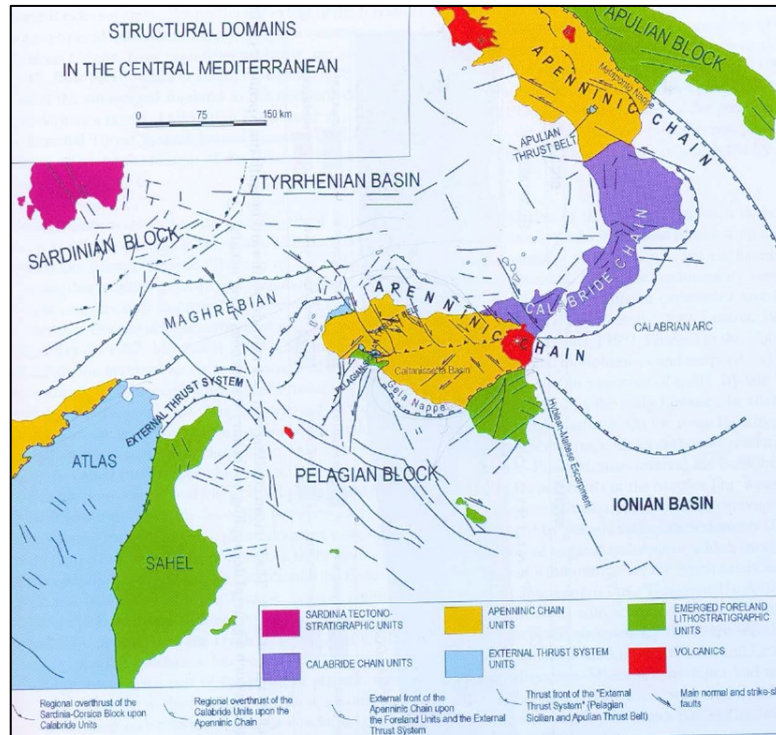


**Fig. 2.19** - Regional scheme of the distribution of the structural domains in the central Mediterranean area (Finetti et al., 2005).

The study area is located in the Marina di Ragusa offshore, along the southeastern coastline of Sicily, in the area that connects the Gela-Catania foredeep to the Hyblean plateau foreland (Fig. 2.20).

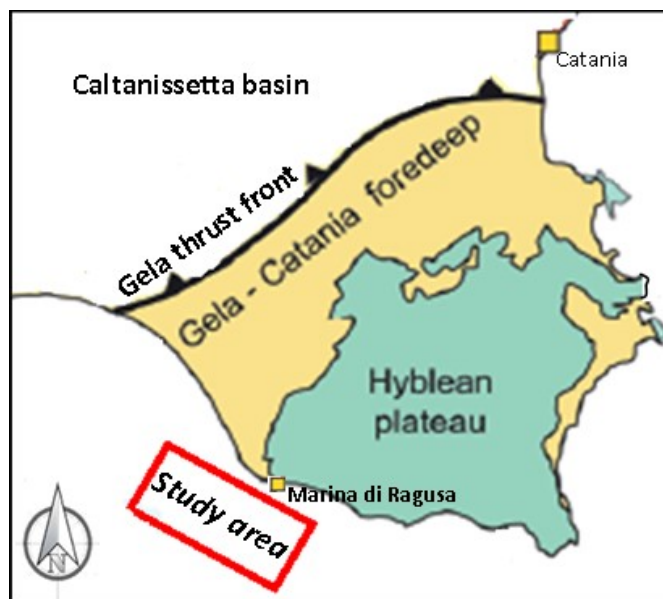


**Fig. 2.20** – Location of the study area in the Sicilian geodynamic context. Modified from Butler et al., 2015.

The Hyblean plateau consists of two morpho-structural elements, the Ragusa Domain and the Siracusa Domain (**Fig. 2.21**) (Carbone et al., 1982, Bonforte et al., 2015). The two sectors are separated by the Tellaro Line interpreted as a left transtensive fault active during lower Pliocene. In turn, the middle part of the Ragusa Altopiano is crossed by the N10° trending Scicli-Ragusa-Irminio (named in the literature also “Scicli Line”) dextral transtensive fault system (**Fig. 2.21**), active during the Early-Middle Pliocene (Ghisetti and Vezzani, 1980).

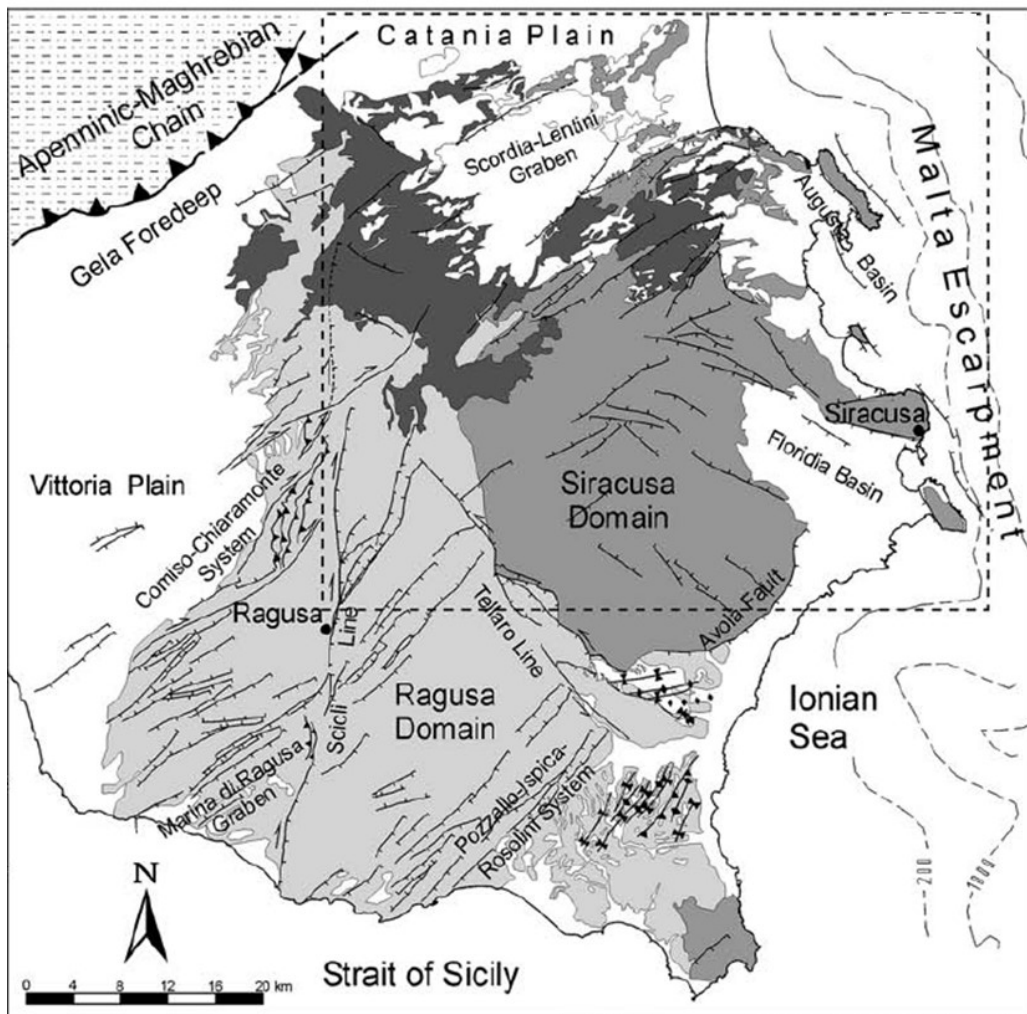


**Fig. 2.21** - Tectonic sketch map of the Hyblean plateau. The Tellaro Line divides two stratigraphic-structural domains: Siracusa and Ragusa Domains. The Scicli Line crosses the Ragusa Altopiano with a N10° trending (by Bonforte et al., 2015).

The geometry of the Scicli Line is the product of a prolonged dextral strike-slip deformation that reactivated a Cretaceous–Late Tertiary fault zone (Grasso and Reuther,

1988; Catalano et al., 2008). In accordance with the current geological models (Catalano et al., 2008), the Scicli Line would play the role of a major transform fault that developed, to accommodate the NE extension affecting the Sicily Channel during the Neogene–Quaternary age, simultaneously to the development of the Pantelleria–Linosa–Malta Rift (Reuther and Eisbacher, 1985; Grasso and Reuther, 1988; Reuther, 1990; Boccaletti et al., 1987) (Fig. 2.22).

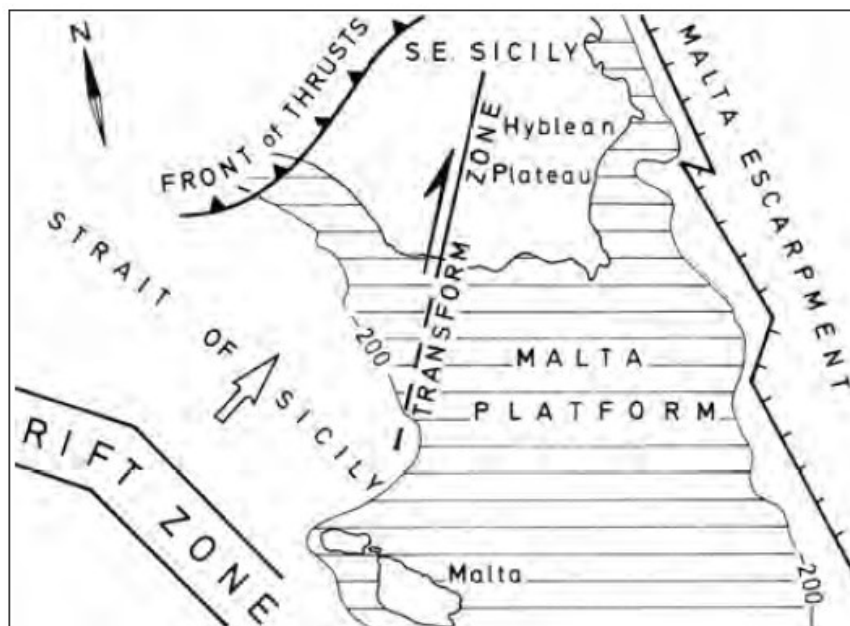


**Fig. 2.22** - Simplified model illustrating the relationships between the frontal wedge of the Apenninic-Maghrebian Chain (Gela Nappe) and the Hyblean plateau as the northern emerged part of the Malta platform. In the regional tectonic context, the Scicli shear zone can be interpreted as a transform link between the neotectonic rift zone and the actual zone of underthrusting. By Lentini and Carbone, 2014.

The sedimentary succession of the Hyblean Plateau is known for a thickness of about 5.5 km (Vizzini 1 well) and mainly consist of thick Triassic-Jurassic platform limestones with some volcanic intercalation and subordinate basinal limestones.

In the following section, a brief stratigraphic synthesis of the Hyblean Plateau foreland sedimentary succession (Lentini and Carbone, 2014) is reported. Since the seismic stratigraphic interpretation of this study shows that the available seismic profiles do not penetrate below the Miocene-Oligocene deposits, the following synthesis will focus only on the units from the late-Paleogene to Pleistocene.

The Ragusa Formation (upper Oligocene – lower Langhian) is divided in two members (Rigo and Barbieri, 1959; Pieri, 1967; Carbone and Lentini, 1967): Leonardo and Irminio. The Leonardo Member consists of calcisiltites and white-grey marls with a total thickness of about 100 m. Upwards, the Irminio member consists of yellow-grey calcarenite and calcirudite with thickness variable from 10 m up to 200 m.

The Tellaro formation (Serravallian-lower Messinian, Rigo and Barbieri, 1959) is characterized by calcisiltite and white-grey marls, with slump intercalations (up to 10 m thick). Its total thickness varies from 50 m up to 400 m. The Tellaro formation is associated locally (e.g. Valle Guffari) with thick volcanoclastic deposits, covered by yellow marls.

The Palazzolo formation (Rigo and Barbieri, 1959) develops in the central sector of the Hyblean Plateau and is laterally heteropic with the Tellaro formation. It consists of calcarenites and marls of lower Messinian age, with a thickness variable from few meters up to 250 m.

The well-known Messinian evaporitic sequence - recording the Messinian salinity crisis (Hsü & alii, 1973, 1977; Rouchy & Caruso, 2006; Roveri & alii, 2008, 2012) – outcrops only in the marginal areas of the Hyblean Plateau. As an example, on the northwestern edge of the Hyblean plateau, an evaporitic succession (limestones and white gypsum with thickness up to 70 m) is present. Similar evaporitic deposits never crop out in the central Plateau (named “horst” by Lentini and Carbone, 2014). In this sector, the Miocene succession ends upwards with the Monte Carrubba Formation that represents a pre-evaporitic deposit.





A general stratigraphic scheme of the evaporitic sequence has been reconstructed for the Caltanissetta Basin (Decima & Wezel, 1971, 1973; Decima et al., 1988, Manzi et al., 2009), also defined “Caltanissetta pit” (Patacca and Scandone, 2004) because it is filled by allochthonous units of the Appenine-Maghrebides front.

In general, the evaporitic sequence consists of (Manzi et al., 2009): (i) a lower composite unit made up of interfingering massive selenite, evaporitic limestone (Calcere di Base Formation) and gypsum turbidites; (ii) an intermediate halite-K-Mg salt unit with a basal marly-anhydritic breccia; and (iii) the Arenazzolo Formations, a thin siliciclastic unit extending over the whole Caltanissetta Basin, unconformably overlying the lower and



intermediate units. A peculiar feature of the evaporitic deposits is their highly lateral heterogeneity and structural complexity due to their deposition within different sedimentary basins. Butler et al., (2015) highlight the variations in evaporite stratigraphies across different thrust-top basins, and how these rapid lateral facies variations have controlled subsequent deformation styles within the Gela Nappe. In fact, in compressional tectonic regimes, numerous studies have stressed the role of evaporitic formations, especially those formed principally of halite, in acting as regional detachment surfaces, and local shear planes thus dictating the style of the deformation.

**Table 2.1** shows the stratigraphic sketch of the middle Miocene-Pleistocene Hyblean foredeep-foreland succession (offshore sector).

Units	Main reflectors	Formation	Age		
P7		Argo formation	middle Pleistocene	Plio-Pleistocene succession	
P6					
P5		Ponte Dirillo formation	middle Pliocene upper Pleistocene		
P4					
P3					
P2		Trubi Formation	early Pliocene		
P1					
					
M4		Gessoso-Solfifera Formation: Upper Gypsum unit	upper Messinian		Oligo-Miocene succession
					
M3		Gessoso Solfifefa Formation: Lower Composite Unit	middle Messinian		
					
M2		Tellaro and Palazzolo formations	Serravallian- lower Messinian		
					
M1		Ragusa Formation	upper Oligocene- lower Langhian		

**Table 2.1** - Stratigraphic sketch of the middle Miocene-Pleistocene Hyblean foredeep-foreland succession (offshore sector) on the basis of the stratigraphic reconstruction of various authors (Lentini and Carbone, 2014; Ghielmi et al., 2012). The names of the stratigraphic units and the main reflectors identified in the seismic profiles discussed in this thesis are also reported in this table.

Following the Messinian, during the first part of early Pliocene, the Gela Basin (GB), located west of the Hyblean Plateau area, is affected by no deposition or subaerial

erosion and is still included in the Hyblean and Sicily Channel forelands. Thin intervals (10-20 m) of transgressive grey-whitish fossiliferous marls of the Trubi Formation were deposited only in a relatively limited onshore areas north around Gela (Ghielmi et al., 2012).

During this time interval (the Intra-Zanclean Phase), an important contractional deformation event caused an episode of rapid subsidence of the GB area, controlled by the flexural subsidence induced by active thrust advancement in the southern Apennine chain connected with the dynamics of the plate subduction. Several areas of the GB rapidly passed to an open-marine environment with sedimentation of the Trubi fossiliferous marls (average thickness of 40-60 m). A hiatus, probably due to condensation/non-deposition in a marine environment, has been recognized on the top of the Trubi formations and interpreted in Ghielmi et al., 2012 as a tectonically driven unconformity, widely recognized in the Central Mediterranean Sea (Zijderveld et al., 1986).

After the deposition of the Trubi, over the whole GB, the Ponte Dirillo Formation consists of 20-70 m of middle Pliocene grey-green fossiliferous clays deposited in the foreland area. Subsequently, another middle Pliocene deformative event caused the reactivation of the high-angle faults of the carbonate substratum with the rapid subsidence and tilting of large sectors of the Hyblean Plateau. The main consequence of this tectonic event is an abrupt deepening of the foreland ramp and the establishment of widespread deep-water conditions along the Gela-Catania foredeep. As a consequence, from the middle Pliocene-to-Holocene, relatively thick section of marine grey and grey-green clays of the Ponte Dirillo Formation were deposited with draping geometry on the foreland ramp and foreland of the GB.

During lower Pleistocene, the advancement the Gela Nappe towards the south and the southeast determines the deposition of turbidite sands and clays of the Sabbie di Irene formation in the GB foredeep, to the west of the study area. On the basis of the available seismic and well data, the Sabbie di Irene Formation turbidites have been attributed to a highly-efficient turbidite system (Mutti et al., 1999) that achieves its maximum development (thickness up to 900 m) in the main offshore depocenter located south of the Gela Nappe. Instead, in the onshore depocenter, north of the town of Gela,

the sand-rich turbidites (thickness up to 100 m) have been referred to poorly-efficient turbidite systems fed by different areas of the Gela Nappe. During middle Pleistocene, the deposition of the turbidite deposits (clays and sands) continues, and it is attributed to Argo Formation (thickness up to 1300 m), bounded at the base by an unconformity of tectonic origin. Mass-transport deposits (mainly represented by slumps) are often intercalated in the middle-upper Pleistocene foredeep succession of the Argo Formation (Patacca and Scandone, 2004; Ghielmi, et al., 2009; Ghielmi et al., 2012).

There are several reasons that have motivated the acquisition of new seismic profiles in the Marina di Ragusa offshore, along the southeastern coastline of the Sicily: i) the improvement of the knowledge concerning the Cenozoic stratigraphic-structural setting of the areas that connect the Gela-Catania foredeep and the Hyblean foreland ramp and, in particular, to detail the Plio-Pleistocene sedimentary deposits and their areal distribution, ii) the identification in the offshore area of the main structural lineaments (Scicli-Ragusa-Irminio line) and iii) understanding the role of these faults on the geodynamic evolution of the Sicily Channel.

### **2.5.2 DATA DESCRIPTION AND INTERPRETATION**

In order to achieve the best results in terms of acoustic resolution and depth of investigation and therefore to reach the aims of the research, the Sparker System was chosen. Through this technology, 5 seismic profiles (about 77 km) have been acquired during an oceanographic cruise in August 2015, led by the Department of Biological, Geological and Environmental Sciences of the Catania University in the frame of the Simit Project (Integrated Italy-Malta Cross-Border System of Civil Protection). These seismic profiles highlight a depth of the seabed between the 40 and 120 m, located between the lower shoreface and the continental shelf in s.s. The wells that lie in the southeastern Sicily offshore are numerous but unfortunately those (Mila 1-6, Licata, Archimides, Merluzzo, Delfino, Pellicano Ovest, Pancrazio Sud) around the study area do not provide information about the first 300 m of sediment below of the seabed.

**Fig. 2.23** shows the schematic tectonic context of the study area, the wells location and the georeferenced position of the seismic profiles that in the following are described and interpreted.

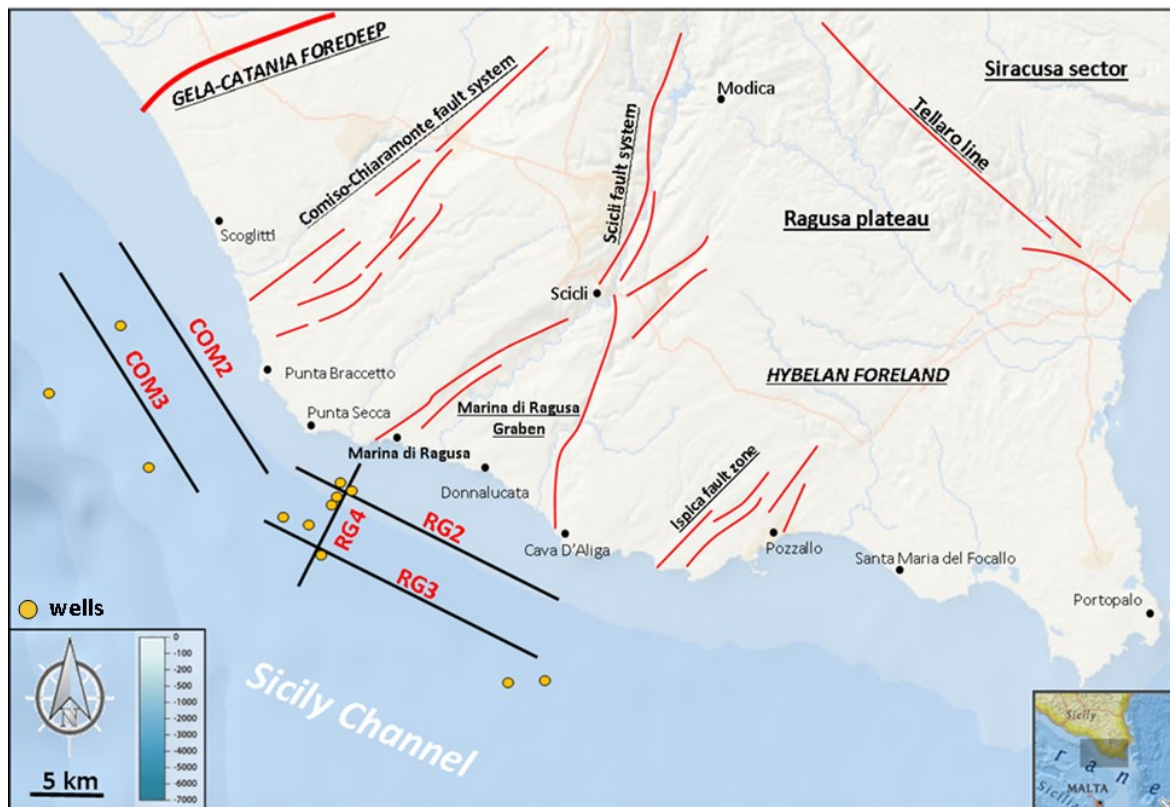


**Fig. 2.23** - Schematic tectonic context (modified from Bonforte et al., 2015) of the study area and the position of the seismic profiles during the oceanographic cruise between the Cava d'Aliga and Scoglitti coastlines.

The **COM-2** seismic profile is oriented in NNW-SSE direction and runs in the offshore between the Punta Braccetto and Scoglitti (**Fig. 2.24**), to an average distance from the coastline of about 7 km.

The profile is characterized by a marked seismic reflector (named B-reflector), corresponding with a widespread irregular erosional surface, that cuts the underlying units and is interpreted as the base of the Messinian evaporitic succession. In the southeastern part of the profile, the B-reflector is a very rough surface with local channelized forms. Furthermore, the B-reflector gradually deepens northwestward where it has a more flat trend.

Below the B-reflector, a widely deformed unit with a seismic stratified facies is interpreted as corresponding with the Tellaro and Palazzolo formations (named M2) of the Serravallian-lower Messinian. The lateral continuity of the reflectors of the M2 unit is

interrupted by several sub-vertical normal faults, that are the evidence of a late Miocene deformation since faults never affect the overlying evaporitic deposits.

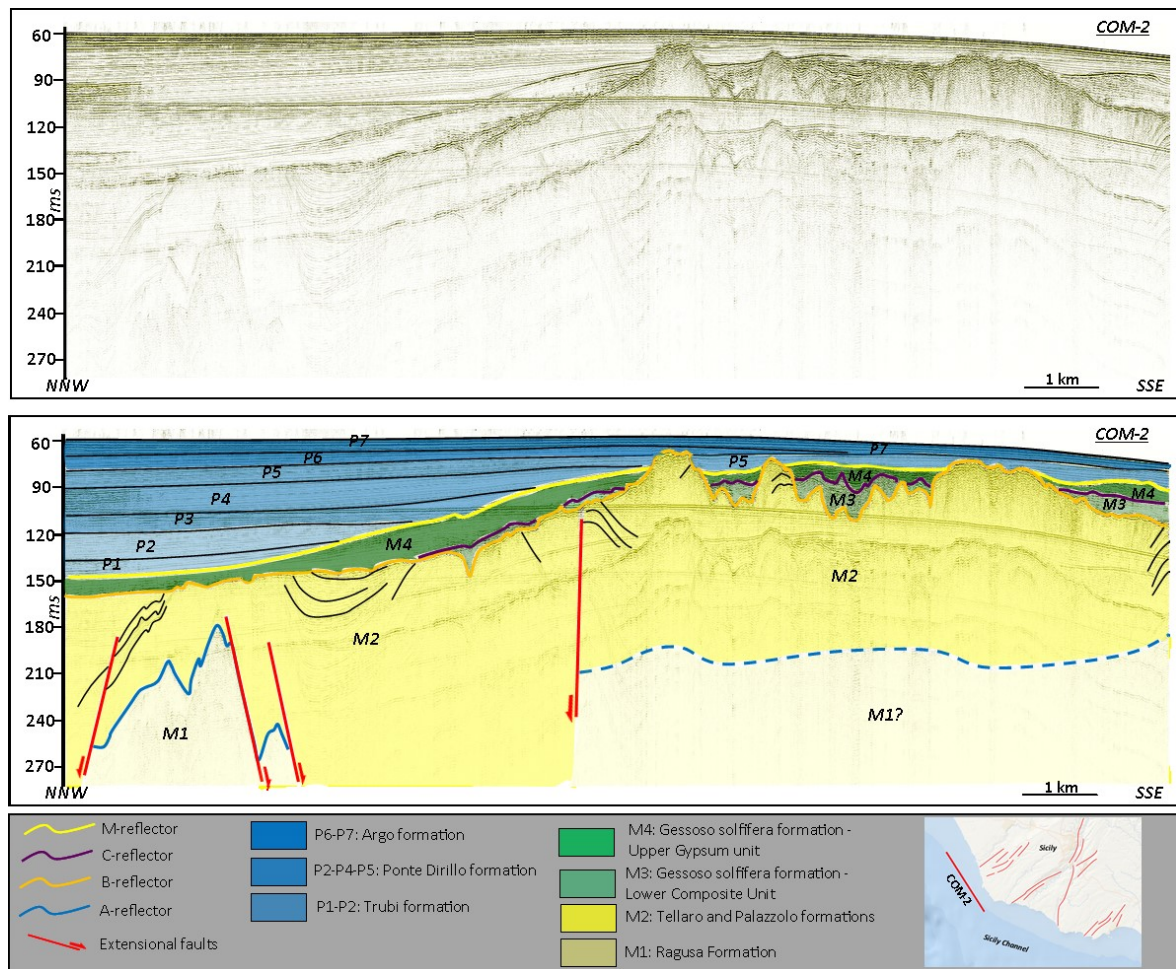


**Fig. 2.24** - The COM-2 seismic profile. The interpretation shows the late-Miocene tectonic activity and the preferential deposition of the Lower Composite Unit (M3) within the channelized area. In the NNW sector is maximum (about 90 m) the thickness of the Plio-Pleistocene succession and decrease considerably (thickness about 30 m) in the SSE sector.

The unit M2 is locally bounded at its base by a strong reflector (A-reflector) that is here interpreted as corresponding with the top of the Ragusa Formation (calcisiltites and white-grey marls of the upper Oligocene – lower Langhian). This depositional unit is named here M1. In particular, in the NNW portion of the profile, the M1 and M2 unit form a prominent horst bounded by two vertical normal-faults dipping respectively towards the SSE and the NNW. These faults are associated with extensional tectonic activity that has involved the foreland ramp in Oligocene-Miocene age (Lentini and

Carbone, 2014). The A-reflector and M2 units are well visible only in the northwestern extremity of the line, since to the SE they are masked by the multiple reflectors.

Above the B-reflector, two evident horizons, respectively named C-reflector and M-reflector, bound two units with laterally marked facies and thickness variations that correspond with the Messinian evaporitic deposits. In particular, the C-reflector is the top of a rather transparent and poorly stratified facies that represents the infill of channels. It probably represents the Lower Composite Unit of the evaporitic succession (here named M3), made up of interfingering massive selenite, evaporitic limestone (Calcare di Base Formation) and gypsum turbidites (Manzi et al., 2009). The M-reflector, instead, represents the top of a unit with great lateral facies variations: stratified above the channelized area of the underlying M3 unit and rather transparent in the NNW part, where the C-reflector is absent. This unit probably represents the siliciclastic unit (named here M4) of the Upper Gypsum unit (Arenazzolo formation, upper Messinian; Manzi et al., 2009). In NNW part of the profile, it directly lies in unconformity on the underlying Tellaro-Palazzolo evaporitic formations.

Above the M-reflector, the Plio-Pleistocene succession has been divided on the basis of its vertical facies variations in 7 depositional units (fig). The P1, P2, P3, P4 and P5 units are characterized by a rather transparent facies. P1, P2, P3 and P4 units show horizontal reflections with progressively onlap terminations towards the SE on the M-reflectors and present only in the NNW part of the seismic profile, probably due to the greater accommodation space creating by the flexure ramp foreland. The P5 depositional unit, instead, drapes the underlying units along the whole profile. In particular, P1 and P2 cover in unconformity the underlying evaporitic succession and, therefore, are interpreted as the Trubi formation (early Pliocene), whose deposition records the deepening of the Gela-Catania foredeep and restoring of the basinal conditions (Carbone and Lentini, 2014). The P3, P4 and P5 depositional units prove that the deep-sea conditions are preserved in the time: they are interpreted as belonging at the Ponte Dirillo formation (middle Pliocene-upper Pleistocene; Ghielmi et al., 2012), with maximum thickness of about 40 m. The P6 and P7 depositional units are characterized by a gradual increase in the acoustic reflection strength. The reflectors are laterally continuous and show evident sub-parallel stratifications along the whole seismic profile. The thickness of

the P6 and P7 units is variable along the seismic profile, decreasing towards the SSE, where P6 unit tends to zero meters. These units are probably correlated with a turbidite system that feeds several areas of the foredeep area (Ghielmi et al., 2012) during the Pleistocene and, therefore, are interpreted as belonging at the Argo formation (middle Pleistocene).

The **COM-3** seismic profile is oriented in a NNW-SSE direction, parallel to COM-2 seismic profile and lies about 10 km from the coastline (**Fig. 2.25**). Also this profile is characterized by the marked seismic B-reflector that cuts the underlying units and represents the base of the Messinian evaporitic succession. Similarly to the line COM-2, in the southeastern part of the profile, the B-reflector is characterized by marked channelization and an irregular surface. Northwesterward, the B-reflector gradually deepens and shows a more flat trend.

Below the B-reflector, a widely deformed unit with seismic stratified facies is interpreted as corresponding with the Tellaro and Palazzolo formations (M2) of the Serravallian-early Messinian. The lateral continuity of the M2 unit is interrupted by several sub-vertical normal faults, that are the evidence of a late Miocene deformation since they never involve the overlying evaporitic deposits.



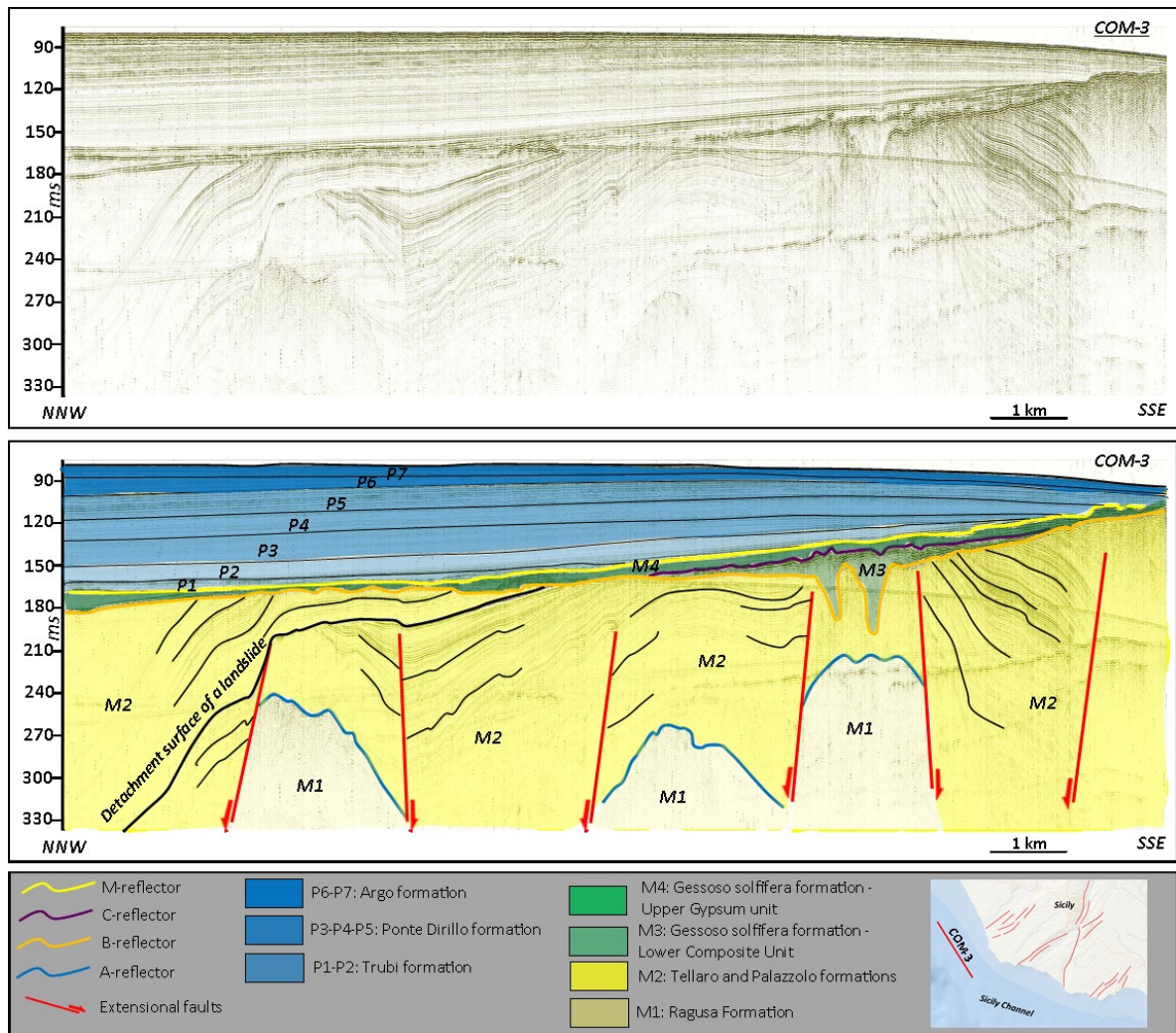


**Fig. 2.25** - The COM-3 seismic profile. The interpretation shows the widespread horst and graben setting within the late-Miocene formation. The deposition of the Lower Composite Unit (M3) is preferential within the channelized area, in the SSE sector. In the NNW sector an evident reflector (in black) cuts the deformed horizons and is interpreted as the detachment surface of a submarine landslide.

In the central and NNW part of the seismic profile, in the upper portion of the M2 unit, a further evident reflector cuts the deformed horizons and is here interpreted as the detachment surface of a submarine landslide development on a structural high. In fact, in an area affected by an intense late-Miocene tectonic activity, it is very widespread the development of landslides - on different scale (from tens to hundreds of meters) - especially in the proximity of structural highs. In the adjacent lowered block, it is overlain by a transparent package that corresponds with the landslide deposit (Fig. 2.25).



The good penetration of the acoustic signal allowed to identify the strong reflector (A-reflector) that bounds at the top the Ragusa Formation (M1) of the upper Oligocene – early Langhian along of whole profile COM-3. In several sectors of the profile, M1 and M2 are arranged in a prominent horst bounded by vertical normal-faults dipping towards SSE and NNW (**Fig. 2.25**). These faults show widespread slope variation and are associated with the extensional tectonic activity that has involved the foreland ramp in Oligocene-Miocene age (Lentini and Carbone, 2014), giving to this area a graben and horst setting.

Above the B-reflector, two evident horizons, respectively named C-reflector and M-reflector, bound two units with marked lateral variations, that correspond with the Messinian evaporitic deposits. In particular, the C-reflector bounds upwards a unit with a rather transparent poorly stratified facies with little lateral extent being restricted within two prominent channels, localized in the SSE sector. It probably represents the Lower Composite Unit of the evaporitic succession (M3) (Manzi et al., 2009). The M-reflector, instead, bounds a unit with extremely laterally variable facies with alternations of a transparent facies to a rather stratified one. This unit is very extensive laterally and is here interpreted as representing the siliciclastic unit (M4) of the Upper Gypsum unit (Arenazzolo formation, upper Messinian; Manzi et al., 2009). Its thickness is rather constant and it does not exceed the 15 m.

Above the M-reflector, the Plio-Pleistocene succession has been divided on the basis of its vertical facies variations in 7 seismic-stratigraphic units. The P1, P2, P3, P4 and P5 units are characterized by a rather transparent facies and show horizontal reflections with progressively onlap terminations towards the SE on the M reflector. In particular, P1 and P2 cover in unconformity the underlying evaporitic succession and, therefore, are interpreted as the Trubi formation (early Pliocene), whose deposition records the initial deepening of the Gela-Catania foredeep and restoring of the basinal conditions (Carbone and Lentini, 2014). The P3, P4 and P5 are interpreted as belonging at the Ponte Dirillo formation (middle Pliocene-upper Pleistocene; Ghielmi et al., 2012), with maximum thickness of about 45 m. The P6 and P7 depositional units are characterized by a gradual increase in the acoustic reflection strength. The reflectors are laterally continuous and show an evident sub-parallel stratification along the whole seismic profile. The thickness of the P6 and P7 units is variable along the seismic profile, decreasing towards the SSE.

These units are probably correlated with a turbidite system that feeds several areas of the foredeep (Ghielmi et al., 2012) during the Pleistocene and, therefore, are interpreted as belonging at the Argo formation (middle Pleistocene).

The seismic profile **RG-2** is oriented in a NNW-SSE direction and runs in the offshore between the Punta Secca and Cava D'Aliga towns (**Fig. 2.26**), to a distance from the coastline of about 7 km.

An evident seismic reflector, corresponding with a widespread irregular erosional surface, cuts the underlying units and is interpreted as the base of the Messinian evaporitic succession (B-reflector). In the southeastern part of the profile, the B-reflector shows a marked large-scale channelization, whereas northwestward it has preserved an irregular surface.

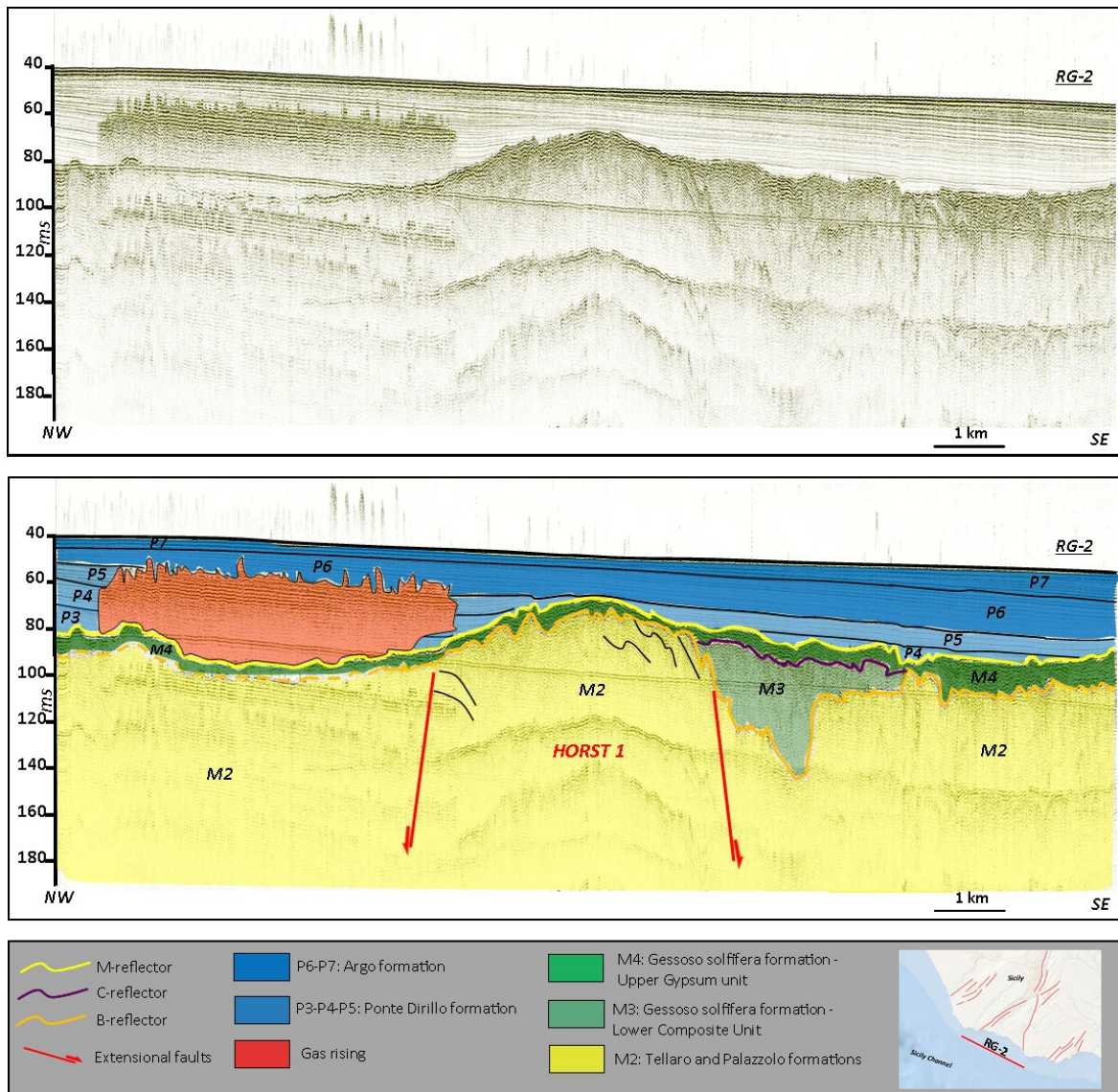


**Fig. 2.26** - The RG-2 seismic profile. The interpretation shows in the central portion the development of the Horst 1 and the preferential deposition of the Lower Composite Unit (M3) within the channelized area. In the northwestern sector, the increase of the acoustic reflectivity is interpreted as the gas rising within the Plio-Pleistocene succession. Trubi Formation (P1 and P2 units) of the Plio-Pleistocene succession is absent

Below the B-reflector, the penetration of acoustic signal is good only in the central part. Here a stratified and deformed depositional unit is interpreted as corresponding with the Tellaro and Palazzolo formations (M2) of the Serravallian-lower Messinian. The lateral continuity of the M2 unit is interrupted by two sub-vertical normal faults, respectively dipping NW and SE, that form a prominent structural high (Horst 1). The latter is connected to extensional tectonic activity that has involved the foreland ramp in Oligocene-Miocene age (Carbone and Lentini, 2014), with no tectonic deformation of the

overlying evaporitic deposits. Along the RG-2 seismic profile, the A-reflector corresponding with the top of the Ragusa Formation (M1) (Oligocene – lower Langhian) is not imaged, probably because the acoustic penetration is lower than that of the previous seismic profiles (COM-2 and COM-3).

Above the B-reflector, two evident horizons (C-reflector and M-reflector) bound two units with laterally marked facies variations that correspond with the Messinian evaporitic deposits. In particular, the C-reflector bounds at the top a rather transparent and poorly stratified facies that infills only the main channel in SE sector of the profile. It probably represents the Lower Composite Unit of the evaporitic succession (M3), made up of interfingering massive selenite, evaporitic limestone (Calcare di Base Formation) and gypsum turbidites (Manzi et al., 2009) and probably in continuity of sedimentation with the overlying unit (M4). The M-reflector bounds upwards a unit with very evident lateral facies variations: stratified near the channelized area (SE sector) and rather transparent in NW part, where the C-reflector is absent. This facies probably represents the siliciclastic unit (M4) of the Upper Gypsum unit (Arenazzolo formation, upper Messinian) and, in NW part of the profile, it directly lies in unconformity on the underlying M2 unit, corresponding with the Tellaro-Palazzolo formations.

Above the M-reflector, the Plio-Pleistocene succession shows a clear vertical facies variations but the lower depositional units (P1 and P2), recognized in the COM-2 and COM-3 seismic profiles and interpreted as corresponding with the Trubi formation) are not present in this offshore sector.

In the NW part of the RG-2 profile, a wide area (extending for about 6 km) within the Plio-Pleistocene succession shows a seismic facies characterized by a sudden increase of its acoustic reflectivity, with an extremely irregular top surface. This seismic facies hides the lateral continuity of the reflectors of much of P3, P4 and P5 depositional units and is interpreted as the reflectivity from the gas within the Plio-Pleistocene succession. Furthermore, some acoustic anomalies in localized area of the water column can be the evidences of the possible gas rising.

However, on the basis of the vertical facies variations, 5 depositional units have been recognized. The P3 and P4 units are characterized by rather transparent facies and show onlap geometry with the thickness that decreases near the late-Miocene structural

high (Horst 1). In particular, the P3 unit is present only the NW sector and the P4 unit reaches maximum thickness in the NW sector, whereas in the SE sector infills some depressions at the top of the M-reflectors. The P5 depositional units tends to drape the underlying units along the whole profile. The P3, P4 and P5 depositional units overall show acoustic facies typical of basinal deposition and is interpreted as belonging at the Ponte Dirillo formation (middle Pliocene-upper Pleistocene), with maximum thickness of about 20 m.

The P6 and P7 depositional units are characterized by a gradual increase in the acoustic reflection strength. The reflector are laterally continuous and show evident sub-parallel stratifications along the whole seismic profile. The thickness of the P6 and P7 units is variable along the seismic profile, increasing towards SE, where overall reaches about 30 m. These units are probably correlated with a turbidite system that feeds several areas of the foredeep area (Ghielmi et al., 2012) during the Pleistocene and, therefore, are interpreted as belonging at the Argo formation (middle Pleistocene).

The seismic profile **RG-3** is oriented in a NW-SE direction, in parallel to COM-2 seismic profile and lies at 10 km from the coastline (**Fig. 2.27**).

Also this profile shows a marked evident seismic reflector (B-reflector) that cuts the underlying units and represents the base of the Messinian evaporitic succession. In the southeastern and central part of the profile, the B-reflector shows a marked large-scale channelization and northwestward became flatter but preserves the erosional character.



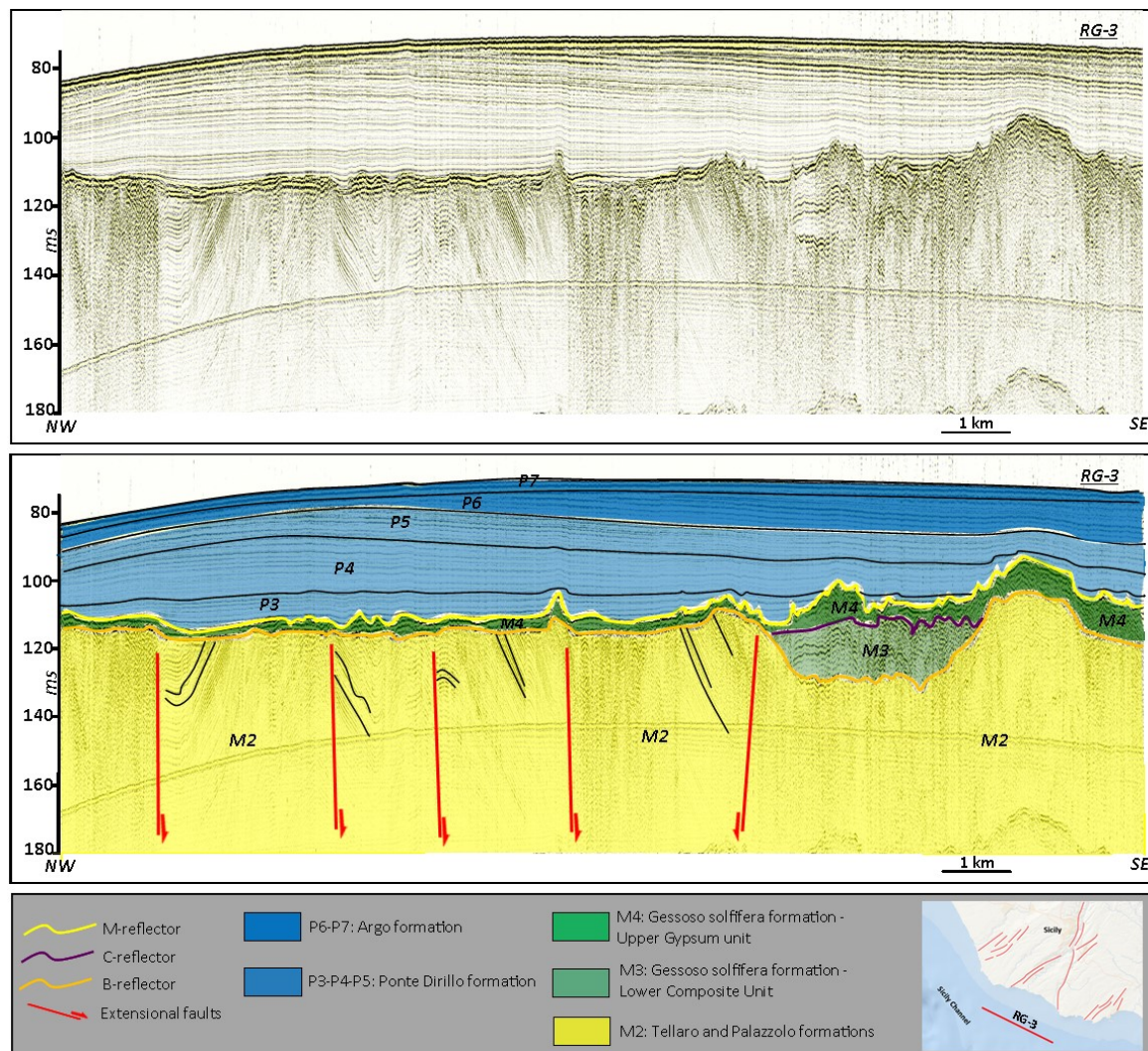


**Fig. 2.28** - The RG-3 seismic profile. The interpretation shows the widespread horst and graben setting within the late-Miocene formation. The deposition of the Lower Composite Unit (M3) is preferential within the channelized area (SE sector). The deposition of the Trubi Formation (P1 and P2 units) of the Plio-Pleistocene succession is absent.

Below the B-reflector, a widely deformed unit with seismic stratified facies is interpreted as corresponding with the Tellaro and Palazzolo formations (M2) of the Serravallian-lower Messinian. The lateral continuity of the M2 unit, together to the slope variation of their acoustic horizons, is interrupted by several sub-vertical normal faults, caused by the late Miocene extensive deformation but without ever involve the overlying evaporitic deposits.

Along the RG-3 seismic profile, the A-reflector corresponding with the top of the Ragusa Formation (M1) (Oligocene – lower Langhian) is not imaged, probably because

the acoustic penetration is lower than that of the previous seismic profiles (COM-2 and COM-3).

Above the B-reflector, a unit with rather transparent and poorly stratified facies is present only as infill of the channelized area in SE sector and is bounded at the top by C-reflector. It probably represents the Lower Composite Unit of the evaporitic succession (M3), made up of interfingering massive selenite, evaporitic limestone (Calcare di Base Formation) and gypsum turbidites (Manzi et al., 2009). The M-reflector bounds a unit with laterally variable facies characterized by a little and constant thickness (about 5 m) along the whole profile: This facies probably represents the siliciclastic unit (M4) of the Upper Gypsum unit (Arenazzolo formation, upper Messinian).

Above the M-reflector, as seen in the RG-2 profile, also in the RG-3 profile the Plio-Pleistocene succession shows a clear vertical differentiation. In this area the P1 and P2 units (interpreted as the Trubi formation) are not deposited, and the Plio-Pleistocene deposition starts with the depositional units stratigraphically younger (P3 and P4 units). In fact, on the basis of the vertical facies variations, 5 depositional units have been recognized. The P3 and P4 units are characterized by rather transparent facies and show an onlap geometry with a thickness roughly constant (about 20 m). The P5 depositional unit tends to drape the underlying units along the whole profile. The P3, P4 and P5 depositional units overall show acoustic facies typical of basinal deposition and is interpreted as belonging to the Ponte Dirillo formation (middle Pliocene-upper Pleistocene).

The P6 and P7 depositional units are characterized by a gradual increase in the acoustic reflection strength. The reflectors are laterally continuous and show evident sub-parallel stratifications along the whole seismic profile. The thickness of the P6 and P7 units is variable along the seismic profile, increasing towards SE, where overall reaches about 20 m. These units are probably correlated with a turbidite system that feeds several areas of the foredeep area (Ghielmi et al., 2012) during the Pleistocene and, therefore, are interpreted as belonging to the Argo formation (middle Pleistocene).

The seismic profile **RG-4** is oriented in NE-SW direction and localized in the Marina di Ragusa offshore, orthogonally to the RG-2 and RG-3 seismic profiles (**Fig. 2.29**).

This profile is characterized by a marked evident seismic reflector (B-reflector), corresponding with a widespread irregular erosional surface, that cuts the underlying units and significantly deepens towards the SE. It is interpreted as corresponding to the basis of the Messinian evaporitic succession.

Below the B-reflector, especially in the SW sector of the profile, the seismic facies shows a stratified and deformed depositional unit interpreted as corresponding with the Tellaro and Palazzolo formations (M2) of the Serravallian-lower Messinian. The lateral continuity of the M2 unit is interrupted by some sub-vertical normal faults connected to extensional tectonic activity that has involved the foreland ramp in Oligocene-Miocene age, without ever involve the overlying evaporitic deposits (Carbone and Lentini, 2014). Along the RG-2 seismic profile, the A-reflector corresponding with the top of the Ragusa Formation (M1) (Oligocene – lower Langhian) is not imaged, probably because the acoustic penetration is lower than that of the previous seismic profiles (COM-2 and COM-3).



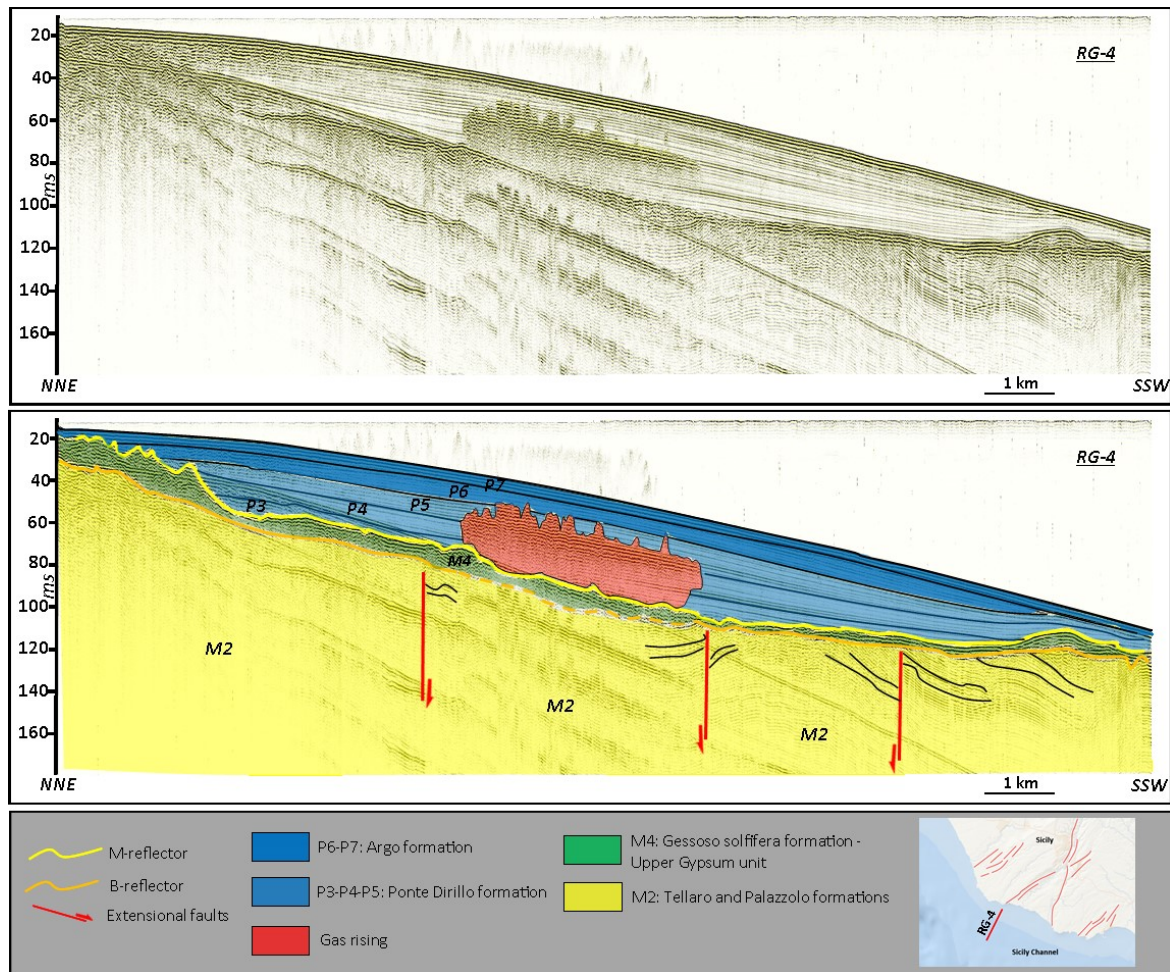


**Fig. 2.29** - The RG-4 seismic profile. The interpretation shows some tectonic discontinuities interpreted as extensional faults within the late-Miocene formation. The deposition of the Lower Composite Unit (M3) is absent. The deposition of the Trubi Formation (P1 and P2 units) of the Plio-Pleistocene succession is absent. In the central portion, the increase of the acoustic reflectivity is interpreted as the gas rising within the Plio-Pleistocene succession.

Above the B-reflector, an evident horizons (M-reflector) bounds units with a well-reflective facies with some laterally variations, that corresponds with the Messinian evaporitic deposits. In particular, the M-reflector bounds dominant stratified facies that alternate to limited transparent area. This facies probably represents the siliciclastic unit (M4) of the Upper Gypsum unit (Arenazzolo formation, upper Messinian). The C-reflector and the Lower Composite Unit (M3) are not present in this offshore sector.

Above the M-reflector, the Plio-Pleistocene succession shows an clear vertical seismic facies variations and the lower depositional units (P1 and P2, recognized in the

COM-2 and COM-3 seismic profiles and interpreted as corresponding with the Trubi formation) are not present.

In central part of the RG-2 profile, an wide area (extended for about 6 km) within the Plio-Pleistocene succession shows a seismic facies characterized by a sudden increase of the acoustic reflectivity, bounded at the top by an extremely irregular surface. This seismic facies hides the lateral continuity of several depositional units and is interpreted as the evidence of the presence of the gas within the Plio-Pleistocene succession. Furthermore, acoustic anomalies in the water column can be evidences of the gas that from the sedimentary succession rising towards the sea surface.

However, on the base of the vertical facies variations, 5 depositional units have been recognized. The P3 and P4 units are characterized by rather transparent facies and show an onlap geometry with the maximum thickness in the central part (35 m) and minimum in the southwestern sector. The P5 depositional units tends to drape the underlying units along the whole profile. The P3, P4 and P5 depositional units overall show acoustic facies typical of basinal deposition and is interpreted as belonging at the Ponte Dirillo formation (middle Pliocene-upper Pleistocene), with maximum thickness of about 30 m.

The P6 and P7 depositional units are characterized by a gradual increase in the acoustic reflection strength. The reflectors are laterally continuous and show evident sub-parallel stratifications along the whole seismic profile. The thickness of the P6 and P7 units decreases towards SE, where reaches about 5 m. These units are probably correlated with a turbidite system that feeds several areas of the foredeep area (Ghielmi et al., 2012) during the Pleistocene and, therefore, are interpreted as belonging at the Argo formation (middle Pleistocene).

### **2.5.3 DISCUSSION**

Based on the seismic stratigraphic interpretation of new profiles acquired along the southeastern offshore of Sicily, this work contributes to the improvement of our knowledge concerning the stratigraphic and structural context in the area between the Gela-Catania foredeep, the Hyblean foreland and its ramp.

A simplified model (**Fig. 2.30**) of the stratigraphic-structural setting of this offshore area has been reconstructed through the interpretation of these new seismic profiles and the comparison with preexisting model yet known in literature (Ghielmi et al, 2012).

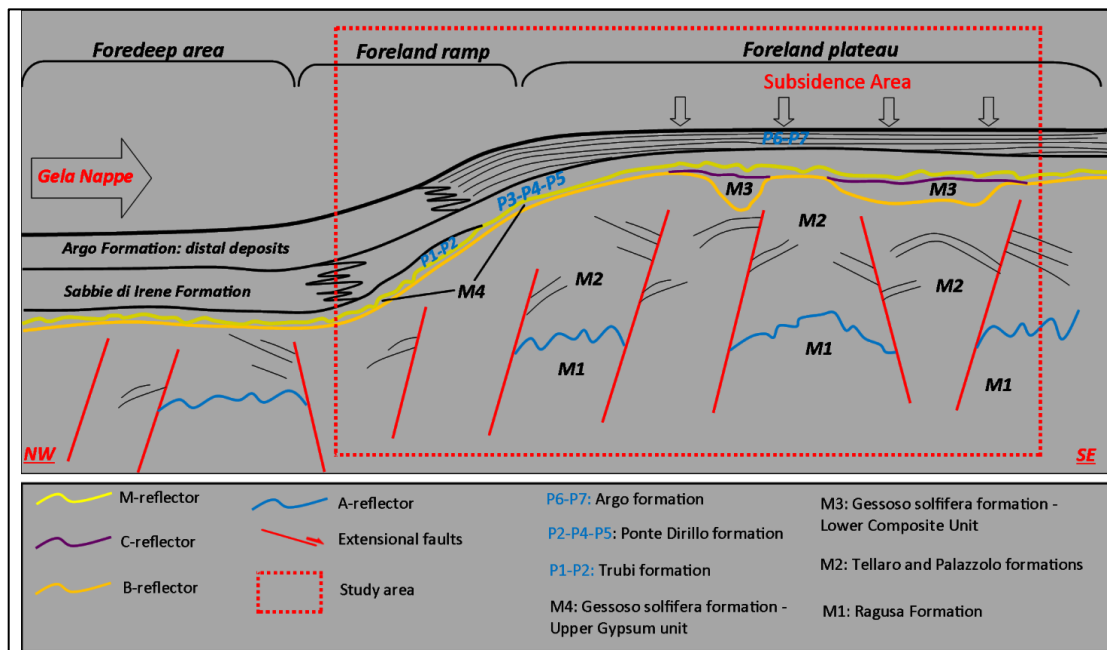


**Fig. 2.30** - Schematic reconstruction of the stratigraphic-structural setting in the area between the Gela-Catania foredeep, the Hyblean foreland and its ramp.

The good penetration of the acoustic signal (in particular, COM-2 and COM3 seismic profiles) allowed to identify the stratigraphy and the structural setting of upper Miocene units of the Hyblean foreland ramp. In the southeastern study area, instead, the gas rising, numerous multiples reflections and the considerable thickness of the Plio-Pleistocene succession mask the underlying M1 and M2 units. Therefore the identification of the structures and their late Miocene activity cannot be reliably reconstructed. Regarding the better imaged northwestern area, an acoustic horizon (A-reflector) bounds at the top the M1 unit interpreted as corresponding with the Ragusa formation (late Oligocene – early Langhian; Lentini and Carbone, 2014). A stratigraphically higher horizon (B-reflector), that represents an erosional surface laterally rather continuous, bounds at the top the M2 unit, interpreted as corresponding with the Tellaro and Palazzolo formations (Serravallian-lower Messinian age; Lentini and Carbone, 2014). M1 and M2 units are arranged in a series of structural highs and basins, bounded by sub-vertical

normal faults that are the evidence of late Miocene deformation. This extensional deformative phase within the foreland ramp never involve younger deposits since already the Messinian evaporitic succession (M3 and M4 units) seals the tectonic structures.

In **Fig. 2.31**, the main extensional faults that involve the upper Miocene formations in this sector of the Hyblean foreland and its ramp are mapped. Their main orientation is NE-SW and determines the horsts and graben setting in the most northwestern and central study area. These faults are probably connected to the history of the Scicli Line and to polyphase kinematic evolution of the N50 oriented faults, controlling also the Marina di Ragusa Graben. The interpretation here presented confirms the seismic data in the Cava d'Aliga offshore described by Grasso (1999), that extend the Scicli Line and Comiso-Chiaramonte fault system in the offshore area. Furthermore, it supports more recent interpretations (Finetti and Del Ben, 2006; Catalano et al., 2008) that identify offshore prolongation of the NE-SW oriented faults of the Marina di Ragusa Graben.

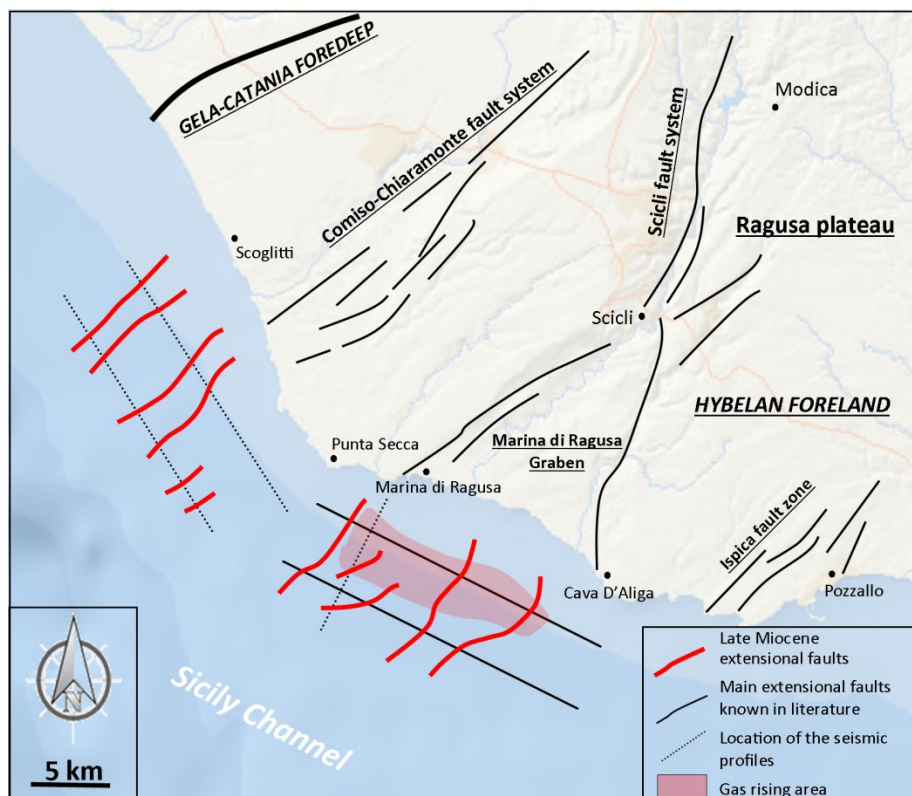


**Fig. 2.31** - Main late Miocene extensional faults identified in the southeastern Sicily offshore and comparison with structural data on land yet known in literature (Lentini and Carbone, 2014).

Instead, the Plio-Pleistocene succession is not affected by any tectonic activity, since the extensional faults within the analyzed seismic profiles involve only the upper Miocene deposits of the M1 Ragusa Formation and M2 Tellaro-Palazzolo Formations. In fact, the stratification of the Plio-Pleistocene succession is distinctly laterally continuous along all the study area, showing a deposition that overall cover the Messinian successions and preserves the Late-Miocene tectonic setting (**Fig. 2.32**). This interpretation is also in agreement with the data of the Geological Map of South-East Sicily (Carbone et al., 1984). Onshore, the Ragusa Domain shows in outcrop the middle-upper Miocene calcareous succession (Ragusa Formation and Tellaro-Palazzolo Formation, from upper Oligocene to early Messinian) widely offset by the Scicli Line and Comiso-Chiaramonte fault system but sutured by calcarenite and sand of the Pleistocene succession in some areas of the southern sector (Scicli Graben). Therefore, the seismic interpretation of this work confirms that the Late Miocene extensional tectonic activity (Carbone et al., 1984; Lentini and Carbone, 2014) involves widely the offshore portions of the Hyblean foreland and its ramp, preserving also the main NE-SW direction, but it does not show evidences that this activity has continued during the Plio-Pleistocene age (Ghisetti and Vezzani, 1980).

Furthermore, the seismic data show that the late Miocene tectonic activity can be the cause of submarine gravity instability. Within the M2 unit (Tellaro and Palazzolo Formations) an evident unconformity corresponds probably with an erosional surface on the top of a horst and is interpreted as the detachment surface of a submarine landslide. At the basis of this horst, in the adjacent basin, a transparent facies corresponds with a mass-transport unit and is interpreted as a wide landslide (**Fig. 2.25**).

The seismic interpretation shows that the deposition of the Gessoso-Solfifera succession (M3 and M4 units) also has widely involved the offshore sector of the Hyblean foreland ramp. In particular, the stratigraphic seismic interpretation provided in this Thesis shows that the Lower Gypsum unit (named in the literature also Primary Lower Gypsum, PLG), interpreted as corresponding with the M3 unit, does not is a peculiarity only of the deposits within the semi-isolated and marginal sub-basins (Manzi et al., 2009; 2012) or of the thrust top mini-basins of the Appennine-Maghrebides belt (Butler et al., 2015). In fact, our data show that the development of the lower part (M3 unit) of the

Messinian evaporitic sequence can take place also along the Hyblean foreland ramp that, instead, represents the outer portions of the chain. In particular, the M3 unit fills numerous channels localized in several parts of the study area above the B-reflector (interpreted as an erosional surface), also reaching significant thicknesses (20-25 m in depocenter area of the channels). Upwards the M4 unit, interpreted as corresponding with the Upper Gypsum unit, is bounded at the basis by a secondary reflector (named here C-reflector) that laterally covers unconformably the pre-evaporitic successions. In the literature (Manzi et al., 2009; 2012; Butler et al., 2015) this unit has only been recognized within the thrust top-basins of the chain and consists of deposits derived from the resedimentation of the PLG mainly accumulated in the deeper settings. Conversely, our seismic profiles show that the M4 unit involves also the Hyblean foreland ramp shows, keeping a constant thickness (in average 5 m) along all the study area. This highlights that the deposition of the Upper Gypsum unit (M4 unit) is not exclusive of the compressional context but extend also in areas where the extensional tectonic have been dominant, at least during the pre-Messinian age.

All the analyzed seismic profiles show a significant thickness (on average 30 m, maximum 50 m) of the Plio-Pleistocene stratigraphic succession, allowing their correlation with at least three regionally important formations described in Ghielmi et al., (2012).

In the NW offshore of the study area, in particular, the COM-2 and COM-3 seismic profiles, show deposits (P1 and P2 units) with progressively onlap terminations towards the SE on the M-reflector and with poor lateral continuity interpreted as the Trubi formation (early Pliocene). Their deposition records the initial deepening of the Gela-Catania foredeep and a gradual establishment of basinal conditions.

Above the Trubi formation, the P3, P4 and P5 units are interpreted as belonging the Ponte Dirillo formation, laterally correlative with the lower Pleistocene turbidite sands and clays of The Sabbie di Irene Formation. They took place in the ramp and foreland area during middle Pliocene-upper Pleistocene (Ghielmi et al., 2012) and represent part of the sedimentary succession of the progradational feeding system. The thickness of the Ponte Dirillo Formation keeps roughly constant thickness along all area between the Gela-Catania foredeep and the Hyblean foreland ramp, because probably of the tectonic

flexure of Hyblean foreland ramp is associated a continuous subsidence (**Fig. 2.30**). The Plio-Pleistocene succession ends with an evident sub-parallel stratification of two units (P6 and P7), characterized by a variable lateral thickness belonging at the Argo Formation (middle Pleistocene) that completes upward the sedimentary succession of the progradational feeding system in the Hyblean foreland area.

Within the Plio-Pleistocene succession, a wide area (extended for about 6 km) is characterized by a seismic facies that hides the lateral continuity of several depositional units and is interpreted as the evidence of the presence of gas. The location of the gas rising in the study area is mapped in **Fig. 2.31**. Furthermore, some acoustic anomalies are recorded in the water column and can be evidences of the gas that from the sedimentary succession rises towards the sea surface.

#### **2.5.4 CONCLUSIONS**

Through the seismo-stratigraphic interpretation of seismic profiles recently acquired in the south-east Sicily, between Scoglitti and Cava d'Aliga offshore, a detailed tectono-stratigraphic framework of the area has been performed.

The main results can be synthetized as follows:

- From the comparison with some preexisting models known in literature, an update stratigraphic-structural model of the area between the Gela-Catania foredeep, the Hyblean foreland and its ramp is proposed.
- The extensional faults system is characterized by a main NE-SW orientation and involves only the late Miocene formations, determining a horsts and graben setting, especially in the most northwestern and the central study area. These faults are probably connected to history of the Scicli Line and to polyphase kinematic evolution of the N50 oriented faults, supporting recent interpretations that identify offshore prolongation of the NE-SW oriented faults of the Marina di Ragusa Graben.
- the Plio-Pleistocene succession is not affected by any tectonic activity, showing a stratification distinctly laterally continuous along all the study area and covering widely the underlying Messinian successions. Therefore, the seismic interpretation confirms that the late Miocene extensional tectonic activity involves widely the



- offshore portions of the Hyblean foreland and its ramp, but it does not show evidences that this activity has continued during the Plio-Pleistocene age.
- The deposition of the Gessoso-Solfifera succession has been widely recognized in the offshore sector of the Hyblean foreland ramp, demonstrating that the Lower Gypsum unit does not is a peculiarity only of the deposits within the semi-isolated and marginal sub-basins or of the thrust top mini-basins of the Appennine-Maghrebides belt. In fact, the Lower Gypsum unit infills widely several channelized areas and the Upper Gypsum unit keeps a constant lateral extension along all the study area. Therefore, this highlights that the deposition of the Gessoso-Solfifera succession is not exclusive of the compressional context but extends also in areas where the extensional tectonic have been dominant, at least during the pre-Messinian age.
  - Within the Plio-Pleistocene succession, a wide area in the Marina di Ragusa offshore is involved from the gas rising and, furthermore, the presence of the gas is recorded also within the water column (acoustic anomalies), where tends to rise towards the sea surface.
  - The offshore identification of the main on-land structural lineaments in the south-east Sicily is a goal that has only partially been achieved in this Thesis, because the available seismic lines do not cover completely the offshore area involved by the tectonic activity of the Scicli-Ragusa-Irminio lineament. Therefore, in the future, during further oceanographic cruises, new seismic profiles will be acquired in order to cover the sector localized immediately to southeastern of the study area and, then, to define the possible offshore involvement of the Plio-Pleistocene deposits with the activity of the Scicli-Ragusa-Irminio lineament.



### **PART III: SHALLOW-WATER DEPOSITIONAL SYSTEM: GEOMORPHOLOGICAL EVOLUTION OF THE NORTH-EAST SICILY**

#### **3.0 INTRODUCTION**

The continental shelf is the typical physiographic place where is located the coastal interface between the terrestrial and marine environments. In this Part of the Thesis, a detailed study of the physical processes in shallow water conditions and main sedimentary structures, with particular reference to the north-east offshore sector of Sicily, is discussed.

In particular, the physical features of depositional systems of transgressive coasts are described, because in the study area the waves motion predominate over the others physical agents, such as currents and tides. The genesis and the development of the main sedimentary structures (ripples, dunes, barriers) are described, highlighting the interaction of sedimentary processes with the erosive and depositional action of the rivers. About that, the delta and its physiographic features are also defined. Owing to variations in sediment input, outflow velocity, wave and current energy, and other factors, the depositional features of deltas exhibit a high degree of variability from one delta to another. These factors determine the geometric features, the lateral facies relationships and the vertical facies variations of a delta, and that represent the peculiar features for the characterization and the reconstruction of a paleo-deltaic system.

Part 3 focuses on the stratigraphic and geomorphological reconstruction of the Sicily north-east continental shelf, in particular of the sector comprised between Capo Milazzo and Saponara river. The bathymetric interpretation of the Multibeam data and the seismic profiles (CHIRP) allowed to individuate several geomorphic elements connected with the last eustatic sea level cycle and with the sedimentary input by the numerous rivers that flow into this sector of Tyrrhenian Sea. The sedimentary deposits detect in the study area belong to the transgressive and highstand wedges and develop above an erosive widespread surface that delimits at the top a succession made up of continental margin clinofolds (lowstand succession).

### 3.1 TRANSGRESSIVE WAVE-DOMINATED COASTS

The marginal-marine setting lies along the boundary between the continental and the marine depositional environmental and is a narrow zone dominated by river, wave and tidal processes (**Fig. 3.1**) (Boggs, 2006). Salinities may range in different parts of the system from freshwater to supersaline, depending on the river discharge and the climatic conditions. Owing to intermittent exposure, high-energy conditions, or marked variations in salinity or temperature, much of the marginal-marine realm is a high-stress environment for organisms.

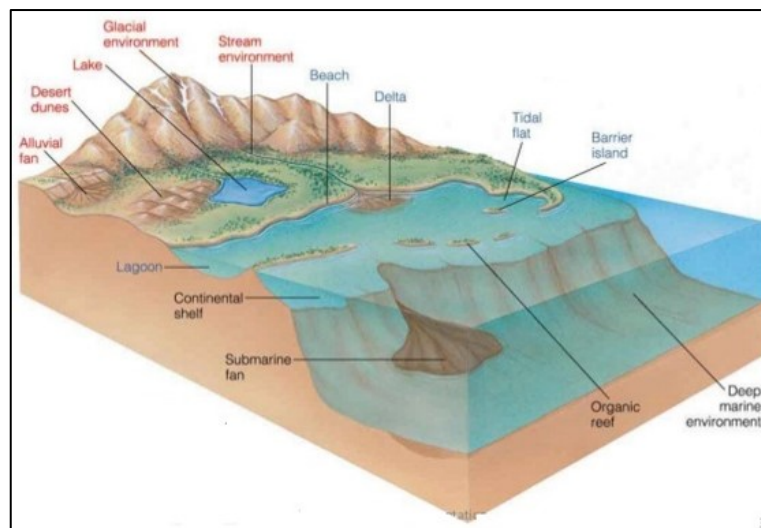


**Fig. 3.1** – *The marginal-marine setting; in red: continental environments; in blue: transitional environments (study area); in black: marine environments.*

A wide variety of sediment types (including conglomerates, sandstones, shales, carbonates and evaporates) can accumulate in marginal-marine environments. Owing to the large quantities of siliciclastic sediment delivered by rivers to the coastal zone throughout geologic time, the volume of marginal-marine deposits preserved in the geologic record is significant. The principal depositional settings for marginal-marine sediments are deltas, beaches, strand plains, barriers, estuaries, lagoons, and tidal flats.

About 80% of the world's coast and shelf areas are dominated by hydraulic and sedimentary processes related to wave motion and storms (Boyd et al., 2006). These

processes are reflected in an abundance of sedimentary rocks that preserve evidence of wave processes, and episodic erosional-depositional event.

Furthermore, the coast is particularly sensitive to the potential impact of the global warming and sea-level rise. The coastal interface between terrestrial and marine environments is constantly changing at both the human and geological time scale. This change is expressed as the interplay between coastal transgression and regression that, in turn, are the result of the interaction between coastal erosion/deposition and sealevel rise/fall. Therefore, the transgression and regression represent a composite response to the interaction of coastal sediment flux and changes in relative sea level resulting from the sum of tectonic and eustatic components (Curry, 1964).

A shelf is considered to be wave-dominated when the wave related processes dominate over tidal processes (Davis and Hayes, 1984). The sediment transport on the beach and upper shoreface is driven by waves, which generated both oscillatory currents through the orbital motion of water under the wave, and along-shore and off-shore directed rip currents (Clifton, 2006). The gradient of the beach and upper shoreface is strongly influenced also by the grain size of the sediment. Coarse-grained beaches are steep, and waves break close to shore, whereas sandy beaches slope more gently, and waves dissipate their energy across a wide zone (Clifton, 2006). The shelves include a continuum of depositional environments from beach and shoreface through inner to outer shelf settings. Deposition commonly takes place in relatively shallow-water (< 100 m) and on surfaces with a low topographic gradient. As a result, the shorelines have the potential to move laterally for many ten of kilometers, both as a result of sediment accumulation along the coast, and also result of relative rise and falls in sea level (Harris et al., 2002).

The transgressive wave-dominated coasts occur at the critical interface between land and sea and include such important components as estuaries, lagoons and barrier islands. Classification of coastal morphology and sediments is often accomplished by reference to the dominant physical process controlling the coastal zone: wave motion and tidal currents (Hayes, 1975).

Wave-dominated coasts are commonly in areas of strong persistent winds and relatively low tidal power. On transgressive coasts, the wave-dominated region consists of

the eroding linear coastlines, barrier-lagoon shorelines occupying embayments with little fluvial input, and wave-dominated estuaries at the mouths of river valleys (Harris et al., 2002) (**Fig. 3.2**).

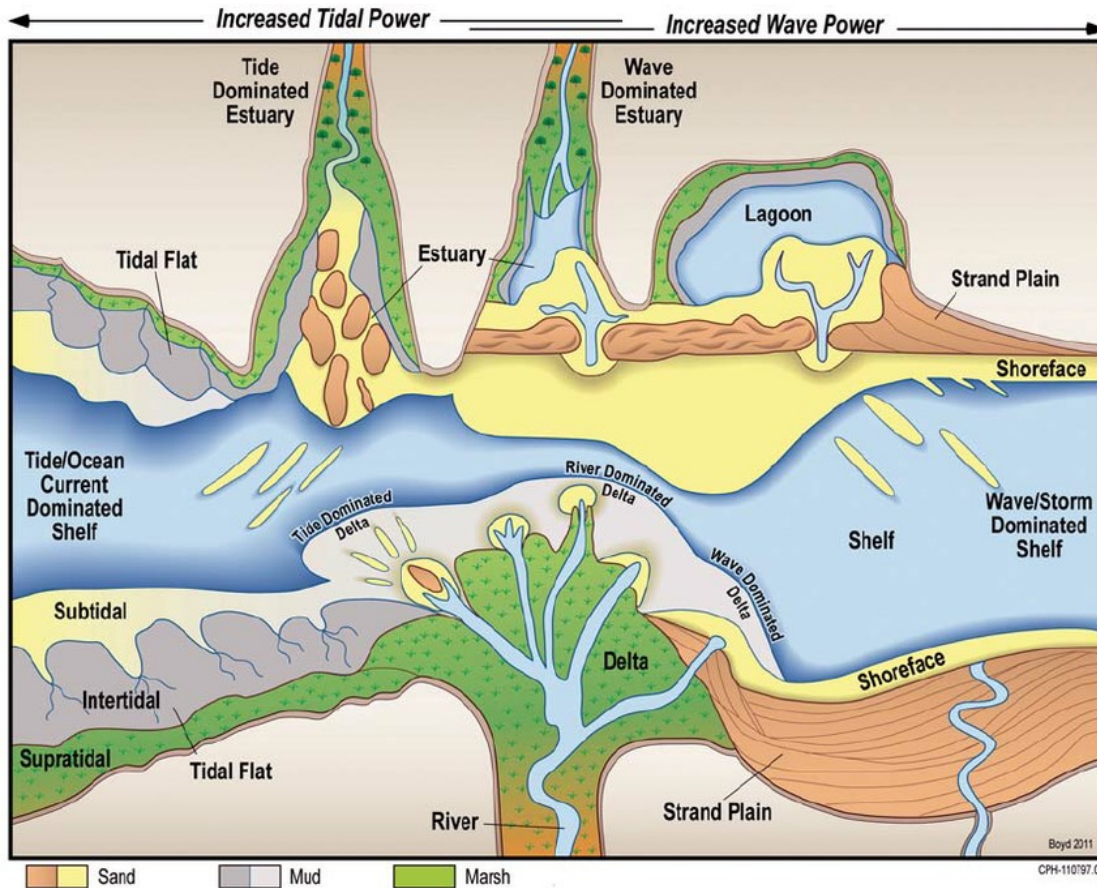


**Fig. 3.2** – Coastal classification, illustrating organization of all major clastic coastal depositional environments based on shoreline translation direction and relative power of waves, tidal currents and river currents. The upper coastline is transgressive whereas the lower coastline is regressive. Transgressive wave-dominated shorelines occupy the upper right-hand portion of this figure (Boyd et al., 1992).

Transgressive coasts receive sediment from two sources: the river that reach the coast and wave processes that erode pre-existing deposits.

The rivers that supply sediment to the coast create a variety of fluvial-channel and floodplain geomorphological elements in the area upstream of the tidal limit and contain channel, bar/sand flat and floodplain elements.

### **3.2 PHYSICAL PROCESSES AND MAIN SEDIMENTARY STRUCTURES**

Classification of coastal morphology and sediments is often accomplished by reference to the dominant physical process controlling the coastal zone: wave motion and tidal currents (Dalrymple et al., 1992).

Wave-dominated coasts are commonly in areas of strong persistent winds and relatively low tidal power. On transgressive coasts, the wave-dominated region consists of the eroding linear coastlines, barrier-lagoon shorelines occupying embayments with little fluvial input, and wave-dominated estuaries at the mouths of river valleys. Transgressive coasts receive sediment from two sources: the river that reach the coast and wave processes that erode pre-existing deposits. The rivers that supply sediment to the coast create a variety of fluvial-channel and floodplain geomorphological elements in the area upstream of the tidal limit and contain channel, bar/sand flat and floodplain elements (Davies, 1964).

As a result, the sediments that accumulate on shelves have very complex stratigraphy, that record both wave scour in transgressive shorelines and also sub-aerial erosion, as shelf deposits were exposed to fluvial processes during regression and relative sea level fall (Davis and Hayes, 1964). Stratigraphic and facies complexity is further increased by potentially rapid changes in the intensity of wave and tidal processes linked to changes in the width and depth of shelves, and by changes in the caliber of sediment delivered to the shoreline (Yoshida et al., 2007).

The physical sedimentary structures are generated primarily by combined flows. The nature of these flow types is very different (Swift et al., 1986) and the most important sedimentary structures found in shelf deposits are various types of small wave ripples, large wave ripples, hummocky cross-stratification, planar stratification and dunes. It is important to highlight that the types of sedimentary structures that develop on a shelf are dependent not on the hydraulic conditions but also on the sediment grain sizes available (Clifton, 2006).



### 3.2.1 RIPPLES AND HUMMOCKY CROSS-STRATIFICATION

The hummocky cross-stratification (HCS) is generally formed in coarse silt to fine sand and experimental studies (Dumas et al., 2005) have greatly clarified the hydraulic conditions under which ripples and HCS form. When oscillatory currents ( $U_0$ ) are between 20-50 cm/sec and the unidirectional component of flow ( $U_u$ ) is small ( $< 10$  cm/sec), the stable bedforms are small symmetric ripples (height about 1 cm) (**Fig. 3.3**).

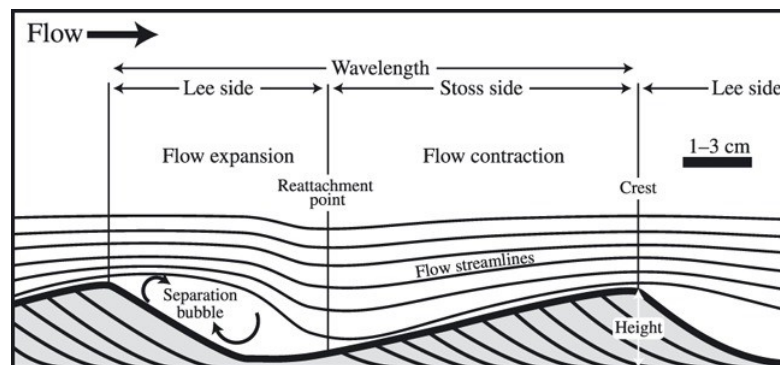


**Fig. 3.3** - *Ripple morphology and terminology.*

As  $U_u$  increases (10-25 cm/sec), ripples wavelength and height increase. When the  $U_0$  increases to 50-100 cm/sec, large symmetric ripples with a wavelength of 1-2 m and sharp discontinuous crests are the stable bedform.

Instead, others experimental results of Dumas (2005) show that HCS is the product of large wave, commonly accompanied by weak currents (**Fig. 3.4**).

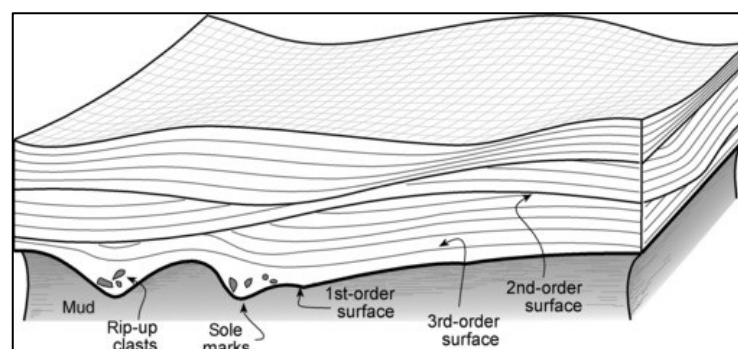


**Fig. 3.4**- *The hummocky cross-stratification and their different order surfaces in HCS beds.*

### 3.2.2 PLANAR STRATIFICATION

The planar stratification develops in fine to very fine sand under combined flows where the unidirectional component may only be a small fraction of the oscillatory component (Arnott and Southarh, 1990) (**Fig. 3.5**). Planar lamination is typically developed immediately above erosional base and may grade up into HCS or wave ripples.

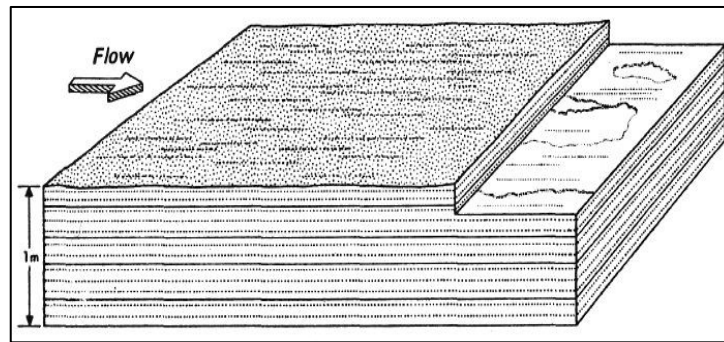


**Fig. 3.5** - Example of Planar lamination, also called horizontal, parallel, and flat lamination

### 3.2.3 DUNES

The dunes are very common on modern shorefaces and sandy shelves where they develop in upper fine- to coarse grained sand under longshore and onshore currents. In shorefaces composed of fine sand, dune crossbedding is typically preserved only in the upper shoreface where the longshore bars provide protection from waves. The dunes that have spacing of tens to hundreds of meters and heights of a few decimeters to a few meters also widely developed on modern shelves they indicate broadly along-shelf flows (Swift et al., 1979).

### 3.2.4 BARRIERS AND BEACHES

Barrier and beach complexes are best developed on wave-dominated coasts where tidal range is small to moderate (Fitzgerald and Buynevich, 2001).

Coastal *barriers* form due to the combined action of wind, waves, and longshore currents whereby thin strips of land are built a few to several tens of meters above sea level (Fitzgerald and Miner, 2013). They are called barriers because they protect the mainland coast from the forces of the sea, particularly during storms. Barriers are wave-built accumulations of sediment that accrete vertically due to wave action and wind processes. Most are linear features that tend to parallel the coast, generally occurring in

groups or chains. Barriers are separated from the mainland by a region termed the *backbarrier* consisting of tidal flats, shallow bays, lagoons and/or marsh systems. Barriers may be less than 100 m wide or more than several kilometers in width (Swift, 1968). Generally, barriers are wide where the supply of sediment has been abundant and relatively narrow where erosion rates are high or where the sediment was scarce during their formation. Barrier length is partly a function of sediment supply but is also strongly influenced by wave versus tidal energy of the region (Forbes et al., 1991). Coastal barriers consist of many different types of sediment depending on their geological setting. Sand, which is the most common constituent, comes from a variety of sources including rivers and deltaic deposits, eroding cliffs, and biogenic material (**Fig. 3.6**).

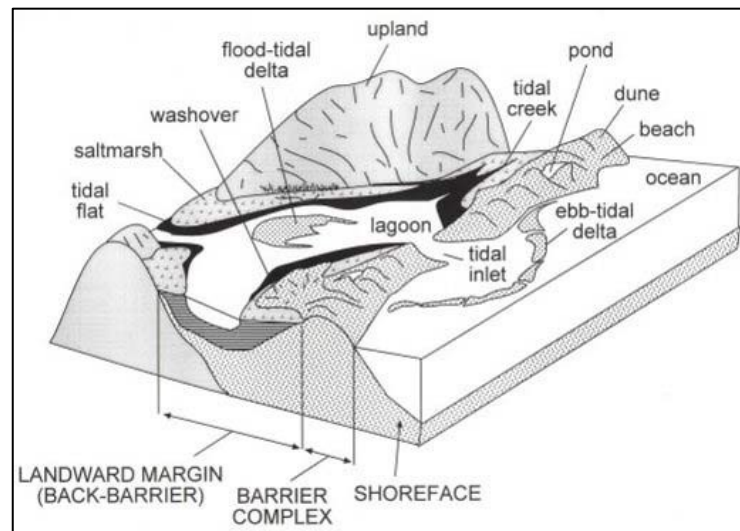


**Fig. 3.6** - Barrier shoreline environments from Fitzgerald and Buynevich, 2001

Due to continual sediment reworking by wind, waves, and tides, the *beach* is the most dynamic part of the barrier. The beaches are long and narrow accumulations of sand aligned parallel to the shoreline and attached to land. Bodies of beach sand are typically cut across by headlands and sea cliffs, estuaries, river deltas, tidal inlets, bays and lagoons. The barriers are also commonly dissected by tidal channels or inlets. Beaches may occur within delta systems, along depositional strike from deltas, or in other marine or even lacustrine settings that have no connection with deltas. In contrast to deltas, which are influenced by both fluvial and marine processes, beach and barrier systems are

generated predominantly by marine processes, aided to a minor degree by eolian sand transport.

### 3.3 DELTA

A delta is a discrete bulge of the shoreline formed at the point where a river enters an ocean, sea, lake, lagoon or other standing body of water (Giosan et al., 2005). The bulge is formed because sediment is supplied more rapidly than it can be redistributed by basinal processes, such as waves and tides. Deltas are thus fundamentally regressive in nature, which means that their deposits record a seaward migration or progradation of the shoreline (Bhattacharya, 2006). The terrestrial feeder systems can be alluvial (rivers, alluvial fans, braidplains) or non-alluvial (volcanic lavas or pyroclastic flows). Most of the sediment in a delta is derived directly from the river that feeds it; in contrast with estuaries in which much of the sediment is derived from the marine realm and in which deposits are fundamentally transgressive (Bhattacharya, 2006).

This chapter focuses on river deltas as a depositional system in which both environments and their deposits will be described.

The distribution and characteristics of alluvial deltas are controlled by a complex set of interrelated fluvial and marine/lacustrine processes and environmental conditions (Elliot, 1986). These factors include climate, water and sediment discharge, river-mouth processes, nearshore wave power, tides, nearshore currents, and winds (Coleman, 1981). Alluvial deltas can be classified on the basis of delta-front regime (Galloway, 1975) in: fluvial-dominated, tide-dominated or wave-dominated.

In function of contrast of density of the sediments with sea water (Boggs, 2006), it is possible to distinguish:

- *homopycnal flows*, when the density of the river water is equal to the density of the standing water in the basin. This type of flow is associated with rapid mixing and abrupt deposition of much of the sediment load (**Fig. 3.7**);

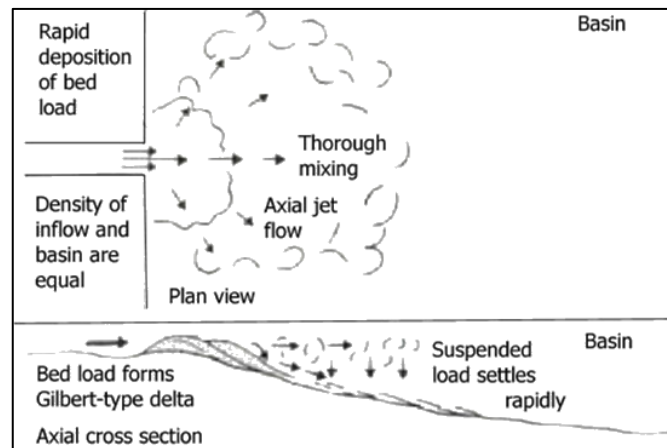


**Fig. 3.7** – Schematization of a homopycnal flows and depositional effects.

- *hyperpycnal flows*, in which the density of the suspended sediment flow is more than that of the water. This type of flow moves along the bottom as a density current that may be erosive in its initial stages but eventually deposits its load along the more gentle slopes of the delta front to form turbidites;

- *hypopycnal flows*, in which the density of the suspended sediment flow is less than that of the water. In this flow, fine sediment may be carried in suspension some distance outward from river mouth before it flocculates and settles from suspension.

### 3.3.1 PHYSIOGRAPHY AND RECONSTRUCTION OF A DELTAIC SYSTEM

Owing to variations in sediment input, outflow velocity, wave and current energy, and other factors, the depositional features of deltas exhibit a high degree of variability from one delta to another. Nevertheless, all deltas can be divided into subaerial and subaqueous components (Giosan et al., 2005). The subaerial component of deltas is generally larger than the subaqueous component and is divided into an *upper delta plain*, which lies largely above high-tide level, and a *lower delta plain*, lying between low-tide mark and the upper limit of tidal influence. The upper delta plain is commonly the oldest part of the delta and is dominated by fluvial processes. The lower delta plain is exposed during low tide but is covered by water during high tide. Thus, it is subjected to both fluvial and marine processes. The upper most part of the subaqueous delta, lying at water

depths down to 10 m, is commonly called the *delta front*. The remaining seaward part of the subaqueous delta is called the *prodelta* (Fig. 3.8).

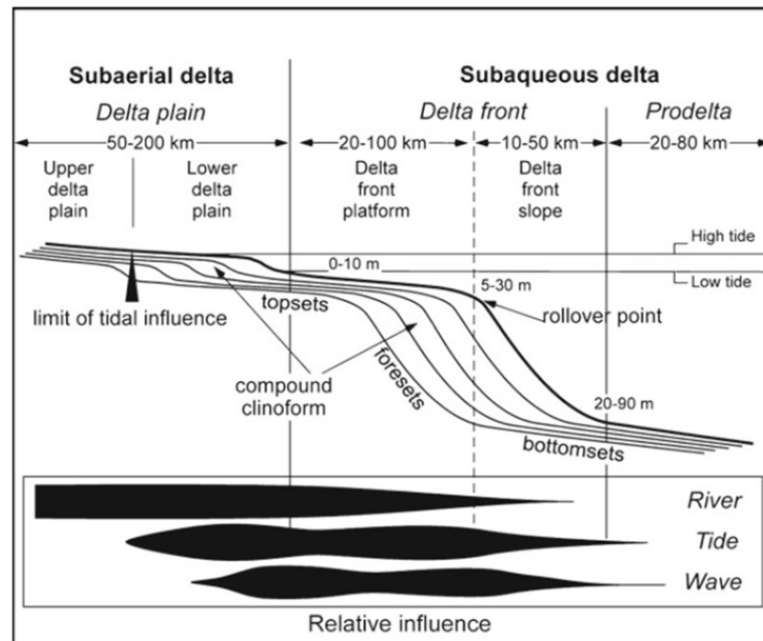


**Fig. 3.8** - Major physiographic and morphologic features of tide-dominated delta systems shown in cross-section scheme.

The sub-environments of delta systems range from normal marine (beach, barrier, lagoonal) to nonmarine (fluvial, marsh, eolian), and a variety of different sediment types can be deposited. Deltaic sedimentary successions are characterized by assemblages of lithofacies, each of which can occur in other environments, such as fluvial, lacustrine, and shallow-marine environments. Some general characteristics of delta deposits that can be useful in their recognition include geometry, lateral facies relationships, vertical successions of facies and sedimentary structures (Broussard et al., 1975; Bhattacharya, 2006).

### *Geometry*

Ideally, deltas are triangular in areal shape; however, much variation from this ideal shape can occur, particularly with tide- and wave-dominated deltas. In cross section, deltas are typically wedge- or lens-shaped bodies extending laterally to several hundred kilometers.

#### *Lateral Facies Relationships*

On a smaller scale, lateral facies relationships are likely to be complex. Delta-plain deposits may range from coarse distributary-channel deposits to finer-grained marsh or interdistributary-bay or lacustrine deposits. The lateral associations of delta-front sediments can also be highly variable depending upon whether deposition was dominated by fluvial, wave, or tidal processes.

#### *Vertical Facies Successions*

The progradation of deltaic deposits during active delta growth produces a generally coarsening-upward sedimentary succession. Migration of delta-front sands over prodelta silts and clays generates fairly well-defined coarsening-upward successions. Locally, filling of abandoned channels may even cause fining-upward successions to develop. Although the generalized coarsening-upward progradational model for deltas serves as a useful norm for comparison, the variations in delta behavior can produce vertical successions that differ from this idealized model. The lithologic types, sedimentary structures, textures, and other features preserved in the progradational facies depend upon the type of delta.

#### *Sedimentary Structures*

Numerous types of sedimentary structures - such as cross-bedding, ripple marks, bioturbation structures, and slump structures - occur in deltaic deposits. All of these structures are found also in many other environments, but the suites of structures may help to define a particular type of deltaic deposit such as fluvial deposits. Paleocurrent directions in deltaic deposits can be highly variable, ranging from unidirectional patterns in fluvial-dominated portions of deltas to bidirectional patterns in tide-dominated portions.



### **3.4 GEOMORPHOLOGICAL RECONSTRUCTION OF THE NORTH-EAST SICILYCONTINENTAL SHELF**

#### **3.4.1 GEOLOGICAL SETTING**

The study area is located along the NE Sicily margin, between the Milazzo Promontory and the area offshore from the Saponara River (**Fig. 3.9a**). On land, the Peloritani Mountains are the southern portion of the Calabrian Arc where the tectonic basement nappes of the Kabilo-Calabride units, that tectonically overlie the Apenninic–Maghrebian Chain, crop out (Lentini et al., 1996; Gamberi et al., 2014). The orogenic wedge was affected by the extensional tectonics that led to the opening of the Tyrrhenian backarc basins at the rear of the Maghrebian thrust belt (Patacca et al., 1987). As a result, NNE–SSW-trending normal faults and NW–SE trending strike–slip faults gave rise to the horst and graben structural setting of NE Sicily (Di Stefano and Lentini, 1995; Lentini et al., 2000). Basement nappes of the Kabilo–Calabride units are exposed on the NE–SW elongated horsts (i.e. Castanea Ridge), whereas Miocene to Quaternary sediments fill the grabens (i.e. Barcellona Trough; **Fig. 3.9a**).

Within this complex tectonic setting, the largest tectonic feature of the Calabrian Arc is the Siculo-Calabrian Rift Zone (SCRZ) (**Fig. 3.9b**), a 370 km long belt that runs continuously along the inner side of the Calabrian Arc, through the Messina Straits and along the Ionian coast of Sicily and extends also westwards into the Aeolian Islands Arc (Monaco and Tortorici, 2000).

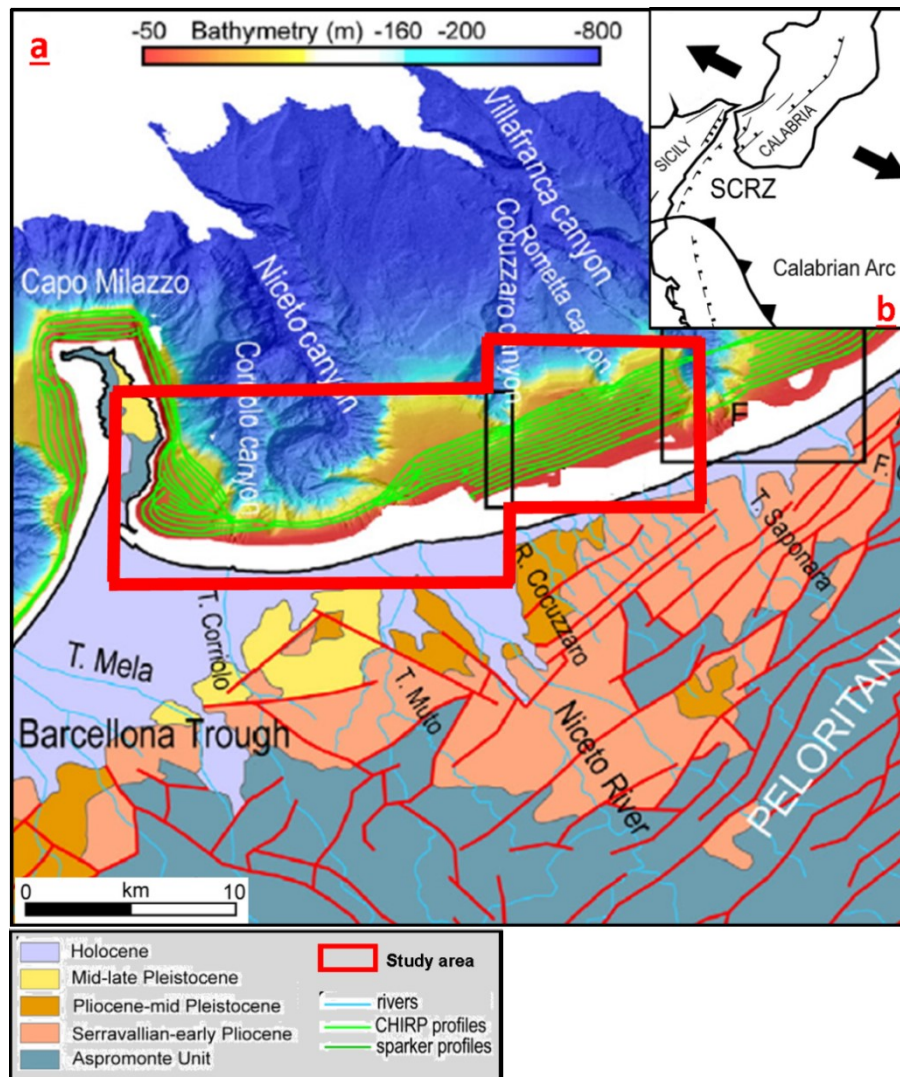


**Fig. 3.9** - - Bathymetric map of the NE Sicily shelf and schematic tectonic setting of the Peloritani Mt. (**Fig. 3.9a**) resulting from the compilation of different multibeam surveys (Gamberi et al., 2017). Regional location of the study area (**Fig. 3.9b**): the black arrows show the extensional regime responsible for the Siculo-Calabrian Rift Zone above the Calabrian Arc subduction zone (Lentini et al., 2000).

High regional uplift rates affect the NE Sicily area (Westaway, 1993) and are amplified by local uplift connected with the vertical movements of single fault blocks of probably active structures (Catalano et al., 2003; Scicchitano et al., 2011).

The tectonic pattern of northeast Sicily also controls the on-land drainage basin morphologies, with rivers that are short with small drainage basins on the eastern side and become progressively longer with larger drainage basins to the west. In NE Sicily, rivers are mainly represented by 1st order streams (Strahler, 1952). On the northeastern Sicilian shelf, the sediments deposited during the present highstand of sea level can reach

a thickness of about 50 m and are arranged in a prograding sediment wedge, in places covering the whole shelf (Pepe et al., 2003; Caruso et al., 2011; Sulli et al., 2013).

Furthermore, the continental shelf of the northeastern Sicily is dominated by the canyons that in some cases (Muto and Niceto Canyon) have their heads in proximity of the coast and of the homonymous deltas, and in other cases (Cocuzzaro and Rometta Canyon) at almost 3 km from the Sicily coastline and, therefore, at a significant distance from the river mouths. Canyon heads are usually thought as retrogradational features where erosional processes prevail (Pratson and Coakley, 1996; Piper and Normark, 2009; Gamberi et al., 2017). It is a common understanding that canyon heads with amphitheatre shaped margins are formed by the headward migration of landslide scars and associated with erosional processes extending upslope until eventually reaching the shelf break (Farre et al., 1983; Arbues et al., 2007; Dakin et al., 2013).

The aim of this work is to provide an update characterization of the geomorphological setting of the north-east Sicily continental shelf deposits, through Multibeam bathymetric data, taking to account the variable river drainage basins along the margin. Furthermore, through high-resolution CHIRP seismic profiles, a reconstruction of the last eustatic sea level cycle is provided, on the basis of the morpho-stratigraphic description of the transgressive and highstand wedges.

#### **3.4.2 DATA DESCRIPTION AND INTERPRETATION**

The interpretation of the Multibeam bathymetric data and of the CHIRP seismic profiles aims at interpreting on the geomorphological description and the stratigraphic evolution of the northeastern Sicily continental shelf. In order to provide a clear description and interpretation of the available data, the study area (localized between Milazzo town and Saponara River) was divided into three shelf sectors (**Fig. 3.10**).

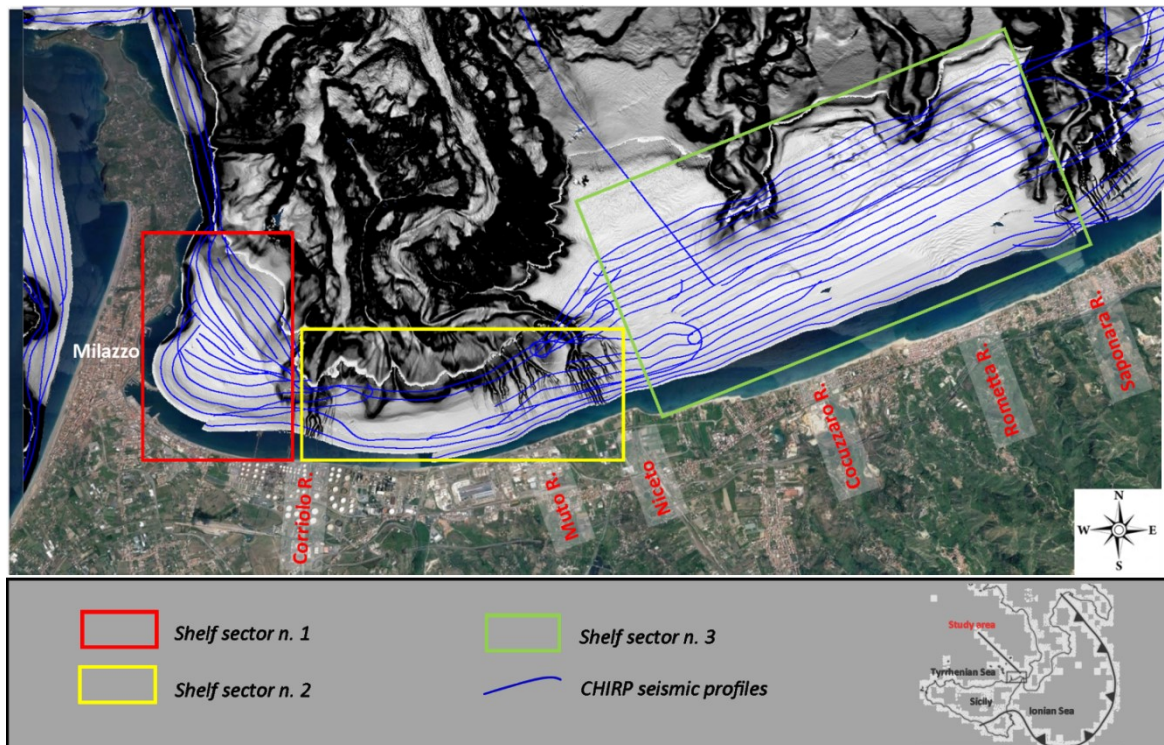


**Fig. 3.10** - Location of the CHIRP seismic profiles and the Multibeam data interpreted in this Thesis. The study area has been divided in three sectors for a clearer description

In the following, a description of the main surfaces that have been used to discriminate the transgressive and highstand wedges deposits above the lowstand succession is provided. Through the CHIRP seismic profiles interpretation, in fact two main reflectors, characterized by an intense contrast of acoustic impedance, have been recognized.

The first reflector (named here L-reflector and found at a depth between 5 and 40 m below the seafloor (b.f.s.) is characterized by a persistent lateral continuity that defines an irregular surface interpreted as the top of the *lowstand succession* and the basis of the *transgressive wedge*. The transgressive deposits show variable acoustic features (from well-stratified to transparent facies) and a different thickness along all the study area.

Upwards, the transgressive wedge is bounded by a second main reflector (named here T-reflector), characterized by an irregular lateral trend and interpreted as a Maximum Flooding Surface (MFS). In turn, the T-reflector bounds at the base the *highstand wedge*, characterized by downlap termination on the T-surface, and consisting of the deposits (deltas) of the rivers that lie along the northeastern Sicily coastline (Gamberi et al., 2014) and of their distal fine-grained equivalent. Within the highstand



wedge, in particular along the central-eastern sector of the study area, the good resolution of numerous available CHIRP data has allowed to describe the distribution of several depositional units and, the reconstruction of their evolution in time and space.

#### 3.4.2.1 Shelf sector n. 1

The shelf sector n. 1 (area of about 15 km<sup>2</sup>) is located in the western margin of the study area. The sector is located to the west of the Corriolo river delta and is represented by the highstand deposits sited to the east of the Milazzo Promontory. All the CHIRP seismic profiles available are sub-parallel to the southern coastline and cover all the continental shelf, up to the beginning of the Corriolo canyon.

The **MAG599** seismic profile runs very close to the coastline and shows the stratigraphic feature of the inner part of the continental shelf (**Fig. 3.11**).

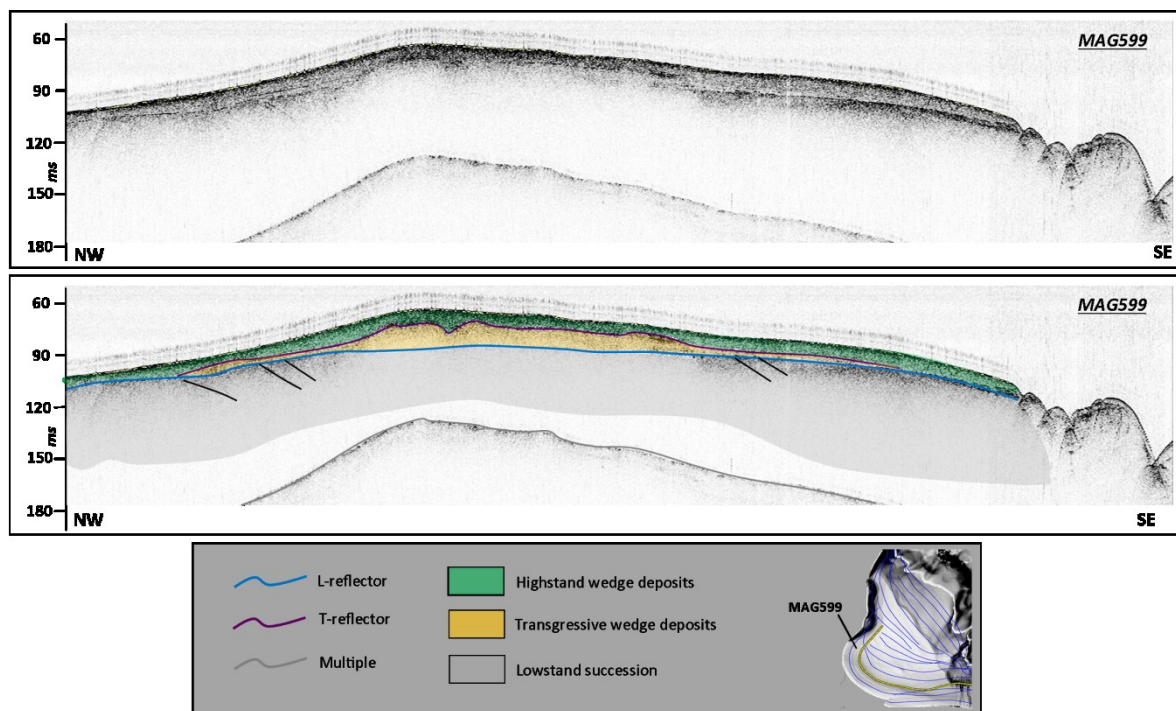


**Fig. 3.11** – The MAG599 CHIRP seismic profile. The interpretation shows the stratigraphic feature of the inner part of the continental shelf sector n. 1.

The L-reflector coincides with an erosional surface with a good lateral continuity and follows the bathymetric trend of the seabed, with an average depth of about 15 m b.s.f. The T-reflector, instead, is the top boundary of a unit with a poorly stratified facies

and with a maximum development in the central portion (thickness about 10 m), interpreted as a coastal transgressive wedge that due to its facies probably consists of coarse deposits. Above the T-reflector, a facies characterized by an increase in the acoustic reflection strength coincides with the the highstand wedge, represented by the laterally distal well stratified unchanneled deposits of the delta of the Corriolo River.

Towards the NNE, the **MAG597** seismic profile, located roughly in the central part of the shelf sector 1 (**Fig. 3.12**), shows the L-reflector that is partially exposed at the seafloor in the central portion and increases considerably its depth eastwards, where it reaches at least 60 m of depth b.s.l.

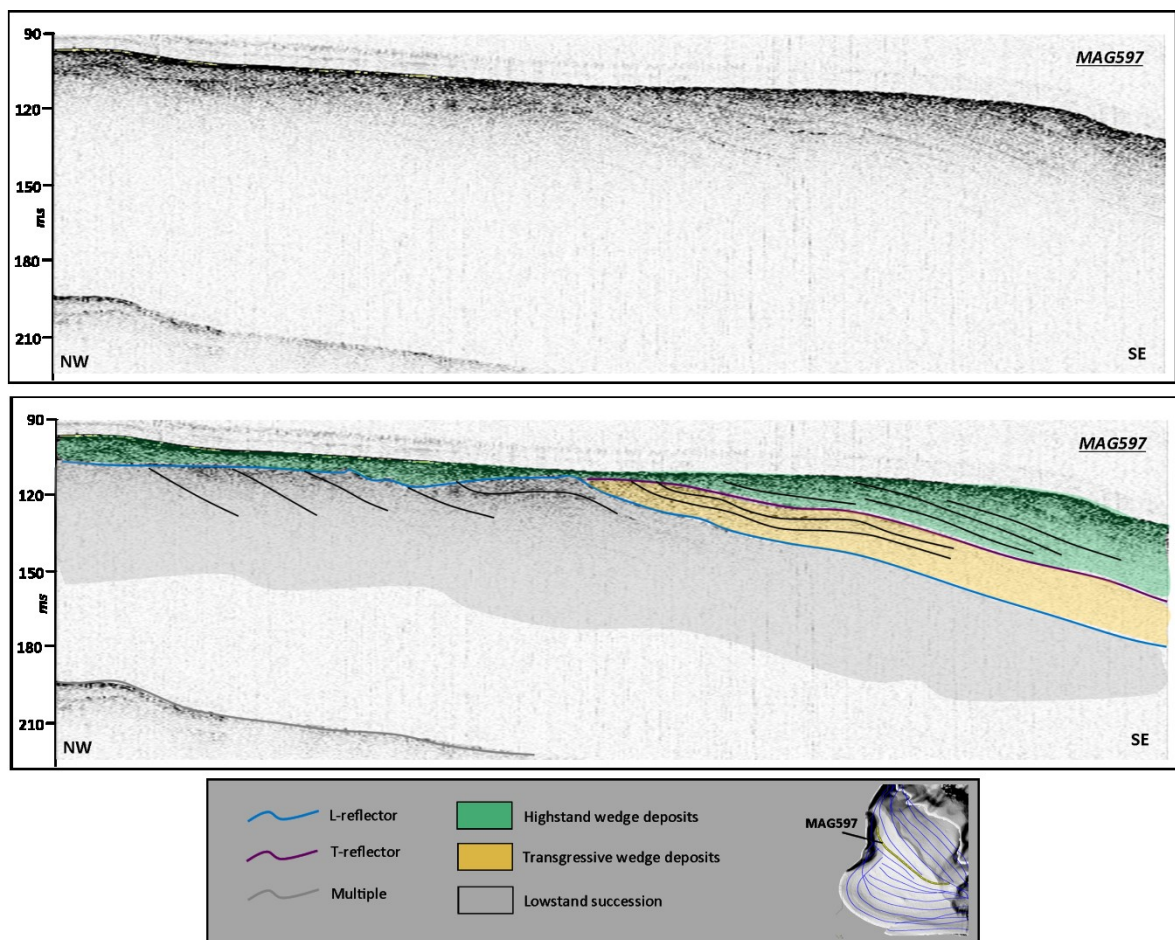


**Fig. 3.12** – The MAG597 CHIRP seismic profile. The interpretation shows that the lowstand succession is almost outcropping at the seafloor in the central portion of the shelf sector n.1 and increases considerably its depth eastward.

In the western portion of the seismic profile there are not evidences of the transgressive wedge deposits. Here, the highstand deposits cover in unconformity the lowstand succession and show a distinctive acoustic facies typical of proximal deposit (relatively coarse deposit) belonging probably to the sediment fed by the eastern coast of the Milazzo Promontory. Eastwards, instead, an evident reflector shows that the transgressive wedge is present above the lowstand succession and characterized by a well-stratified and laterally continuous facies. Upward, this facies is bounded by the T-reflector, on which lies in unconformity another well-stratified deposit interpreted as belonging to distal highstand deposit.

In the seismic profile **MAG564**, located in the outer part of the continental shelf (**Fig. 3.13**), the L-reflector remains at an average depth of about 25 m b.s.f. and roughly follows the bathymetric trend of the seabed.

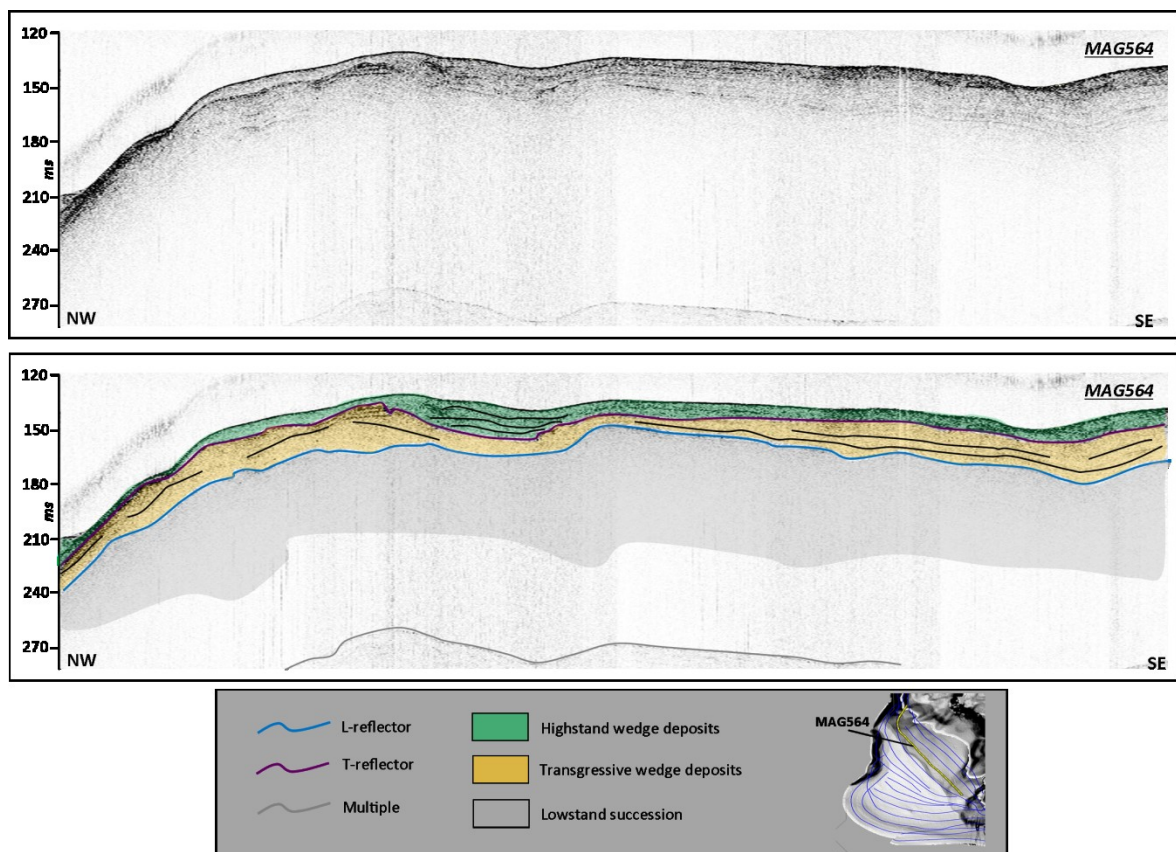


**Fig. 3.13** – The MAG564 CHIRP seismic profile. The interpretation shows the stratigraphic feature of the outer part of the continental shelf sector n. 1.



Above the L-reflector, the transgressive wedge shows along all the profile a well-stratified facies, with thickness decreasing (about 5-7 m) only in central portion, where the T-reflector, that bounds at the top the transgressive wedge, shows an evident channelization. Upwards and along all the seismic profile, the highstand wedge deposits alternate with a well-stratified facies (within the central channelized area) and with poorly-stratified facies in the SE portion, corresponding to coarser deposits.

In the **Fig. 3.14** a schematic geological profile (named *profile 1*), arranged about orthogonally to coastline, has been reconstructed from the intersection of the 15 available seismic profiles in this area. It shows the development and the main stratigraphic features of the transgressive and highstand wedge along this part of the Sicilian continental shelf.

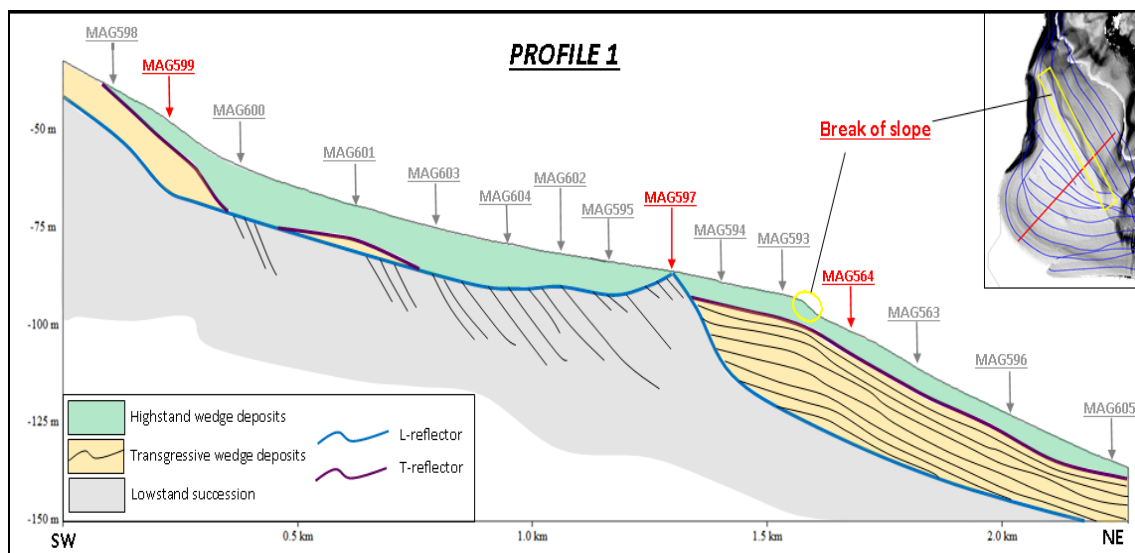


**Fig. 3.14** – The Profile 1, arranged orthogonally to coastline and reconstructed from the intersection of the 15 available seismic profiles, shows the main stratigraphic features of the transgressive and highstand wedges.

In the SW part of the profile, the top of the lowstand succession (L-reflector) maintains a constant depth (about 15 m b.s.f.) and, on the whole, due to the good penetration of the acoustic signal, the falling stage and lowstand deposits are imaged with a stratification dipping to the NE, interpreted here as corresponding with the foreset of the prograding clinoforms of the continental margin successions. In this part of the profile, the transgressive wedge shows a discontinuous development and the thickness of

the deposits tends gradually to zero towards the central portion, where the lowstand succession crops out. In proximity of the seismic profiles MAG601 the deposition of the transgressive facies shows a convex up body. Therefore, in this part, the highstand wedge deposits widely cover directly in unconformity the lowstand succession. Furthermore, the seabed morphology (slightly concave) is equivalent to trend of the erosional surface of the lowstand (see L-reflector trend), highlighting that it the highstand deposits uniformly draped the lowstand erosional surface.

In the central part of the *profile 1*, a widespread break of slope is present (extended in NW-SE direction for about 2500 m) (**Fig. 3.14**). It was interpreted by Gamberi et al. (2014) as a normal fault but that the seismic stratigraphic interpretation in this thesis does not highlight any offset of recent sediments and thus an interpretation as due to depositional processes is here preferred.

Seawards from this break of slope, in the NE part of the profile, the L-reflector tends quickly to deepen, due to a sudden gradient increase to about 6°. The lowstand bedding is not imaged in the seismic profiles of the area, probably owing to the greater thickness of the overlying succession, belonging to the transgressive deposits. In particular, the transgressive wedge shows a significant and constant thickness (about 20 m), with a maximum lateral development of a well-stratified facies typical of distal deposits. Upwards, the T-reflector bounds the base of the highstand wedge that, conversely, shows a poorly-stratified facies and characterized by a small and regular thickness (5-7 m).

In synthesis, in the shelf sector n. 1, the transgressive wedge deposits are characterized by marked areal variations in their seismic facies. In particular, some areas without transgressive deposition (to the SW) alternate with the areas (toward the NE) where the deposition is significant and laterally continuous. In order to reconstruct and identify these variations an isopach map of the transgressive wedge thickness has been produced (**Fig. 3.15**).

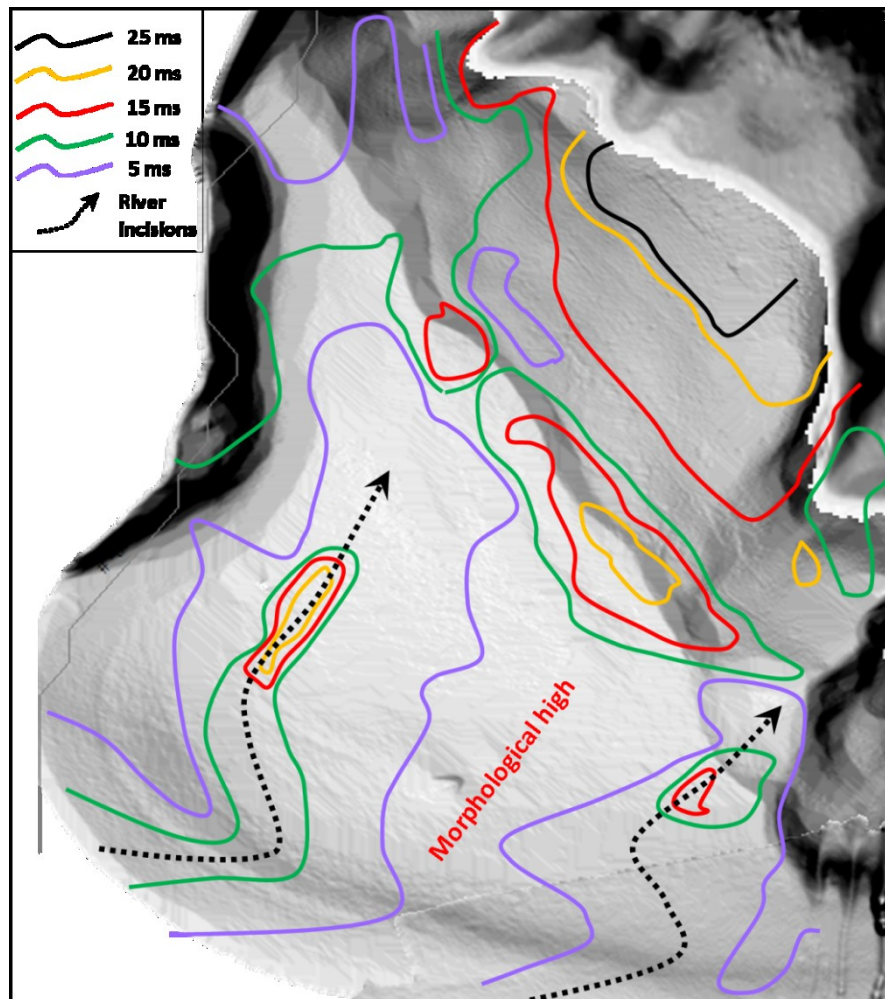


**Fig. 3.15** - Isopach map (in ms) of transgressive deposits in sector 1. The black arrows show the main direction of the paleo-river incisions.

The isopach map shows two areas elongated in about NNE-SSW direction, with two depocenter points respectively to 20 m and 15 m, and interpreted as the paleo-river incisions and separated by a morphological high where the transgressive deposits are absent. The isopach map (**Fig. 3.15**) shows the main direction of the paleo-river incisions. The direction of these paleo-river incisions is congruent with the present position of the canyons heads, and in particular of the Corriolo canyon, where the rivers tended to discharge their deposits during the last sealevel rise .

Furthermore, in the shelf sector n. 1, the highstand wedge reaches a bathymetry of at least 150 m, at a distance from the coast of about 3.3 km. This significant areal development may be due to: i) abundant supply by the Corriolo river or ii) oceanographic

processes connected with the physiographic trend of the Capo Milazzo that represents an obstacle to long-shore sediment transport and capture sediments.

### 3.4.2.2 Shelf sector n. 2

The shelf sector n. 2 (area of about 20 km<sup>2</sup>) is located in a sector dominated by the Corriolo, Muto and Niceto canyons and developed in front of the homonymous rivers (Fig. 3.16).

The Corriolo canyon head has a semi-circular area with a width of about 2 km and is characterized by a sudden gradient increase to 12° seawards (*profile 2*; Fig. 3.16). Upslope from the canyon head, a channelized area is present on the shelf, with a gradient of about 5° (Fig. 3.16).

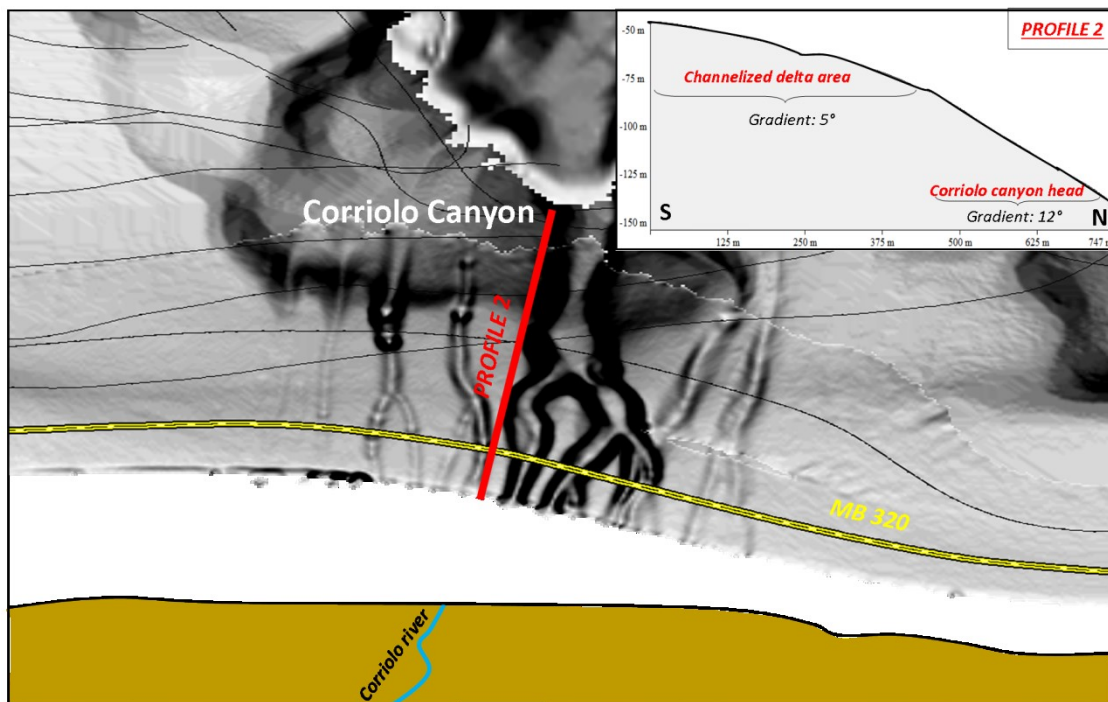


**Fig. 3.16** – Location of the profile 2 and the MB320 CHIRP seismic profile in proximity of the Corriolo canyon. The profile 2 shows the gradient variation in proximity of the Corriolo canyon head area.

In Fig. 3.17, in order to evidence the morphology and stratigraphic features of the channelized area, a comparison between bathymetric (*profile 3*) and CHIRP data is provided (MB320 CHIRP seismic profile). In particular, two main channels, which are 15 m

deep and 150 m wide, are located in front of the Corriolo river mouth, which is only 800 m shorewards. Smaller channels are present eastwards and westwards from the two main ones, showing decreasing relief on a seabed that gently slopes westwards from the main channels (**Fig. 3.17a**).

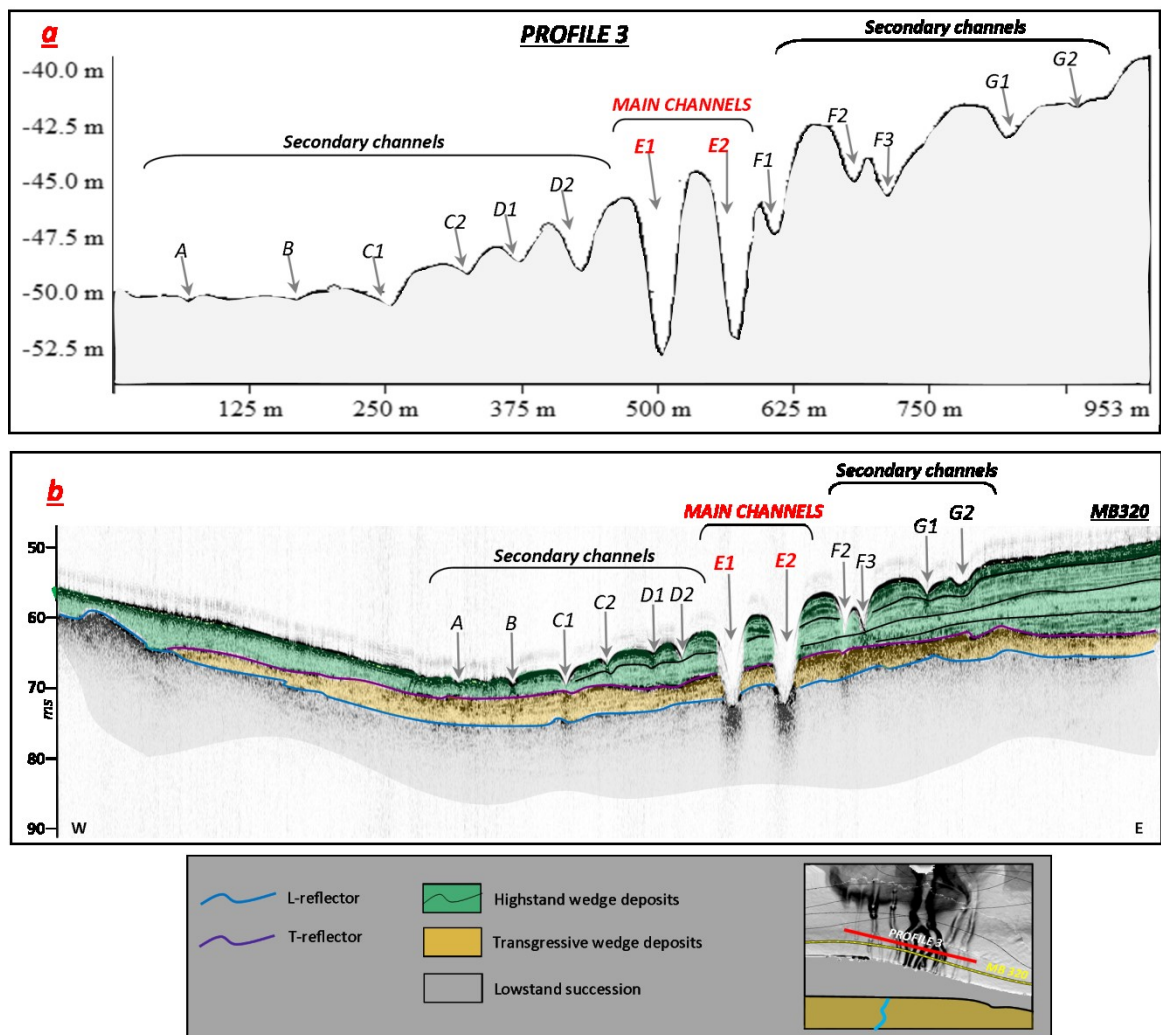


**Fig. 3.17** - Comparison between the bathymetric profile 3 (**Fig. 3.17a**) and the MB320 CHIRP seismic profile (**Fig. 3.17b**).

The MB320 seismic profile (**Fig. 3.17b**) shows that the erosional activity is focused within the two main channels, while the adjacent smaller channels have a more marked depositional character. This area is interpreted as the channelized offshore part of the Corriolo river delta.



Also in this sector, the L-reflector and the T-reflector have been well-recognized within the available CHIRP seismic profiles (MB320; **Fig. 3.17b**). The first reflector bounds the base of a poorly-stratified transgressive wedge that shows a lateral constant thickness (about 5 m) along the whole of the profile. The second reflector, instead, bounds the base of the highstand wedge, represented by the delta convex up deposits of the Corriolo River, that tend to deepen and thin to the west of the two main channels. As a result, the overlying highstand wedge deposits show a thickness increase eastward, where it reaches about 15 m. Therefore, on the whole, the Corriolo delta shows the physiographic feature of an asymmetric delta. Furthermore, eastward, some secondary acoustic reflectors within delta deposits have been detected (**Fig. 3.17b**), and correspond with the boundaries of the depositional units that are well represented especially in the shelf sector n. 3 and that will be described in the next chapter (see chapter 6.2.3).

The Muto canyon head has a semi-circular area characterized by a sudden increase of the seafloor dip to  $15^\circ$  (*profile 4*), occurring at about 80 m water depth (**Fig. 3.18**). Landward, the shelf is less steep with a gradient of about  $4^\circ$  and consists of a channelized area that connects with the eastern portion of the Niceto canyon head (**Fig. 3.18**).

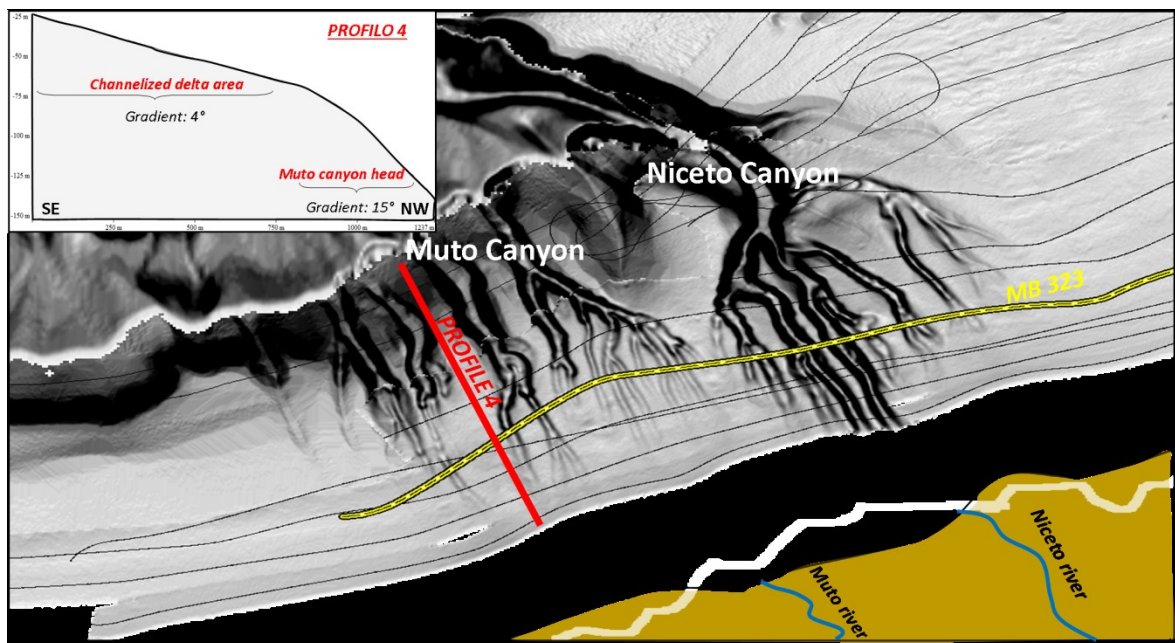


**Fig. 3.18** – Location of the profile 4 and the MB323 CHIRP seismic profile in proximity of the Muto and Niceto canyons. The profile 4 shows the gradient variation in proximity of the Muto canyon head area.

Towards the east, further channels face the Muto river mouth with a relief that decreases progressively westward. The MB323 CHIRP seismic profile (crossing also the channelized area of the Muto delta; **Fig. 3.18**) shows that the channels could be erosional or depositional, whereas the inter-channel areas are always depositional (**Fig. 3.19**). The delta of Muto and Niceto delta tend partly to overlap forming a coalescing delta structure. The numerous channels show essentially depositional character, except for two main erosional channels of the Niceto delta located directly off the mouth of the Niceto River (**Fig. 3.19**).

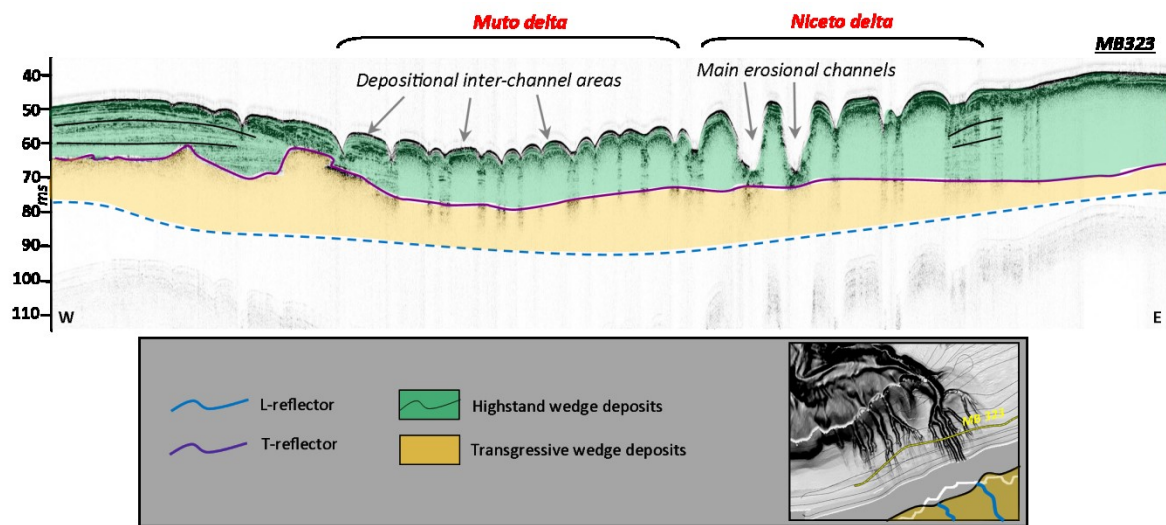


**Fig. 3.19** – The MB323 CHIRP seismic profile shows that the channels could be erosional or depositional, whereas the inter-channel areas are always depositional.

The MB323 CHIRP seismic profile, acquired at a distance of about 1 km off the coastline, shows that the largest channels are located eastwards and directly face the Niceto river mouth. A network of smaller tributary channels joins the main channel.

In proximity of the Muto and Niceto rivers, the significant thickness of the highstand wedge deposits (20 m on average) probably restricts the penetration of the acoustic signal and, therefore, only the T-reflector has been identified and no information is provided about the lowstand succession (**Fig. 3.19**). Here, the acoustic facies of the highstand wedge is widely transparent in the central portion, but below the channels and moving away from channelized area, the acoustic facies show a stratified succession.



### 3.4.2.3 Shelf sector n. 3

The shelf sector n. 3 (area of about 40 km<sup>2</sup>) is comprised between the eastern portion of the Niceto delta and the Saponara delta (**Fig. 3.10**).

To the west, the area between the Niceto and Cocuzzaro canyon heads is characterized by downslope convex contours, straight central channels and bedforms (**Fig. 3.20**). The straight central channels die out downslope, whereas the lateral channels converge seawards into the Cocuzzaro and the Niceto canyon heads. This area is interpreted (in agree with Gamberi et al., 2014) as the offshore channelized eastern continuation of the Niceto river delta. This part is also characterized by the presence of bedforms, which have 50–100 m wavelength and are 0.5–1.5 m in height.

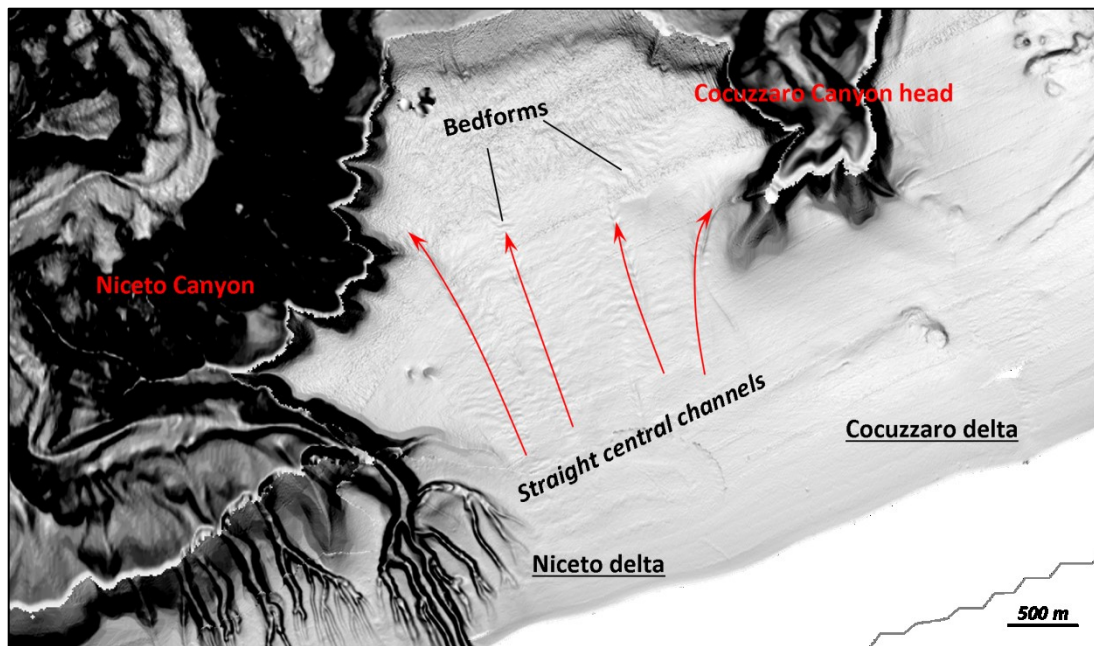


**Fig. 3.20** - The area between the Niceto and Cocuzzaro is interpreted as the offshore channelized eastern continuation of the Niceto delta and is characterized by downslope convex contours, straight central channels and bedforms.

Eastwards, the offshore part of the Cocuzzaro delta has a relief of only 2.5 m and, at a depth of about 50 m, and a width of 1 km. Further downslope, a narrow, 20 m wide and 0.5 m deep channel develops and connects with the Cocuzzaro Canyon head.

The analysis of the numerous CHIRP seismic profiles available in this area has allowed to characterize the highstand wedge deposits, belonging to Cocuzzaro and

Rometta delta deposits. The MB327 seismic profile (**Fig. 3.21a**), located close to the coastline, covers an extended portion of the Cocuzzaro and Rometta delta in the inner portion of the continental shelf. In this area, only the highstand and transgressive wedge are visible and, therefore, the L-reflector, bounding the top of the lowstand succession, is not image. In fact, here, the thickness of the highstand wedge deposits is very consistent (up to 30 m) and the penetration of the acoustic signal is too low. Within the thick highstand wedge, six depositional units have been distinct based on their acoustic facies variations (**Fig. 3.21a**). They show the maximum vertical and lateral development in the inner continental shelf.

The **Fig. 3.21a**, **Fig. 3.21b** and **Fig. 3.21c**, show the distribution and thickness of these six depositional units respectively from the inner to the outer part of the continental shelf, on the basis of the interpretation of three seismic profiles (MB327, MAG559 and MAG552).

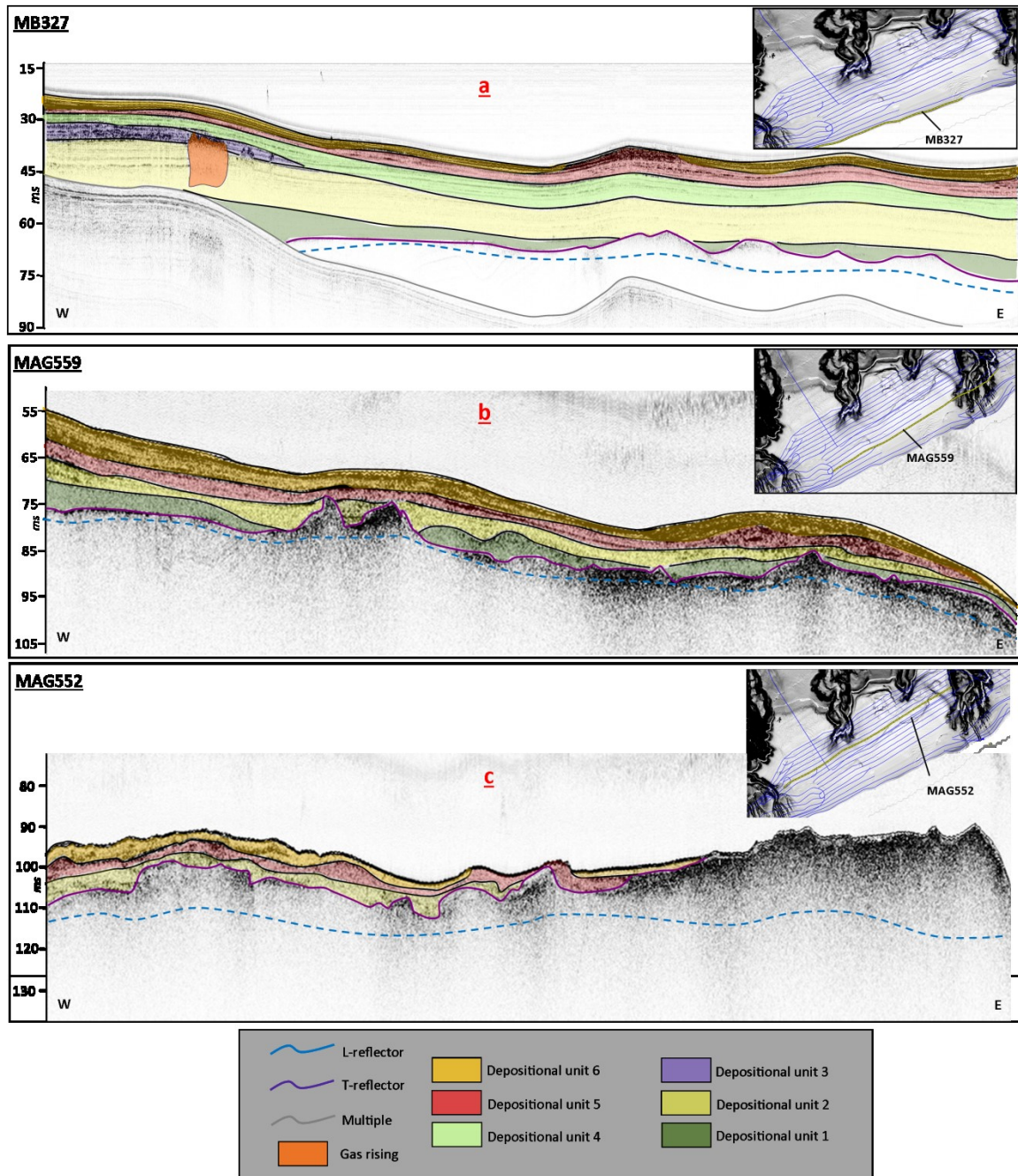


**Fig. 3.21** - On the basis of the interpretation of three CHIRP seismic profiles MB327 (**Fig. 3.21a**), MAG559 (**Fig. 3.21b**) and MAG552 (**Fig. 3.21c**), the areal development of the six depositional units - from the inner to the outer part of the shelf sector n. 3 - is provided.

In the following, the main features of these depositional units are reported and in **Fig. 3.22** their areal distribution along the shelf sector n. 3 is shown:

- the depositional unit 1 (DU1) is the deepest unit, drapes unconformitably the T-Reflector and its lateral continuity along the continental shelf is interrupted by a morphological high in the underlying transgressive wedge;

- the depositional unit 2 (DU2) shows a significant and constant thickness (about 10 m) and it is characterized by a partially transparent facies with a good lateral continuity;
- the depositional unit 3 (DU3) is part of the delta deposits of the Cocuzzaro River and represents an example of distribution of a coarse grained body;
- the depositional unit 4 (DU4) shows a decrease of the thickness (about 7 m) and a lower areal extension, and therefore is interpreted as corresponding with a phase of minor feeding;
- the depositional unit 5 (DU5), conversely, represents an increase of the fluvial supply in the area (greater areal extension; **Fig. 3.22**) and consists of fine grained sediments, as also demonstrated by the well-stratified acoustic facies. It is interpreted as a coalescing phase of the Cocuzzaro and Rometta deltas;
- the depositional unit 6 (DU6) is characterized by very high reflectivity and marks a facies laterally continuous, with a low thickness (< 5 m). Its distribution extends into the outer shelf up to the depth of 85 m, and along a narrow central portion is missing (**Fig. 3.22**). This highlights that in the last phases of the highstand evolution, the Cocuzzaro and Rometta deltas show an independent development.



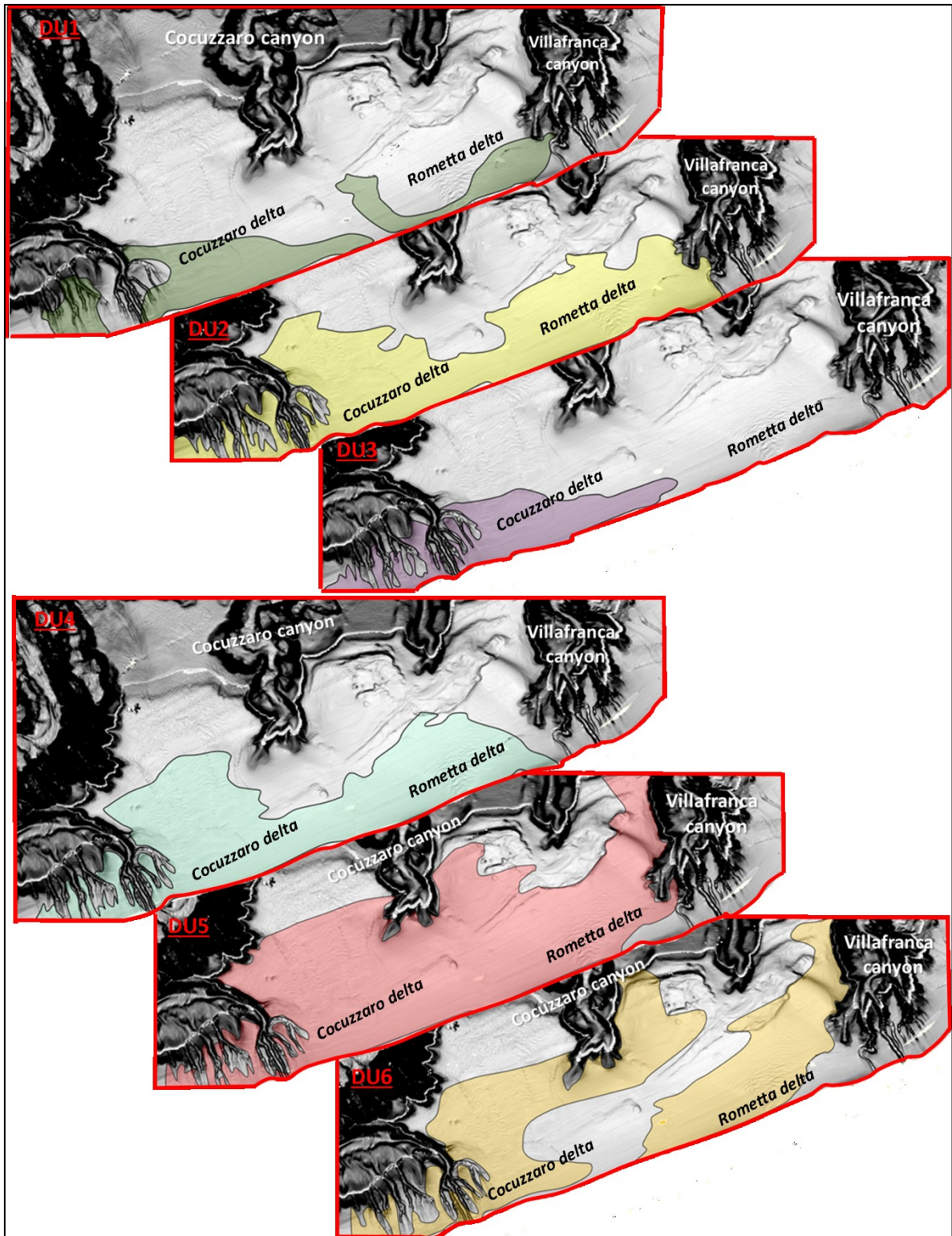


**Fig. 3.22** – Map of the distribution of the six depositional units (DU) belonging to Cocuzzaro and Rometta delta and representing the highstand wedge of the shelf sector n. 3.

Towards the outer part of the continental shelf the continuity of the depositional units considerably decrease and their thickness is on average lower. In 2 km from the coastline, the number of the depositional units decreases from 6 to 3 units (**Fig. 3.21c**) and the thickness of the highstand wedge does not reach the 10 m. In particular, in proximity of the Rometta canyon head, none of the six units occur, and, as a result, the transgressive wedge deposits are exposed widely in the seafloor.

The N-S bathymetric *profile 5* (**Fig. 3.23**; **Fig. 3.24a**) crosses the area located between the Cocuzzaro and Rometta canyons. At a depth of 117 m, the slight convexity of the seabed contours is interpreted as a beach wedge that covers an area of 0.2 km<sup>2</sup>. This beach is located at the basis of a cliff (named here Cliff 1) elongated in ENE-WSW direction for about 1.4 km with a linear trend. With a gradient of 12°, the Cliff 1 reaches a depth of 94 m and is interpreted as the step 1 of the lowstand succession on which the transgressive wedge develop.

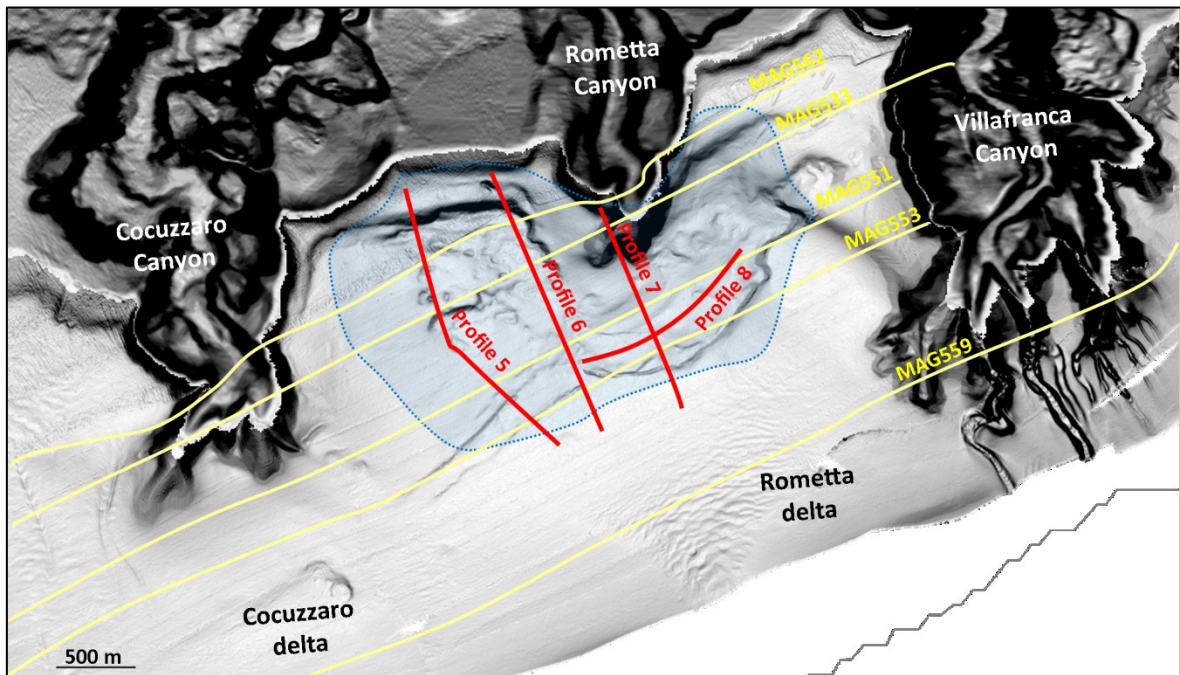


**Fig. 3.23** – Location of the CHIRP seismic profiles (in yellow) and the profiles 5, 6, 7 and 8 (in red) interpreted for the stratigraphic characterization of the area between the Cocuzzaro and Villafranca canyons.



At a depth of 91 m, the irregular morphology of the seabed corresponds with the development of transgressive body (A) extended in N-S direction for about 200 m and characterized by an asymmetric morphology: its northern side shows a gradient of 8° and its southern side shows a gradient of 2° (**Fig. 3.24a**). The MAG562 seismic profile (**Fig. 3.24b**) shows that the transgressive body A corresponds with (thickness of about 5 m) an area characterized by a very reflective acoustic facies

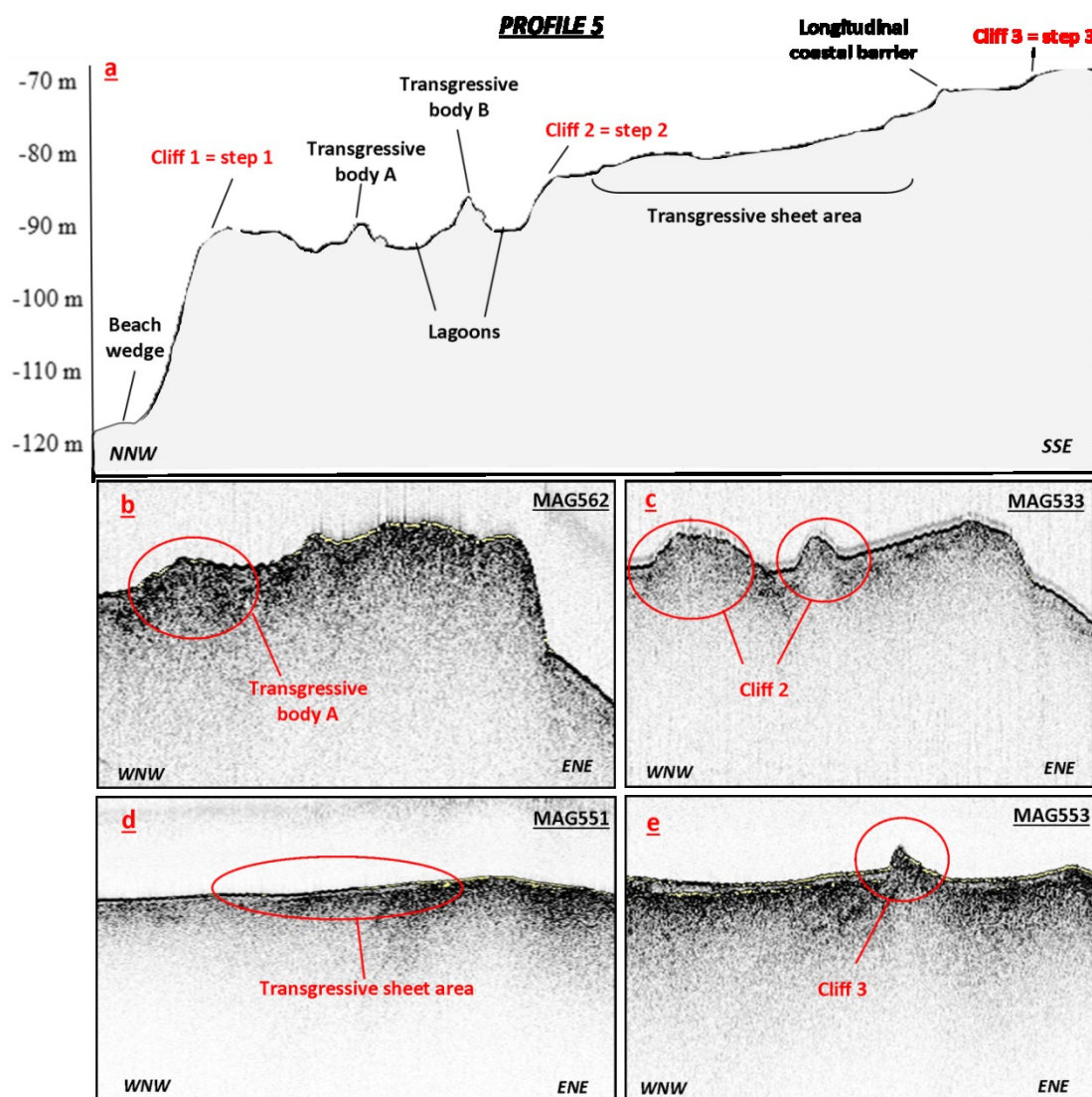


**Fig. 3.24** – The profile 5 (**Fig. 3.24a**) shows main morphological features located between Cocuzzaro and Rometta canyons. The **Fig. 3.24b** shows the acoustic facies of the transgressive body A along the MAG562 CHIRP seismic profile. The **Fig. 3.24c** shows the development of the Cliff 2 along the MAG533 CHIRP seismic profile. The **Fig. 3.24d** shows the transgressive sheet area along the MAG551 CHIRP seismic profile. The **Fig. 3.24e** shows the acoustic facies of the Cliff 3 along the MAG553 CHIRP seismic profile.



Southwards, at the back of the transgressive wedge A, a morphological depression is present on the seafloor with a slight concavity of the contours (**Fig. 3.24a**). At a depth of 89 m a further symmetric (both sides with a gradient of about 6-7°) transgressive body (B) is detected. It shows a thickness of about 5 m and, as the transgressive body A, it is flanked landwards by a further depression. The significance of these depressions and transgressive bodies can be at least three: i) a landward shift during sea level rise of two transgressive barrier-lagoon system; ii) erosional activity by tidal current or oceanic waves; iii) different morphology of the base level (that is the underlying lowstand succession). The bathymetric data and the chirp profiles are more in agreement with hypothesis 1 thus the transgressive bodies A and B probably represent two coastal barriers that were flanked landwards by a small lagoon.

Southwards, at a depth of 84 m, the *profile 5* shows another cliff (named here Cliff 2) with a gradient of about 12°. The MAG533 seismic profile shows the acoustic features of the Cliff 2, characterized by a very reflective facies (**Fig. 3.24c**). It is interpreted as the step 2 of the lowstand succession and represents a new base level on which further transgressive bodies develop. From a depth of about 87 m, the seabed morphology shows a roughly flat area (about 0.1 km<sup>2</sup>) that extends up to a depth of 72 m and that is here interpreted as a reworked transgressive sheet (**Fig. 3.24d**) connected probably to an high power of waves (or tidal currents) that did not allow the same preservation as seen in the deeper transgressive bodies A and B. The development of this wide transgressive sheet ends at a depth of 72 m in proximity of a morphological high with a gradient of about 7°. It shows good lateral development in NW-SE direction for at least 900 m, keeping markedly a straight trend, and is interpreted as a further longitudinal coastal barrier. Only 150 m southwards, at the depth of 68 m, a further slight morphological (gradient of about 4°) variation on the seafloor dip represents a gentle cliff (named here Cliff 3) partially draped from the delta depositional units that tend to close their deposition in this area. The Cliff 3, well-image also in the MAG553 seismic profile (**Fig. 3.24e**), is interpreted as the step 3 of the lowstand succession covered from the highstand wedge deposits, belonging to the delta deposits of the Corriolo and Rometta rivers.

The bathymetric *profile 6* (**Fig. 3.23; Fig. 3.25**), located 500 m northeastwards of the *profile 5*, confirms the development also in this area of many of the geomorphological

features described previously. Also in this area, but at a depth of about 100 m, is present the continuation of the Cliff 1 (gradient of 11°), representing the step 1 of the lowstand succession. At its base (depth of 112 m), a marked convexity of the contours bounds a narrow and elongated body with a relief of about 5 m elongated in NW-SE direction. The latter is interpreted as a coastal spit, probably formed owing to continuous sediment reworking and transport due to wave action.

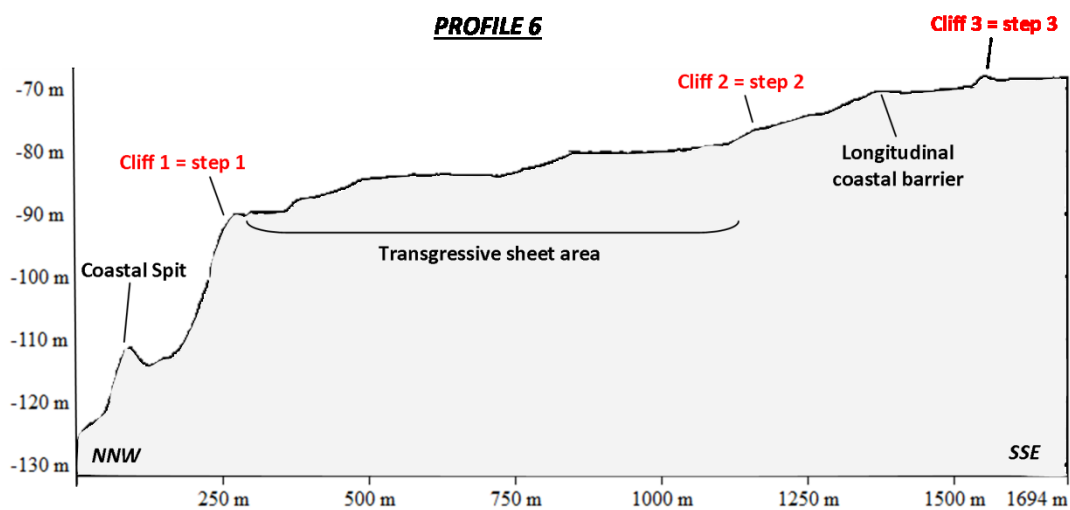


**Fig. 3.25** - The profile 6 shows the presence of several geomorphological features between the Cocuzzaro and Rometta canyons, with a significant areal development of the transgressive sheet area.

Above the Cliff 1, at a depth of 90 m, the slight vertical variations of the bathymetric trend show the presence of widely extended transgressive bodies. They are interpreted as genetically equivalents to the transgressive bodies A and B seen above (**Fig. 3.24b**), but characterized by a minor vertical development and a greater areal extension (about 0.17 km<sup>2</sup>), probably owing to the lateral increase of the action of the oceanographic currents. These transgressive bodies end southwards in proximity of a morphological variation, at a depth of 82 m, and corresponding to a morphological high (gradient about 8°) interpreted as the northeastward continuation of the Cliff 2 (well-imaged also in the MAG 533 seismic profile; **Fig. 3.24c**). Above this latter, interpreted as the step 2 of the lowstand succession, the morphological features are very similar to those seen in the *profile 5*, with only some little bathymetric variations. In fact, from 79 m to 73 m of depth the bathymetric data show the development of the wide transgressive sheet, as imaged in the MAG 551

seismic profile (**Fig. 3.24d**). Southward, at a depth of 72 m, the lateral continuation of the longitudinal coastal barrier is present. And finally, at a depth of 68 m, the continuation of the Cliff 3 develops and is interpreted as the step 3 of the lowstand succession.

The bathymetric *profile 7*, instead, shows a transgressive wedge with some different morphological features (**Fig. 3.26a**). It is located parallel to the two previous profiles (**Fig. 3.23**), but in a sector dominated by the Rometta canyon head. In fact, the northern portion of the *profile 7* shows the Rometta canyon edge, has a gradient of 14°. Southwards, the depth of the 84 m represents the break of slope of the Rometta canyon edge and, roughly, corresponds with the continuation towards the east of the Cliff 1 that here reaches lower depth. This break of slope bounds the base of a first morphological body characterized by a slight convexity in the contours. Also the MAG551 seismic profile shows the morphology of this sector (**Fig. 3.26b**). It is interpreted as a transgressive body (C) that extends along an area of about 0.1 km<sup>2</sup>, up to a depth of about 79 m.

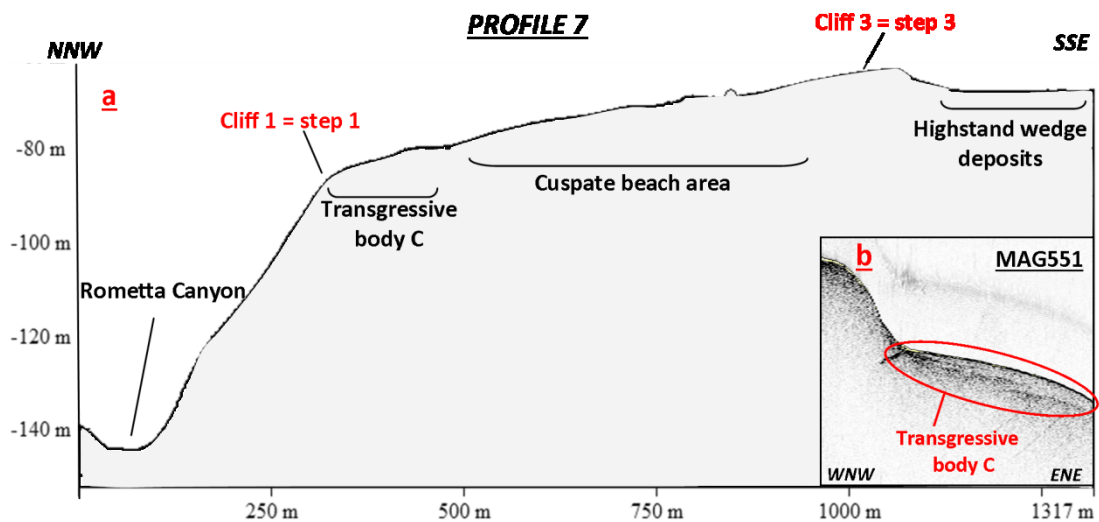


**Fig. 3.26** - The profile 7 (**Fig. 3.26a**) is located in a sector dominated by the Rometta canyon head and shows a transgressive wedge with several morphological structures. In particular, the MAG551 CHIRP seismic profile (**Fig. 3.26b**) shows the transgressive body C.

The transparent high reflective seismic facies is indicative of coarse grained facies and highlights that is probably formed by reworked deposits, connected to an intense wave action. From 79 m to 68 m of depth (Fig. 20), a sector characterized by a low gradient (on average <math><1^\circ</math>) occurs along an area of 0.5 km<sup>2</sup>. Here, the contours, with

cusate trend, cover a length of about 1 km and bound some preserved beach bodies with a vertical development of 1.5 m and a gradient of about 1°, interpreted as cusate beaches. The *profile 8* (**Fig. 3.27**), located orthogonally to the others bathymetric profiles shows the geometry of the cusate beaches and their areal development.

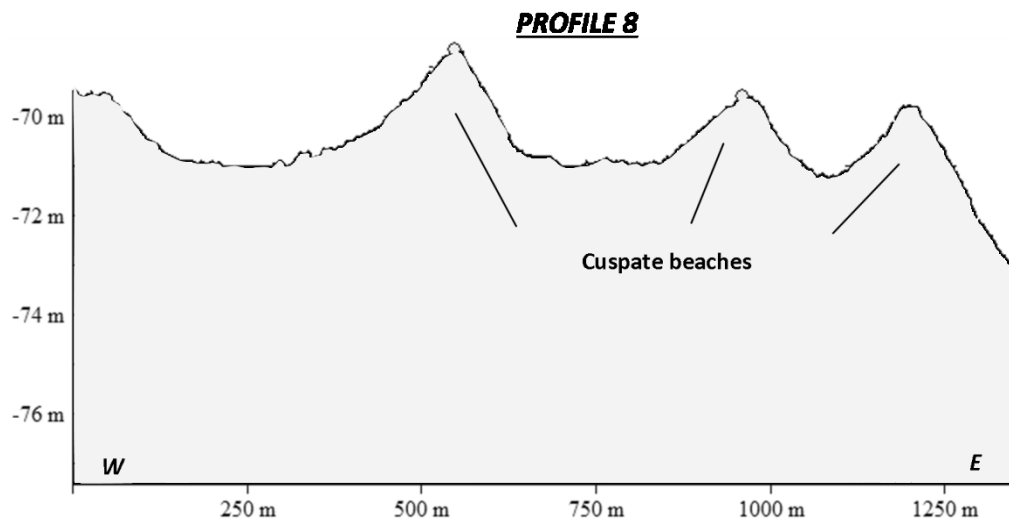


**Fig. 3.27** - The profile 8 shows the geometry of the cusate beaches located in front of the Rometta canyon head.

Southwards (*profile 8*; **Fig. 3.27a**), at a depth of 68 m, the cusate beaches end in proximity of an important morphological variation on the seafloor characterized by a gradient of 4°. It is interpreted as the eastern continuation of the Cliff 3 that in this sector shows overall a concavity seawards. Also in this area, above the Cliff 3, the highstand wedge deposits of the Rometta delta develop widely.

In the inner shelf, to the west of the Villafranca Canyon head, an area with seaward convex bathymetric contours is present. It is located offshore from the Rometta delta and, for this reason, is interpreted as representing its delta front offshore continuation. It has a gradient that from 3° at a depth of 50 m decreases to 1° distally. The delta is 1200-m wide and 6-m high at a depth of about 47 m, being about 2-km wide and only 4-m high at a depth of about 55 m.

Sandwaves occur widespread over the whole surface of the Rometta delta offshore continuation (**Fig. 3.28a**). The sandwaves in front of the delta extend into deeper water eastwards, showing that the delta is asymmetric. The delta asymmetry is confirmed by

the 559 seismic profile (**Fig. 3.28b**), showing that its upward convex lens of sediment with strong and discontinuous reflection thin eastwards, approaching the head of the Villafranca Canyon.

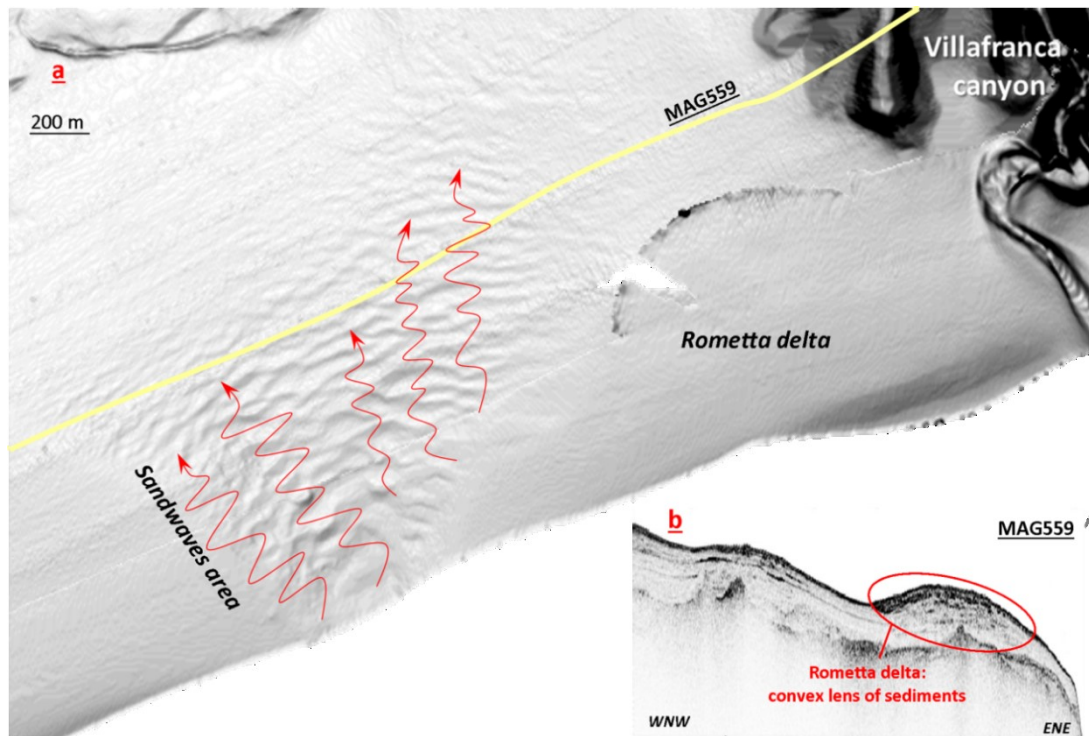


**Fig. 3.28** – The multibeam data show sandwaves area in front of the Rometta delta, extend into deeper water northeastward (**Fig. 3.28a**). Along the MAG559 CHIRP seismic profile, an upward convex lens of sediment (**Fig. 3.28b**) shows the stratigraphic features of the Rometta delta.

### 3.4.3 DISCUSSION

The study area is characterized by several geomorphological elements, belonging to three different sedimentary successions deposited during the last regressive-transgressive cycle.

The lowstand succession is bounded at the top by a widespread erosional surface (L-reflector) and represents the base level of the depositional units formed during the last sea level rise and highstand of the sea level. The evolution of the transgressive and highstand wedges is strongly influenced by the geometry and location of the underlying lowstand succession that shows overall a relatively smooth surface. In fact, the depositional volume and the topmost morphology of the lowstand succession determines

the accommodation space for the sediment that accumulate during the rise of the sea level. For example, along the shelf sector 1 and 2, the seabed morphology is often equivalent to the trend of the erosional surface of the lowstand (L-reflector). Therefore, the highstand wedge tends to drape the base level consisting of the top of the lowstand succession or, locally, of the overlying transgressive deposits. Furthermore, in some areas, where the transgressive and highstand wedges do not show a consistent thickness, the seismic profiles allow to image the lowstand succession (for example in the central portions of the Corriolo delta), formed by clinoforms of continental margin.

The transgressive wedge is bounded at the top by the Maximum Flooding Surface (T-reflector) and consists of the relict geomorphic elements that represent past landscape. These elements include coastal barrier-lagoon systems formed at different locations on the shelf and, therefore, track the variations in coastline position during the last sea-level rise. Past coastal systems are mainly developed in the 80-100 m bathymetric range. The last sea level rise has not occurred continuously but has proceeded in steps, with tracts of rapid rising punctuated by periods of relatively slower rates of rise (Fairbanks, 1989; Lambeck et al., 2011). One of the tracts with a relatively lower rate of rise of seafloor occurred when the sea level rose from about 90 to 70 m below its present position. This corresponds with the depth where, in the northeastern Sicilian relict outer shelf, the coastal systems are best developed. Therefore, in accordance with Gamberi et al., (2014), the transgressive geomorphic elements in the study area could have formed during an interval of relatively reduced rate of sea level rise.

In the study area the highstand wedge is limited to the inner shelf not reaching depths higher than 85 m, leaving sometimes uncovered the past coastal system outcropping at the seafloor of the outer relict shelf. Since the relict shelf areas are located in correspondence with smaller rivers, it is evident that it is the amount of sediment input from the rivers that controls the seaward extent of the inner shelf highstand wedge and the presence of a relict outer shelf. The Corriolo, Muto, Niceto, Cocuzzaro and Rometta delta deposits widely develop on the offshore portions of the inner continental shelf and make up most of the prograding highstand sediment wedge of the study area. The bathymetric data image the deltas from a distance of 600 m from the coastline at an average depth of 40 m. On the whole, the sector shelf 1 and 2 show the development of

the deltas very near to canyon heads also through numerous terminal distributary channels. Conversely, the sector shelf 3, through the greater accommodation space, due to a wider shelf, (about 20 km<sup>2</sup>), allows the maximum areal development of the delta deposits, in particular of the Cocuzzaro and Rometta rivers.

#### **3.4.3.1 Last transgressive stage reconstruction**

With the support of 3D bathymetric maps (output data of Global Mapper software), in the following section, a reconstruction of the geomorphological evolution of past coastal systems during the last transgressive stage is provided. In particular, in the study area there is a portion of the shelf sector 3, where the transgressive wedge widely crops out and some relicts of the lowstand succession are still evident along the current seafloor.

##### *Sealevel -120 m (Fig. 3.29):*

At this time, the Cliff 1 and Cliff 3 already represent the basement of the continental shelf sector and represent respectively the step 1 and step 3 of the lowstand succession on which in particular the transgressive wedge develop. On the basis of the large lateral extension, the Cliff 1 and Cliff 3 are interpreted as connected to regional dynamics, and step in the rate of sea level drop during the last sealevel fall are envisaged as being responsible for these terrace development. Instead, the Cliff 2 (step 2 of the lowstand succession), owing to its smaller areal development, is interpreted as connected to local dynamics and fluvial erosional activity or different lithological features can be advocate for its development.

Wave action tends to support the formation of the beach wedge and of the spit around the basis of the Cliff 1 (in the central portion), while the overlying regressive beach bodies probably undergo sub-aerial erosional activity.

Furthermore, the bathymetric morphology, at a depth in 85-70 m range, suggests that at least three fluvial incisions (named here River 1, River 2 and River 3) affected the shelf sector when the sealevel was at -120 m. In particular, the contour trend on the seafloor evidences that the River 2 flowed directly into the Rometta canyon head.



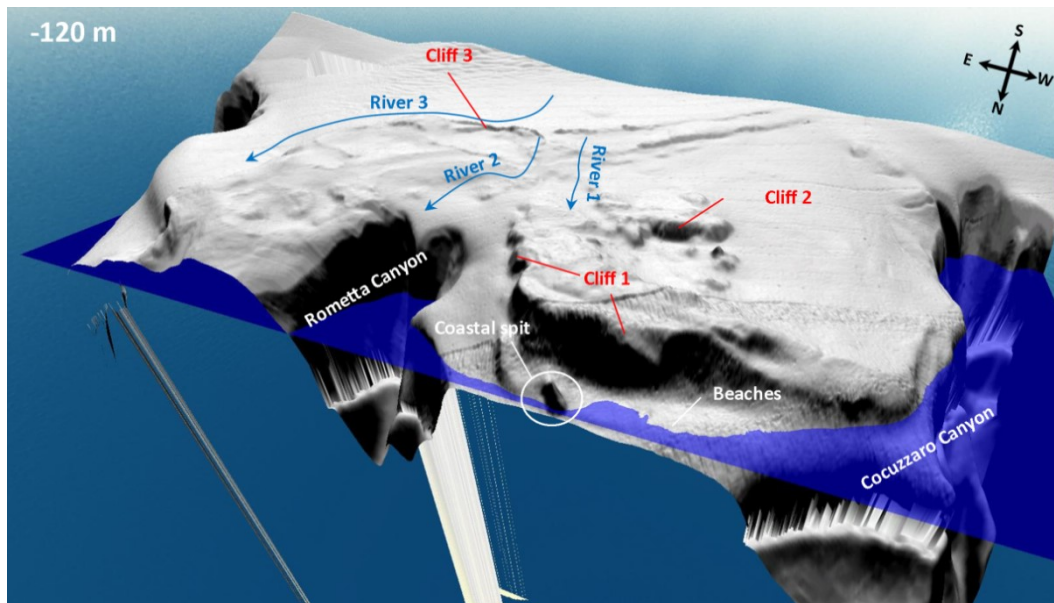


**Fig. 3.29** – On the basis of 3D bathymetric map, reconstruction of the geomorphological evolution of past coastal systems of the area between the Cocuzzaro and Rometta canyons, simulating a sealevel of -120 m.

**Sealevel -100 m (Fig. 3.30):**

This step of sea-level rise evidences that the Cliff 1 has not the same slope along the shelf sector 3, but it dips few degrees towards the west. In fact, the central and eastern portions of the Cliff 1 are not yet submerged and, conversely, the western portion is interested by the formation of beach bodies (beach area 1). The latter represents the first deposits named here the overstep 1.

In the central portions of the continental shelf the geomorphological features do not change, because the Cliff 1 still represents a high coast and the rivers can still feeds the outer part of the continental shelf.

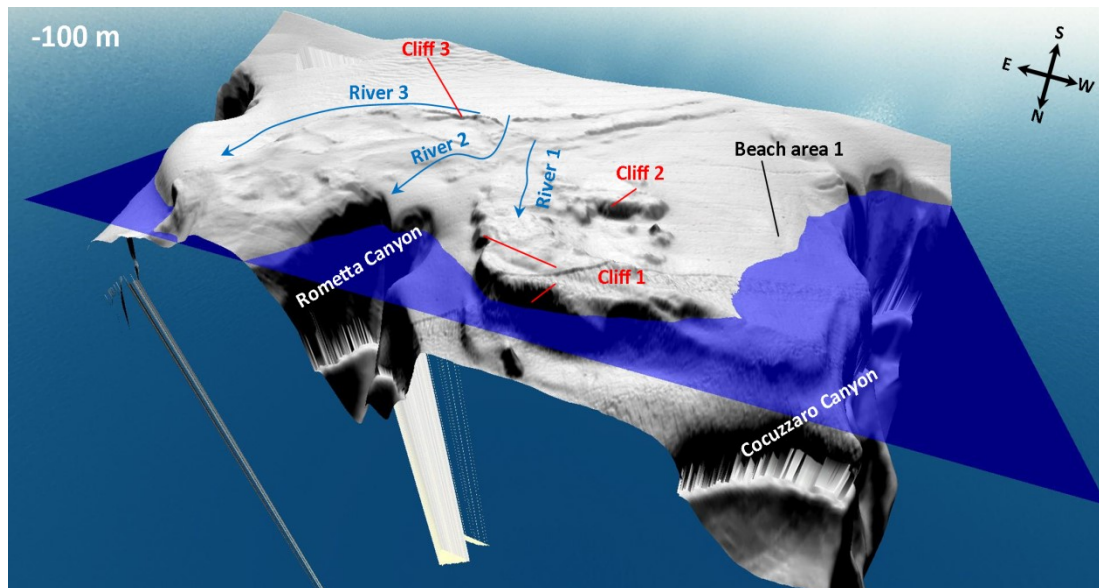


**Fig. 3.30** – On the basis of 3D bathymetric map, reconstruction of the geomorphological evolution of past coastal systems of the area between the Cocuzzaro and Rometta canyons, simulating a sealevel of -100 m.

*Sealevel -90 m (Fig. 3.31):*

When the sea level reaches -90 m also the Cliff 1 is completely submerged. In this phase is evident as the rise of the sealevel causes a different development of the fluvial incisions. The River 1 tends to branch in more parts (with the formation of distributary channels) and, westwards, it changes its direction through a curvilinear trend. Where the River 1 flows until the sea, an estuarine system develops. The **Fig. 3.31** shows in particular two survivor parts of a past single longitudinal coastal barrier and the lagoon at the back. These represent new transgressive bodies belonging to the overstep 1 deposits. Furthermore, with the gradual and progressive rise of the sea level (-85 m), they tend to extend mainly in proximity of the Rometta canyon head, but here they show a greater areal development.

Simultaneously, the western sector is totally submerged and probably the intense oceanic current does not allow the preservation of the beach bodies (transgressive sheet area; **Fig. 3.31**). In the eastern part of the continental shelf, the rivers do not change their trend and the wave action tends to develop only small beach bodies (beach area 2).

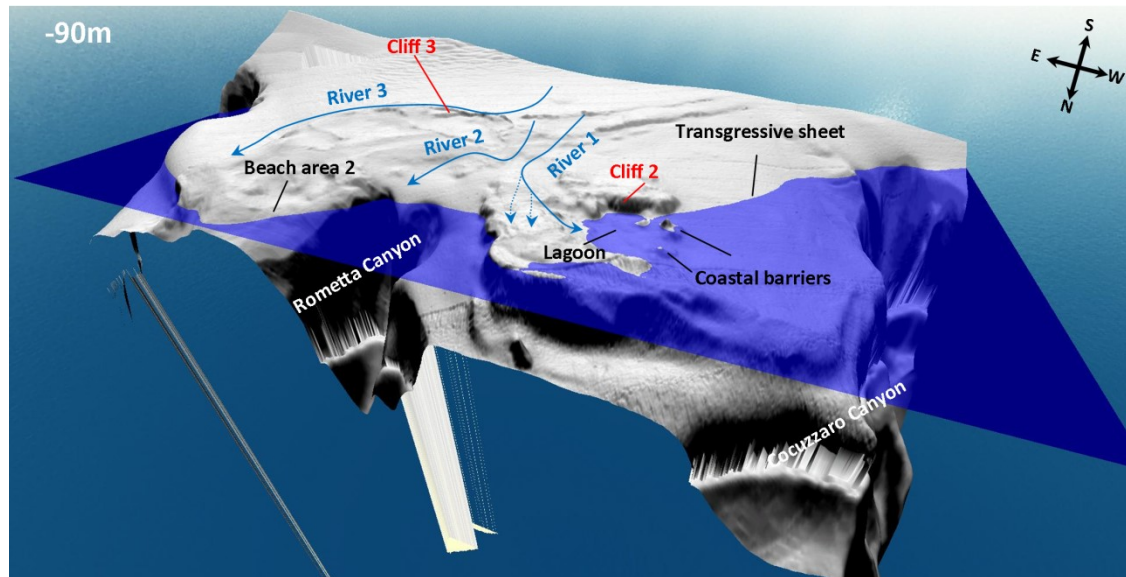


**Fig. 3.31** – On the basis of 3D bathymetric map, reconstruction of the geomorphological evolution of past coastal systems of the area between the Cocuzzaro and Rometta canyons, simulating a sealevel of -90 m.

*Sealevel -80 m (Fig. 3.32):*

Gradually, also in the southeastern portion, the transgressive wedge deposits increase its areal extension, characterized by reworked beaches and connected probably to the intense action of the oceanic waves. The River 2 retreats its course in the inner shelf and, therefore, in the central portion can continue the marked development of transgressive beaches (cusped beaches) and, westwards, also the formation of an extended longitudinal coastal barrier, belonging to overstep 2 deposits.

Only the River 3 keeps the original location and continues to flow at the basis of the Cliff 3, giving a general curvilinear trend. The Cliff 3 represents the step 3 of the lowstand succession and, in the following to further sea level rise (about -70 m), it becomes the place for the highstand wedge deposition that constitutes the overstep 3 deposits.

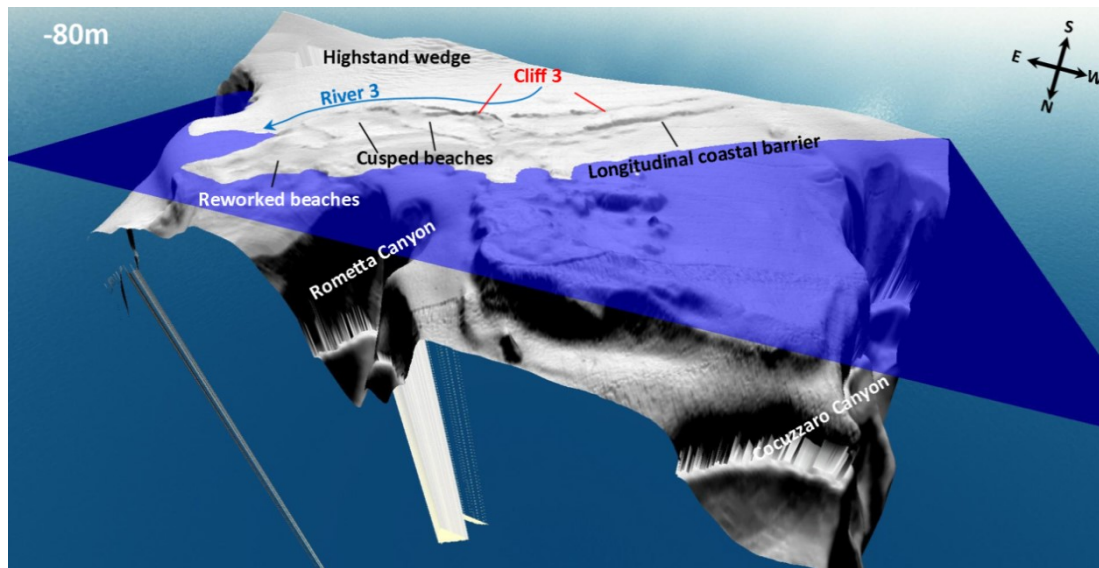


**Fig. 3.32** – On the basis of 3D bathymetric map, reconstruction of the geomorphological evolution of past coastal systems of the area between the Cocuzzaro and Rometta canyons, simulating a sealevel of -80 m.

#### 3.4.4 CONCLUSIONS

Through Multibeam bathymetric data, an update characterization of the geomorphological setting of the north-east Sicily continental shelf, between Milazzo Promontory and the area offshore from the Saponara River, is provided. Furthermore, through high-resolution CHIRP seismic profiles interpretation, a reconstruction of the evolution of the last eustatic sea level cycle is performed, on the basis of the morphostratigraphic description of the transgressive and highstand wedges.

The main results can be synthesized as follows:

- The lowstand succession corresponds with the foreset of the prograding clinoforms of the continental margin successions and represents the base level of the depositional units formed during the last sea-level rise and highstand.
- The lowstand succession determines the accommodation space for the sediment accumulation during the subsequent rise of the sea level. Therefore, the evolution of the transgressive and highstand wedges is strongly influenced by the geometry of the underlying lowstand succession. In fact, the seabed morphology along most study area is often equivalent with the top erosional surface of the lowstand succession, because the highstand wedge deposits tend to widely drape this surface of maximum regression. Conversely, where the transgressive and

highstand wedges do not show a consistent development, the lowstand succession is exposed on the seafloor.

- The transgressive wedge, preferentially developed in the 80-100 m bathymetric range, is bounded at the top by the Maximum Flooding Surface and consisting of the relict geomorphic elements that represent past landscape (coastal barrier-lagoon, transgressive sheet area, cusped beaches). These elements tracked the variations in coastline position during the last sea-level rise. One of the tracts with a relatively lower rate of rise of seafloor occurred when the sea level rose from about 90 to 70 m below its present-day position. This corresponds with the depth where, in the northeastern Sicilian relict outer shelf, the coastal systems are best developed (Gamberi et al., 2014; 2017). Therefore, the transgressive geomorphic elements could have formed during an interval of relatively reduced rate of sealevel rise.
- With the support of 3D bathymetric maps, a reconstruction of the geomorphological evolution of the past coastal systems during the last transgressive stage is provided.
- The highstand wedge consists of the Corriolo, Muto, Niceto, Cocuzzaro and Rometta delta deposits that widely develop on the offshore portions of the inner continental shelf. The bathymetric data image the deltas from a distance of 600 m from the coastline at an average depth of 40 m. The highstand wedge does not reaching depths higher than 85 m, leaving uncovered the past coastal system cropping out at the seafloor of the outer relict shelf.
- The relict shelf areas are located in correspondence of the smaller rivers, therefore the amount of sediment input from the rivers controls the seaward extension towards inner shelf of the highstand wedge.

## REFERENCES

AA.VV. (2000). Multibeam Sonar Theory of Operation. *Seabeam Instruments, L-3 Communications*. Washington Street East Walpole, 141. MA 02032-1155, (2000).

Allen, G. P., & Posamentier, H. W. (1993). Sequence stratigraphy and facies model of an incised valley fill: the Gironde estuary, France. *Journal of Sedimentary Research*, 63(3).

Allen, J. R. L. (1997). Simulation models of salt-marsh morphodynamics: some implications for high-intertidal sediment couplets related to sea-level change. *Sedimentary Geology*, 113(3-4), 211-223.

Antonelli, M., Franciosi, R., Pezzi, G., Querci, A., Ronco, G.P., & Vezzani, F. (1988). Paleogeographic evolution and structural setting of the northern side of Sicily Channel. *Memorie della Società Geologica Italiana*, 41, 141-157.

Arbues, P., Mellere, D., Falivene, O., Fernandez, O., Munoz, J. A., Marzo, M., & De Gibert, J. M. (2007). Context and architecture of the Ainsa-1- quarry channel complex, Spain. In: *Nilsen, T. H., Shew, R. D., Steffens, G. S., Studlick, J. R. J. (Eds), Atlas of Deep-water Outcrops: American Association of Petroleum Geologists Studies in Geology*, 56, CD-ROM, 20.

Argnani, A. (1990). The Strait of Sicily rift zone: foreland deformation related to the evolution of a back-arc basin. *Journal of Geodynamics*, 12(2-4), 311-331.

Arnott, R. W., & Southard, J. B. (1990). Exploratory flow-duct experiments on combined-flow bed configurations, and some implications for interpreting storm-event stratification. *Journal of Sedimentary Research*, 60(2).

Baldassini, N., & Di Stefano, A. (2015). New insights on the phosphatic layers of the Oligo-Miocene succession of the Maltese Archipelago. *Italian Journal of Geoscience*, 134/2, 355366.

Baldassini, N., Barreca ,G., Di Stefano, A. & Monaco, C. (2015). Stratigraphic and structural features of the Lampedusa Island. In: *Baldassini N. & Di Stefano A. (eds): Establishment of an integrated Italy-Malta cross-border system of Civil Protection. Geological Aspects. Aracne Editrice, Ariccia (Italy), 25-45.*

Baldassini, N., & Di Stefano, A. (2017). Stratigraphic features of the Maltese Archipelago: a syntesis. *Natural Hazards, 86*, 233-251.

Ben-Avmham, Z., & Grasso, M. (1990) . Collisional zone segmentation in Sicily and adjacent areas (central Mediterranean). *Ann. Tectonicae, 4*, 131-139.

Bhattacharya, J. P. (2006). Deltas. *Society for Sedimentary Geology Special Publication, 84*, 237.

Bianca, M., Monaco, C., Tortorici, L. & Cernobori, L. (1999) - Quaternary normal faulting in southeastern Sicily (Italy): A seismic source for the 1693 large earthquake. *Geophys. J. Int., 139*, 370-394.

Blum, M. D. (1994). Genesis and architecture of incised valley fill sequences: a Late Quaternary example from the Colorado River, Gulf Coastal Plain of Texas. In: *Weimer, P., Posamentier, H. W. (eds.), Siliciclastic sequence stratigraphy: recent developments and applications. American Association of Petroleum Geologists Memoir 58*, 259–283.

Blum, M. D., & Törnqvist, T. E. (2000). Fluvial responses to climate and sea-level change: a review and look forward. *Sedimentology, 47*(s1), 2-48.

Boccaletti, M., Nicolich, R., & Tortorici, L. (1984). The Calabrian Arc and the Ionian Sea in the dynamic evolution of the Central Mediterranean. *Marine Geology, 55*(3-4), 219-222.

Boccaletti, M., Cello, G., & Tortorici, L. (1987). Transtensional tectonics in the Sicily Channel. *Journal of Structural Geology, 9*(7), 869-876.



Boggs, S., (1995) - Principles of Sedimentology and Stratigraphy, 2nd ed. Prentice-Hall.

Bonforte, A., Catalano, S., Maniscalco, R., Pavano, F., Romagnoli, G., Sturiale, G., & Tortorici, G. (2015). Geological and geodetic constraints on the active deformation along the northern margin of the Hyblean Plateau (SE Sicily). *Tectonophysics*, 640, 80-89.

Boyd, R., & Honig, C. (1992). Estuarine sedimentation on the eastern shore of Nova Scotia. *Journal of Sedimentary Research*, 62(4).

Boyd, R., Dalrymple, R., & Zaitlin, B. A. (1992). Classification of clastic coastal depositional environments. *Sedimentary Geology*, 80(3-4), 139-150.

Boyd, R., Dalrymple, R. W., & Zaitlin, B. A. (2006). Estuarine and incised-valley facies models. *Society for Sedimentary Geology Special Publication*, 84, 171.

Broussard, M. L. (Ed.). (1975). *Deltas: models for exploration*, 2. Houston Geological Society.

Buccheri, G., Renda, P., Morreale, C., & Sorrentino, G. (1999). Il Tirreniano dell'Isola di Lampedusa (Arcipelago Pelagiano, Agrigento, Italia): le successioni di Cala Maluk e Cala Uccello. *Bollettino della Società Geologica Italiana*, 118(2), 361-373.

Burollet, P. F., Mugniot, G. M., & Sweeney, P. (1978). The geology of the Pelagian Block: the margins and basins of Southern Tunisia and Tripolitania. In: *Nairn A., Kaner W. & Stelhi F.G. (eds): The Ocean Basins and Margins. Plenum Press, New York*, 331-339.

Butler, R. W., Maniscalco, R., Sturiale, G., & Grasso, M. (2015). Stratigraphic variations control deformation patterns in evaporite basins: Messinian examples, onshore and offshore Sicily (Italy). *Journal of the Geological Society*, 172(1), 113-124.

Carbone, S., Grasso, M., & Lentini, F. (1982). Considerazioni sull'evoluzione geodinamica della Sicilia sud-orientale dal Cretaceo al Quaternario. *Mem. Soc. Geol. It*, 24, 367-386.

Carter, R. W. G., & Orford, J. D. (1984). Coarse clastic barrier beaches: a discussion of the distinctive dynamic and morphosedimentary characteristics. *Marine Geology*, 60(1-4), 377-389.

Caruso, A., Cosentino, C., Pierre, C., & Sulli, A. (2011). Sea-level changes during the last 41,000 years in the outer shelf of the southern Tyrrhenian Sea: evidence from benthic foraminifera and seismostratigraphic analysis. *Quat. Int.*, 232, 122–131.

Catalano, S., Monaco, C., Tortorici, L., & De Guidi, G. (2003). Morphological evidence of Holocene coseismic deformation in the Taormina region (NE Sicily). *J. Geodyn.*, 36, 193–211.

Catalano, S., Monaco, C., Tortorici, L., Paltrinieri, W., & Steel, N. (2004). Neogene-Quaternary tectonic evolution of the southern Apennines. *Tectonics*, 23(2).

Catalano, S., De Guidi, G., Romagnoli, G., Torrisi, S., Tortorici, G., & Tortorici, L. (2008). The migration of plate boundaries in SE Sicily: Influence on the large-scale kinematic model of the African promontory in southern Italy. *Tectonophysics*, 449(1), 41-62.

Catalano, S., De Guidi, G., Lanzafame, G., Monaco, C., & Tortorici, L. (2009). Late Quaternary deformation on the island on Pantelleria: New constraints for the recent tectonic evolution of the Sicily Channel Rift (southern Italy). *Journal of Geodynamics*, 48(2), 75-82.

Catuneanu, O. (2002). Sequence stratigraphy of clastic systems: concepts, merits, and pitfalls. *Journal of African Earth Sciences*, 35(1), 1-43.

Catuneanu, O. (2006). *Principles of sequence stratigraphy*. Elsevier, (4), 165-178.

Catuneanu, O., Abreu, V., Bhattacharya, J. P., Blum, M. D., Dalrymple, R. W., Eriksson, P. G., Giles, K. A., Fisher, W. L., Galloway, W. E., Gibling, M. R., Giles, K. A., Holbrook, J. M., Jordan, R., Kendall, C. G. St. C., Macurda, B., Martinsen, O. J., Miall, A. D., Neal, J. E., Nummedal, D., Pomar, L., Posamentier, H. W., Pratt, B. R., Sarg, J. F., Shanley,

K. W., Steel, R. J., Strasser, A., Tucker, M. E., & Winker, C. (2009). Towards the standardization of sequence stratigraphy. *Earth-Science Reviews*, 92(1), 1-33.

Catuneanu, O., Galloway, W. E., Kendall, C. G. S. C., Miall, A. D., Posamentier, H. W., Strasser, A., & Tucker, M. E. (2011). Sequence stratigraphy: methodology and nomenclature. *Newsletters on stratigraphy*, 44(3), 173-245.

Cavallaro, D., Monaco, C., Polonia, A., Sulli, A., & Di Stefano, A. (2016). Evidence of positive tectonic inversion in the north-central sector of the Sicily Channel (Central Mediterranean). *Natural Hazards*, 86(2), 233-251.

Cello, G., Crisci, G. M., Marabini, S., & Tortorici, L. (1985). Transtensive tectonics in the Strait of Sicily: structural and volcanological evidence from the Island of Pantelleria. *Tectonics*, 4(3), 311-322.

Cello, G. (1987). Structure and deformation processes in the Strait of Sicily "rift zone". *Tectonophysics*, 141(1-3), 237-247.

Civile, D., Lodolo, E., Zecchin, M., Ben-Avraham, Z., Baradello, L., Accettella, D., Cova, A., & Caffau, M. (2015). The lost Adventure Archipelago (Sicilian Channel, Mediterranean Sea): morpho-bathymetry and Late Quaternary palaeogeographic evolution. *Global and Planetary Change*, 125, 36-47.

Clifton, H.E. (2006). A re-examination of facies models for clastic shorelines. In: Posamentier, H. W., Walker, R. G. (Eds.), *Facies Models Revisited*, Society for Sedimentary Geology Special Publication, 84, 293-337.

Cogan, J., Rigo, L., Grasso, M., & Lerche, I. (1989). Flexural tectonics of southeastern Sicily. *Journal of geodynamics*, 11(3), 189IN1205-204IN2241.

Colantoni, P. (1975). Note di geologia marina sul Canale di Sicilia. *Giornale di Geologia*, 40(1), 181-207.

Coleman, J. M., Roberts, H. H., Murray, S. P., & Salama, M. (1981). Morphology and dynamic sedimentology of the eastern Nile delta shelf. *Marine Geology*, 42(1-4), 301-326.

Corti, G., Cuffaro, M., Doglioni, C., Innocenti, F., & Manetti, P. (2006). Coexisting geodynamic processes in the Sicily Channel. *Geological Society of America Special Papers*, 409, 83-96.

Curry, J. R. (1964). Transgressions and regressions. *Papers in marine geology*, 175-203.

D'agostino, N., & Selvaggi, G. (2004). Crustal motion along the Eurasia-Nubia plate boundary in the Calabrian Arc and Sicily and active extension in the Messina Straits from GPS measurements. *Journal of Geophysical Research: Solid Earth*, 109, B11402.

Dakin, N., Pickering, K. T., Mohrig, D., & Bayliss, N. J. (2013). Channel-like features created by erosive submarine debris flows: field evidence from the Middle Eocene Ainsa Basin, Spanish Pyrenees. *Mar. Petroleum Geol.*, 41, 62-71.

Dall'Antonia, B., Di Stefano, A., & Foresi, L. M. (2001). Integrated micropalaeontological study (ostracods and calcareous plankton) of the Langhian western Hyblean succession. *Palaeog., Palaeoc., Palaeoec.*, 176, 59-80.

Dalrymple, R. W., Zaitlin, B. A., & Boyd, R. (1992). Estuarine facies models: conceptual basis and stratigraphic implications: perspective. *Journal of Sedimentary Research*, 62(6).

Dart, C. J., Bosence, D. W. J., & McClay, K.R. (1993). Stratigraphy and structure of the Maltese graben system. *Journal of the Geological Society*, 150(6), 1153-1166.

Davies, J. L. (1964). A morphogenic approach to world shorelines. *Zeitschrift für Geomorphologie*, 8, 127-142.

Davis, R. A., & Hayes, M. O. (1984). What is a wave-dominated coast?. *Marine geology*, 60(1-4), 313-329.

Decima, A., & Wezel, F. C. (1971). Osservazioni sulle evaporiti messiniane della Sicilia centro-meridionale. *Riv. Min. Sic.*, 132-139.

Decima, A., & Wezel, F. C. (1973). Late Miocene evaporites of the central Sicilian basin, Italy. *Initial Reports of the Deep Sea Drilling Project*, 13(part 2), 1234-1241.

Decima, A., McKenzie, J. A., & Schreiber, B. C. (1988). The origin of " evaporitive" limestones; an example from the Messinian of Sicily (Italy). *Journal of Sedimentary Research*, 58(2), 256-272.

Di Stefano, A., & Lentini, R. (1995). Ricostruzione stratigrafica e significato paleo-tettonico dei depositi plio-pleistocenici del margine tirrenico tra Villafranca Tirrena e Faro Sicilia nord-orientale. *Studi Geol. Camerti*, 2, 219–237.

Dumas, S., Arnott, R. W. C., & Southard, J. B. (2005). Experiments on oscillatory-flow and combined-flow bed forms: implications for interpreting parts of the shallow-marine sedimentary record. *Journal of Sedimentary research*, 75(3), 501-513.

Elliott, T. (1986). Deltas. *Sedimentary Environments and Facies (ed. by Reading)*, 113-154. Blackwell Scientific Publications, Oxford.

Embry, A. F., & Johannessen, E. P. (1992). T-R sequence stratigraphy, facies analysis and reservoir distribution in the uppermost Triassic-Lower Jurassic succession, western Sverdrup Basin, Arctic Canada. In: *Vorren, T. O., Berg - sager, E., Dahl-Stamnes, O. A., Holter, E., Johansen, B., Lie, E., Lund, T. B. (Eds.), Arctic Geology and Petroleum Potential Special Publication, 2. Norwegian Petroleum Society (NPF)*, 121–146.

Fairbanks, R. G. (1989). A 17,000-year glacio-eustatic sea level record: influence of glacial melting rates on the Younger Dryas event and deep-ocean circulation. *Nature*, 342, 637–642.

Farre, J. A., McGregor, B. A., Ryan, W. B., & Robb, J. M. (1983). Breaching the Shelfbreak: Passage from Youthful to Mature Phase in Submarine Canyon Evolution. *Society for Sedimentary Geology Special Publication*, 33, 25-39.

Finetti, I. R. (1984). Geophysical study of the Sicily Channel rift zone. *Bollettino di Geofisica Teorica ed Applicata*, 26(101-102), 3-28.

Finetti, I. R., & Del Ben, A. (2005). Crustal tectono-stratigraphic setting of the Pelagian foreland from new CROP seismic data. In: *Finetti I. R. (eds): CROP project: deep seismic exploration of the central Mediterranean and Italy, Atlases in Geoscience 1. Elsevier, Amsterdam*, 581–595.

Finetti, I. R., Lentini, F., Carbone, S., Del Ben, A., Di Stefano, A., Forlin, E., Guarnieri, P., Pipan, M., & Prizzon, A. (2005). Geological outline of Sicily and lithospheric tectonodynamics of its Tyrrhenian margin from new CROP seismic data. In: *Finetti I. R. (eds): CROP Deep Seismic exploration of the Mediterranean Region, Elsevier*, 319-375.

FitzGerald, D. M., & Buynevich, I. V. (2001). Late Quaternary morphogenesis of a marine-limit delta plain in southwest Maine. *Special Papers-Geological Society of America*, 125-150.

FitzGerald, D. M., & Miner, M. D. (2013). 10.7 Tidal Inlets and Lagoons along Siliciclastic Barrier Coasts. *Treatise Geomorphology*, 149-165.

Forbes, D. L., Taylor, R. B., Orford, J. D., Carter, R. W. G., & Shaw, J. (1991). Gravel-barrier migration and overstepping. *Marine Geology*, 97(3-4), 305-313.

Friedman G. M., (2001): Father of clinof orm, undaform, and fondoform, Abstract, *Annual meeting of GSA Boston*, Paper 24-0.

Galloway, W. E. (1975). Process framework for describing the morphologic and stratigraphic evolution of deltaic depositional systems. In: *Broussard, M.L. (ed) Deltas: models for exploration. Houston Geological Society.*

Galloway, W. E. (2001). The many faces of submarine erosion: theory meets reality in selection of sequence boundaries. *American Association Of Petroleum Geologists, Hedberg Research Conference on "Sequence Stratigraphic and Allostratigraphic Principles and Concepts", Dallas, August 26–29, Program and Abstracts Volume*, 28–29.

Galloway, W. E. (2004). Accommodation and the sequence stratigraphic paradigm. *Reservoir, Canadian Society of Petroleum Geologists*, 31(5), 9–10.

Gamberi, F., & Argnani, A. (1995). Basin formation and inversion tectonics on top of the Egadi foreland thrust belt (NW Strait of Sicily). *Tectonophysics*, 252(1-4), 285-294.

Gamberi, F., Rovere, M., Mercorella, A., Leidi, E., & Dalla Valle, G. (2014). Geomorphology of the NE Sicily continental shelf controlled by tidal currents, canyon head incision and river-derived sediments. *Geomorphology*, 217, 106-121.

Gamberi, F., Breda, A., & Mellere, D. (2017). Depositional canyon heads at the edge of narrow and tectonically steepened continental shelves: Comparing geomorphic elements, processes and facies in modern and outcrop examples. *Marine and Petroleum Geology*.

Ghielmi, M., Amore, M. R., Bolla, E. M., Carubelli, P., Knezaurek, G., & Serraino, C. (2011). The Pliocene to Pleistocene succession of the Hyblean foredeep (Sicily, Italy). In: *American Association Of Petroleum Geologists Internat. Conf. Exhib. Milan, Italy, October, 23-26.*

Ghisetti, F., & Vezzani, L. (1980). The structural features of the Iblean Plateau and of the Mount Judica area (southeastern Sicily); a microtectonic contribution to the deformational history of the Calabrian Arc. *Bollettino della Società Geologica Italiana*, 99(1-2), 57-102.

Giosan, L., Donnelly, J. P., Vespremeanu, E., Bhattacharya, J. P., Olariu, C., & Buonaiuto, F. S. (2005). River delta morphodynamics: Examples from the Danube delta. In: *Giosan, L., Bhattacharya, J. P. (eds) River Deltas – Concepts, Models and Examples. Society for Sedimentary Geology Special Publication*, 83, 393-411.

Giraudi, C. (2004). The upper Pleistocene to Holocene sediments on the Mediterranean island of Lampedusa (Italy). *Journal of Quaternary Science*, 19(6), 537-545.



Goodbred Jr, S. L., & Saito, Y. (2012). Tide-dominated deltas. In: *Principles of Tidal Sedimentology*, 129-149. Springer Netherlands.

Grasso, M. T., & Lentini, F. (1982). Sedimentary and tectonic evolution of the eastern Hyblean Plateau (southeastern Sicily) during Late Cretaceous to Quaternary time. *Palaeogeography, Palaeoclimatology, Palaeoecology*, 39(3-4), 261-280.

Grasso, M., & Pedley, H. M. (1985). The Pelagian Islands: A new geological interpretation from sedimentological and tectonic studies and its bearing on the evolution of the Central Mediterranean Sea (Pelagian Block). *Geologica Romana*, 24(11), 13-34.

Grasso, M., Reuther, C.D., Baumann, H., & Becker, A. (1986). Shallow crustal stress and neotectonic framework of the Malta Platform and the Southeastern Pantelleria Rift (Central Mediterranean). *Geologica Romana*, 25, 191-212.

Grasso, M., & Pedley, H. M. (1988). The sedimentology and development of Terravecchia Formation carbonates (Upper Miocene) of North Central Sicily: Possible eustatic influence on facies development. *Sedimentary Geology*, 57(1-2), 131-149.

Grasso, M., & Reuther, C. D. (1988). The western margin of the Hyblean Plateau: a neotectonic transform system on the SE Sicilian foreland. In *Annales Tectonicae*, 2(2), 107-120.

Grasso, M., & Pedley, H. M. (1990). Neogene and Quaternary sedimentation patterns in the northwestern Hyblean Plateau (SE Sicily): the effects of a collisional process on a foreland margin. *Rivista Italiana di Paleontologia e Stratigrafia*, 96(2-3), 219-240.

Grasso, M., De Dominicis, A., & Mazzoldi, G., (1990). Structures and tectonic setting of the western margin of the Hyblean-Malta shelf, Central Mediterranean. *Annales Tectonicae* 4(2), 140-154.

Grasso, M., Torelli, L., & Mazzoldi, G. (1999). Cretaceous–Palaeogene sedimentation patterns and structural evolution of the Tunisian shelf, offshore the Pelagian islands (central Mediterranean). *Tectonophysics*, 315(1), 235-250.

Harris, J. A., Hobbs, R. J., Higgs, E., & Aronson, J. (2006). Ecological restoration and global climate change. *Restoration Ecology*, 14(2), 170-176.

Hayes, M. O. (1975). Morphology of sand accumulation in estuaries: an introduction to the symposium. *Estuarine research*, 2, 3-22.

Hollenstein, C., Kahle, H. G., Geiger, A., Jenny, S., Goes, S., & Giardini, D. (2003). New GPS constraints on the Africa-Eurasia plate boundary zone in southern Italy. *Geophysical Research Letters*, 30(18), 1935.

Hsü, K. J., Cita, M. B., & Ryan, W. B. F. (1973). The origin of the Mediterranean evaporites. *Initial Report of the Deep Sea Project 13, U.S. Government Printing Office, Washington D.C.*, 1203–1231.

Hsü, K. J., Montadert, L., Bernoulli, D., Cita, M. B., Erickson, A., Garrison, R. E., Kidd, R. B., Melieres, F., Müller, C., & Wright, R. C. (1977). *History of the Mediterranean salinity crisis. Nature*, 267, 399–403.

Hunt, D., & Tucker, M. E. (1992). Stranded parasequences and the forced regressive wedge systems tract: deposition during base-level fall. *Sedimentary Geology*, 81(1-2), 1-9.

Inman, D. L., & Brush, B. M. (1973). The coastal challenge. *Science*, 181(4094), 20-32.

Johnson, J. G., & Murphy, M. A. (1984). Time-rock model for Siluro-Devonian continental shelf, western United States. *Geological Society of America Bulletin*, 95(11), 1349-1359.

Jongsma, D., Jan, E. V., & Woodside, J. M. (1985). Geologic structure and neotectonics of the North African continental margin south of Sicily. *Marine and petroleum Geology* 2(2), 156-179.

Lambeck, K., Antonioli, F., Anzidei, M., Ferranti, L., Leoni, G., Scicchitano, G., & Silenzi, S. (2011). Sea level change along the Italian coast during the Holocene and projections for the future. *Quat. Int.*, 232, 250–257.

Leckie, D. A. (1994). Canterbury Plains, New Zealand--implications for sequence stratigraphic models. *American Association Of Petroleum Geologists bulletin*, 78(8), 1240-1256.

Lentini, F., Catalano, S., & Carbone, S. (1996). The external thrust system in Southern Italy: a target for petroleum exploration. *Pet. Geosci.*, 2, 333–342.

Lentini, F., Catalano, S., & Carbone, S. (2000). Carta Geologica della Provincia di Messina scala 1:50.000. *SELCA*, Firenze.

Lentini, F., Carbone, S., & Guarnieri, P. (2006). Collisional and postcollisional tectonics of the Apenninic-Maghrebic orogen (southern Italy). *Geological Society of America Special Papers*, 409, 57-81.

Lentini, F., & Carbone, S. (2014). Geologia della Sicilia-Geology of Sicily. *Memorie Descr. Carta Geologica d'Italia*, 95, 31-98.

Lipparini, L., Scrocca, D., Marsili, P., & Morandi, S. (2009). Offshore Malta licence in the Central Mediterranean Sea offers hope of hydrocarbon potential. *First break* 27(2), 105-116.

Manzi, V., Lugli, S., Roveri, M., & Charlotte Schreiber, B. (2009). A new facies model for the Upper Gypsum of Sicily (Italy): chronological and palaeoenvironmental constraints for the Messinian salinity crisis in the Mediterranean. *Sedimentology*, 56(7), 1937-1960.

Manzi, V., Gennari, R., Lugli, S., Roveri, M., Scafetta, N., & Schreiber, B. C. (2012). High-frequency cyclicity in the Mediterranean Messinian evaporites: evidence for solar–lunar climate forcing. *Journal of Sedimentary Research*, 82(12), 991-1005.

Mitchum Jr, R. M., & Vail, P. R. (1977). Seismic stratigraphy and global changes of sea-level, Part 6: stratigraphic interpretation of seismic reflection patterns in depositional sequences. In: PAYTON C.E. (Ed.), *Seismic Stratigraphy-Applications to Hydrocarbon Exploration. American Association Of Petroleum Geologists Memoirs*, 26, 117–133.

Mitchum Jr, R. M., & Vail, P. R. (1977). Seismic stratigraphy and global changes of sea-level, Part 6: stratigraphic interpretation of seismic reflection patterns in depositional sequences. In: PAYTON C.E. (Ed.), *Seismic Stratigraphy-Applications to Hydrocarbon Exploration, American Association Of Petroleum Geologists Memoirs*, 26, 135-144.

Mitchum Jr, R. M., Vail, P. R., & Thompson III, S. (1977). Seismic stratigraphy and global changes of sea level: Part 2. The depositional sequence as a basic unit for stratigraphic analysis: Section 2. Application of seismic reflection configuration to stratigraphic interpretation. *American Association Of Petroleum Geologists Special Volumes*, 165, 53-62.

Monaco, C., & Tortorici, L. (2000). Active faulting in the Calabrian arc and eastern Sicily. *J. Geodyn.*, 29, 407–424.

Mutti, E. (Ed.). (1999). An Introduction to the Analysis of Ancient Turbidite Basins from an Outcrop Perspective. *American Association Of Petroleum Geologists Continuing Education Course Note*, 39.

Nummedal, D., & Swift, D. J. (1987). Transgressive stratigraphy at sequence-bounding unconformities: some principles derived from Holocene and Cretaceous examples. In: Nummedal, D., Pilkey, O. H., Howard, J. D. (eds) *Sea-level fluctuation and coastal evolution. Society of Economic Paleontologists and Mineralogists Special Publication*, 41, 241-260.

Patacca, E., Scandone, P., Giunta, G. & Liguori, V. (1979). Mesozoic paleotectonic evolution of the Ragusa zone (southeastern Sicily). *Geologica Romana*, 18, 331-369.

Patacca, E., Royden, L., & Scandone, P. (1987). Segmentation and configuration of subducted lithosphere in Italy: an important control on thrust-belt and foredeep-basin evolution. *Geology*, 15, 714.

Patacca, E., Scandone, P. (2004) The Plio-Pleistocene thrust belt-foredeep system in the Southern Apennines and Sicily (Italy). *Boll. Soc. Geol. Ital. Vol. Spec.*, 93-129.

Pepe, F., Sulli, A., Agate, M., Di Maio, D., Kok, A., Lo Iacono, C., & Catalano, R. (2003). Plio-Pleistocene geological evolution of the northern Sicily continental margin (southern Tyrrhenian Sea): new insights from high-resolution, multi-electrode sparker profiles. *Geo-Mar. Lett.*, 23, 53–63.

Pieri, M. (1967). Caratteristiche sedimentologiche del limite cretacico terziario nella zona di Monterosso Almo, Monti Iblei, Sicilia sud-orientale. *Rivista Italiana Paleontologia Stratigrafia*, 73, 1259-1294.

Piper, D. J. W., & Normark, W. R. (2009). Processes that initiate turbidity currents and their influence on turbidites: a marine geology perspective. *J. Sediment. Res.* 79(6), 347-362.

Plint, A. G. (1988). Global eustacy and the Eocene sequence in the Hampshire Basin, England. *Basin Research*, 1(1), 11-22.

Posamentier, H. W., & Vail, P. R. (1988). Eustatic controls on clastic deposition II—sequence and systems tract models.

Posamentier, H. W., & Allen, G. P. (1993). Siliciclastic sequence stratigraphic patterns in foreland, ramp-type basins. *Geology*, 21(5), 455-458.

Posamentier, H. W., & Allen, G. P. (1999). Siliciclastic sequence stratigraphy: concepts and applications. *SEPM Concepts in Sedimentology and Paleontology Series* 7.

Pratson, L. F., & Coakley, B. J. (1996). A model for the headward erosion of submarine canyons induced by downslope-eroding sediment flows. *GSA Bull.*, 108, 225-234.

Reuther, C. D. (1990). Neotectonic processes in the central Mediterranean region. In: *Proceedings of the Fourth int. conference on the WEGENER-MEDLAS project, Scheveningen, The Netherlands, June 7-9, 1989, Delft University of Technology, De & The Netherlands*, 29-40.

Reuther, C. D., & Eisbacher, G. H. (1985). Pantelleria Rift-crustal extension in a convergent intraplate setting. *Geologische Rundschau*, 74(3), 585-597.

Reuther, C. D., Ben-Avraham, Z., & Grasso, M. (1993). Origin and role of major strike-slip transfers during plate collision in the central Mediterranean. *Terra Nova* 5(3), 249-257.

Rich, J. L. (1951). Three critical environments of deposition, and criteria for recognition of rocks deposited in each of them. *Geological Society of America Bulletin*, 62(1), 1-20.

Rigo, M., Barbieri, F., & Barbieri, F. (1959). Stratigrafia pratica applicata in Sicilia. *Boll. Serv. Geol. d'It.*, 80 (2-3), 351- 441.

Rouchy, J. M., & Caruso, A. (2006). The Messinian salinity crisis in the Mediterranean basin: a reassessment of the data and an integrated scenario. *Sedimentary Geology*, 188, 35-67.

Roure, F., Howell, D. G., Müller, C., & Moretti, I. (1990). Late Cenozoic subduction complex of Sicily. *Journal of Structural Geology*, 12(2), 259-266.

Roveri, M., Manzi, V., Gennari, R., Iaccarino, S. M., & Lugli, S. (2008). Recent advancements in the Messinian stratigraphy of Italy and their Mediterranean-scale implications. *Bollettino della Società Paleontologica Italiana*, 47(2), 71-85.

Roveri, M., Flecker, R., Krijgsman, W., Lofi, J., Lugli, S., Manzi, V., & Govers, R. (2014). The Messinian Salinity Crisis: past and future of a great challenge for marine sciences. *Marine Geology*, 352, 25-58.

Sabato, L., & Tropeano, M. (2004). Fiumara: a kind of high hazard river. *Phys. Chem. Earth A/B/C*, 29, 707–715.

Salvador, A. (Ed). (1994). International stratigraphic guide: a guide to stratigraphic classification, terminology, and procedure. *Geological Society of America*, 30.

Scicchitano, G., Spampinato, C. R., Ferranti, L., Antonioli, F., Monaco, C., Capano, M., & Lubritto, C. (2011). Uplifted Holocene shorelines at Capo Milazzo (NE Sicily, Italy): evidence of co-seismic and steady-state deformation. *Quat. Int.*, 232, 201–213.

Segre, A.G. (1960). Geologia. In: *Zavattari E. (eds.): Biogeografia delle Isole Pelagie. Rendiconti Accademia Nazionale dei Lincei*, 11(4), 115-162.

Serpelloni, E., Vannucci, G., Pondrelli, S., Argnani, A., Casula, G., Anzidei, M., & Gasperini, P. (2007). Kinematics of the Western Africa-Eurasia plate boundary from focal mechanisms and GPS data. *Geophysical Journal International*, 169(3), 1180-1200.

Sloss, L. L., Krumbein, W. C., & Dapples, E. C. (1949). Integrated facies analysis. *Geological Society of America Memoirs*, 39, 91-124.

Sloss, L. L. (1963). Sequences in the cratonic interior of North America. *Geological Society of America Bulletin*, 74(2), 93-114.

Southard, J. B., & Stanley, D. J. (1976). Shelf-break processes and sedimentation. *Marine Sediment Transport and Environmental Management: New York, John Wiley & Sons*, 351-377.

Sprague, A. R., Sullivan, M. D., Campion, K. M., Jensen, G. N., Goulding, F. J., Garfield, T. R., Sickafoose, D. K., Rossen, C., Jennette D. C., Beaubouef, R. T., Abreu, V., Ardill, J., Porter, M. L., & Zelt, F. B. (2002). The physical stratigraphy of deep-water strata:



A hierarchical approach to the analysis of genetically-related stratigraphic elements for improved reservoir prediction. *American Association Of Petroleum Geologists, Annual Meeting, March 10-13, Houston, Texas.*

Strahler, A. N. (1952). Hypsometric (area-altitude) analysis of erosional topology. *GSA Bull.*, 63(11), 1117–1142.

Sulli, A., Lo Presti, V., Gasparo Morticelli, M., & Antonioli, F. (2013). Vertical movements in NE Sicily and its offshore: outcome of tectonic uplift during the last 125 ky. *Quat. Int.*, 288, 168–182.

Swift, D. J. (1968). Coastal erosion and transgressive stratigraphy. *The Journal of Geology*, 76(4), 444-456.

Swift, D. J. (1975). Barrier-island genesis: evidence from the central Atlantic shelf, eastern USA. *Sedimentary Geology*, 14(1), 1-43.

Swift, D., Freeland, G., & Young, R. (1979). Time and space distributions of megaripples and associated bedforms, Middle Atlantic Bight, North American Atlantic Shelf. *Sedimentology*, 26, 389-406.

Tavarnelli, E., Renda, P., Pasqui, V., & Tramutoli, M. (2003). The effects of post-orogenic extension on different scales: an example from the Apennine–Maghrebide fold-and-thrust belt, SW Sicily. *Terra Nova*, 15(1), 1-7.

Torelli, L., Grasso, M., Mazzoldi, G., Peis, D., & Gori, D. (1995). Cretaceous to Neogene structural evolution of the Lampedusa shelf (Pelagian Sea, Central Mediterranean). *Terra Nova*, 7(2), 200-212.

Torelli, L., Grasso, M., Mazzoldi, G., & Peis, D. (1998). Plio–Quaternary tectonic evolution and structure of the Catania foredeep, the northern Hyblean Plateau and the Ionian shelf (SE Sicily). *Tectonophysics*, 298(1), 209-221.

Vail, P. R. (1977). Seismic stratigraphy and global changes of sea level. *Seismic stratigraphy-applications to hydrocarbon exploration: AAPG Memoir, 26*, 49-212.

Van Wagoner, J. C., Mitchum Jr, R. M., Posamentier, H. W., & Vail, P. R. (1987). Seismic stratigraphy interpretation using sequence stratigraphy, Part 2: Key definitions of sequence stratigraphy. *Atlas of seismic stratigraphy, American Association Of Petroleum Geologists Studies in Geology, 27(1)*, 11-14.

Van Wagoner, J. C., Posamentier, H. W., Mitchum Jr, R. M., Vail, P. R., Sarg, J. F., Loutit, T. S., & Hardenbol, J. (1988). An overview of the fundamentals of sequence stratigraphy and key definitions. *Sea-Level Changes – An integrated Approach, SEPM Special Publications, 42*.

Van Wagoner, J. C., Mitchum, R. M., Campion, K. M., & Rahmanian, V. D. (1990). Siliciclastic sequence stratigraphy in well logs, cores, and outcrops: concepts for high-resolution correlation of time and facies. *American Association Of Petroleum Geologists Special Volumes, A174*, III-55.

Van Wagoner, J. C. (1995). Overview of sequence stratigraphy of foreland basin deposits: terminology, summary of papers, and glossary of sequence stratigraphy. In: *Van Wagoner J. C., Bertram GT (eds) Sequence stratigraphy of foreland basins. American Association Of Petroleum Geologists Memoirs, 64*, 9-21.

Westaway, R. (1993). Quaternary uplift of Southern Italy. *J. Geophys. Res.. 98*, 21741–21772.

Wheeler, H. E. (1958). Time-stratigraphy. *American Association Of Petroleum Geologists Bulletin, 42(5)*, 1047-1063.

Winnock, E. (1981). Structure du Bloc Pelagien. In: *Wezel F.C. (eds): Sedimentary basins of Mediterranean margins, Technoprint, Bologna (Italy)*, 445-464.

Yoshida, S., Steel, R. J., & Dalrymple, R. W. (2007). Changes in depositional processes—an ingredient in a new generation of sequence-stratigraphic models. *Journal of Sedimentary Research*, 77(6), 447-460.

Zijderveld, J. D., Zachariasse, J. W., Verhallen, P. J., & Hilgen, F. J. (1986). The age of the Miocene-Pliocene boundary. *Newsletters on Stratigraphy*, 169-181.

## **RINGRAZIAMENTI**

Alla prof.ssa Agata Di Stefano perché da sempre ha creduto nelle mie capacità, dimostrandomi disponibilità e attenzione costanti, che mi hanno consentito non solo di realizzare questo lavoro ma anche di fare innumerevoli esperienze formative e umane;

Al dr. Fabiano Gamberi, per avermi mostrato come professionalità e umanità costituiscano un binomio fondamentale per essere davvero un buon Ricercatore. Per la pazienza dimostratami durante i miei lunghi soggiorni presso l'ISMAR e per la magnifica ospitalità riservatami da lui e famiglia nella bellissima casa di Crespino del Lamone;

Al dr. David Iacopini che mi ha introdotto per la prima volta nel mondo dell'interpretazione dei profili sismici ma soprattutto per avermi accolto nella sua casa di Aberdeen con garbo e rara disponibilità;

Ai revisori della mia Tesi di Dottorato, la dr.ssa Francesca Budillon e il prof. Sergio Longhitano, per gli attenti commenti e per i preziosi consigli che hanno contribuito certamente a valorizzare e migliorare il lavoro finale;

Al mio amico Niccolò - rigorosamente con due "C" - del quale non conservo gelosamente solo un'impetosa tazza violacea, ma soprattutto il ricordo di tre anni trascorsi nell'intesa, nella comprensione e nel sostegno reciproco;

Alla mia amica Laura che, alternando "vegetariane" chiacchierate a "indifferenziate" dissertazioni ecologiche, ha mostrato da subito lodevole pazienza nel so(u)pportarmi;

A mamma, papà e Anna, l'amorevole trio che da 35 anni riempie le mie giornate, sostiene i miei alti e bassi, mi mostra cosa significa veramente Famiglia, dà linfa e motivazione alle mie giornate;

A te, Clara, semino in crescita, perché tu possa sapere un giorno – se ti capiterà di leggere qui – che non ci sarà mai un'occasione di troppo per dirti quanto ti amo già.

Ad Ele, la donna della mia vita, perché con lei ogni giorno "le cose diventano tutte nuove"...